CHALMERS
UNIVERSITY OF TECHNOLOGY

Novel Control of Run-around Heat Recovery System

Evaluation of the novel control method's performance through laboratory experiments

Master's thesis in the Master's Programme
Sustainable Energy Systems

SUJITH PRIYANTHA
LORENSU HEWA WELLE KAMKANAMGE

DEPARTMENT OF ARCHITECTURE
AND CIVIL ENGINEERING

CHALMERS UNIVERSITY OF TECHNOLOGY
Gothenburg, Sweden 2025
www.chalmers.se

MASTER'S THESIS ACEX30

Novel Control of Run-around Heat Recovery System

Evaluation of the novel control method's performance through laboratory experiments

Master's Thesis in the Master's Program Sustainable Energy Systems

SUJITH PRIYANTHA, LORENSU HEWA WELLE KAMKANAMGE

EXAMINER and SUPERVISOR:

Jan-Olof Dalenbäck

Department of Architecture and Civil Engineering
Division of Building Services Engineering
CHALMERS UNIVERSITY OF TECHNOLOGY
Gothenburg, Sweden 2025

Novel Control of Run-around Heat Recovery System
Evaluation of the novel control method's performance through laboratory experiments

Master's Thesis in the Master's Program Sustainable Energy Systems

SUJITH PRIYANTHA, LORENSU HEWA WELLE KAMKANAMGE

Examensarbete ACEX30
Institutionen för arkitektur och samhällsbyggnadsteknik
Chalmers tekniska högskola, 2025

Department of Architecture and Civil Engineering
Division of Building Services Engineering
Chalmers University of Technology
SE-412 96 Gothenburg
Sweden
Telephone: + 46 (0) 31-772 1000

Department of Architecture and Civil Engineering.
Gothenburg, Sweden 2025

Novel Control of Run-around Heat Recovery System
Evaluation of the novel control method's performance through laboratory experiments

Master's thesis in the Master's Programme Sustainable Energy Systems

SUJITH PRIYANTHA, LORENSU HEWA WELLE KAMKANAMGE

Department of Architecture and Civil Engineering
Division of Building Services Engineering
Chalmers University of Technology

ABSTRACT

Run-around coil (RAC) systems are particularly well-suited for applications requiring complete separation between supply and exhaust airflows, such as hospitals, laboratories, and other facilities with stringent hygiene or contamination control requirements. Unlike rotary or plate-type heat exchangers, RAC systems ensure full airstream separation while offering design flexibility and modular installation, making them appropriate for complex and specialized ventilation scenarios. However, their efficient operation critically depends on the accurate control of the circulating liquid flow rate to achieve optimal heat recovery performance.

Traditional control strategies regulate liquid flow based on balancing the heat capacity flow rates of air and liquid media, which requires accurate real-time knowledge of their thermophysical properties. This approach becomes challenging in dynamic operational environments, especially under demand-controlled ventilation (DCV) conditions, where airflows fluctuate in response to changing occupancy. Moreover, accurately measuring flow rates and properties in real-time often increases system complexity, limiting the practicality of such control strategies.

To address these challenges, a novel temperature-based control method was developed and evaluated through laboratory experiments. This new approach relies on temperature measurements, rather than flow measurements or thermophysical property estimations, to regulate the system. The method aims to enhance system adaptability, reduce measurement uncertainties, and maintain stable heat recovery performance across a wide range of ventilation demands and external conditions. The experimental evaluation focused on testing this strategy's effectiveness, robustness, and responsiveness compared to conventional flow-based control methods.

The results demonstrate that the temperature-based control method (Xt) offers a reliable and efficient alternative, particularly in applications where fluid properties are variable or where accurate flow sensors are impractical. With appropriate tuning of control parameters, specifically the proportional and integral settings, the method achieved consistently high effectiveness and system stability across variable conditions. The findings suggest strong potential for integrating this novel control approach into both new and existing RAC installations, supporting improved energy efficiency and simplified operation in real-world DCV systems.

Key words: Run-around Coil (RAC), Heat Recovery, Temperature-Based Control, Demand-Controlled Ventilation (DCV), Energy Efficiency

Table of content

List of tables

List of figures

Preface

In this master's thesis, the performance of a newly implemented novel control system for run-around heat recovery system was analysed and evaluated using a laboratory test rig. During this period, the performance of the control unit was thoroughly tested under various conditions. Additionally, the associated web application was improved by integrating multiple regulation options, enabling the execution of diverse test scenarios for both balanced and unbalanced demand-controlled ventilation systems. This project was conducted at the Division of Building Services Engineering at Chalmers University of Technology.

I would like to express my sincere gratitude to Professor Jan-Olof Dalenbäck, who served as both my supervisor and examiner. His continuous support, guidance, and readiness to answer my questions were invaluable throughout this work. I would also like to thank Håkan Larsson at the Building Services Laboratory for his assistance with the experimental testing, which was essential for the success of this study. Special thanks to Peter Filipsson at CIT Renergy for providing the initial introduction that helped initiate this project.

I am also grateful to all members of the Division of Building Services Engineering at Chalmers for their valuable feedback. Finally, I would like to extend my heartfelt thanks to Despoina Teli, whose guidance helped me find this thesis opportunity.

Gothenburg, June 2025

Sujith Priyantha, Lorensu

Abbreviations

AHU	Air handling unit
ASHRAE	American society of heating, refrigerating and air-conditioning engineers
DCV	Demand controlled ventilation
Eff	Effectiveness
EG	Ethylene glycol
ERVs	Energy recovery ventilators
HRU	Heat recovery unit
HRVs	Heat recovery ventilators
HVAC	Heating ventilation and air conditioning
HX coil	Heat exchange coil
Max	Maximum
PID values	Proportional, integral and derivative values
RAC	Run-around coil
RAHR	Run-around heat recovery
RAHRS	Run-around heat recovery system
RAHRU	Run-around heat recovery unit
VAV	Variable air volume
VFD	Variable frequency drive

Nomenclature

A	Area	[m^2]
Cp	Specific heat capacity	[kJ/kgK]
k	Thermal conductivity	[W/mK]
μ	*V*iscosity	[mPas]
NTU	Number of transfer units	[-]
ρ	Density	[kg/m^3]
T, t	Temperature	[°C]
U	Heat transfer coefficient	[W/m^2K]
V	Volumetric flow rate	[m^3/s]
X	Heat capacity ratio	[-]

Subscripts

a	*air*
c	*cool*
ea	*extract air*
eha	*exhaust air*
l	*liquid*
oa	*outdoor air*
sa	*supply air*
t	*temperature*
v	*flow*
w	*warm*

Index numbers

1	*before pump*
2	*after pump, unbalanced airflow*

1. Introduction

1.1 Background

Heat recovery technologies, including widely used fixed plate heat exchangers, rotary heat exchangers with desiccant wheels and run-around heat recovery (RAHR) systems, significantly reduce the energy demand of ventilation systems in buildings. RAHR systems play a crucial role in modern ventilation, particularly in applications where cross-contamination between air streams is not acceptable due to air quality requirements, in buildings with complex ducting and multiple exhaust locations, and in retrofit projects with space limitations. These systems are commonly used in hospitals, commercial buildings and industrial facilities to improve energy efficiency while meeting strict sustainability and environmental goals.

Run-around heat recovery systems employ a closed-loop liquid medium, typically a water-glycol mixture, to transfer heat between extract and supply air streams, recovering waste heat and reducing the overall energy demand of heating, ventilation and air conditioning (HVAC) systems. Although RAHR systems offer unique advantages compared to other ventilation heat recovery systems, their design and operation are more complex, especially in ventilation systems with variable airflow rates which are commonly used in modern building applications.

Optimizing heat recovery efficiency in RAHR systems requires precise control of liquid flow rates. Conventional control strategies regulate the system by adjusting the heat capacity flow rate in response to airflow variations, ensuring that the heat capacity rates of both the air and liquid media remain equal. However, in real-world applications, fluctuations in temperature, pressure and flow conditions make it challenging to maintain optimal heat recovery performance. Additionally, demand-controlled ventilation (DCV) systems introduce further complexity, as variations in airflow require real-time adjustments to the liquid flow rate to achieve optimum heat recovery efficiency.

To address these challenges, a novel temperature-based control method has been developed to optimize the regulation of liquid flow rates and achieve optimal system performance. Unlike conventional control strategies, which depend on dynamic thermophysical properties and precise flow measurements, this method uses temperature-based indicators to regulate system performance. By reducing the dependence on dynamic thermophysical properties and accurate flow measurements, this approach enhances system reliability, simplifies operation and lowers maintenance requirements. The method's ability to improve system robustness and accuracy is essential for effectively optimizing liquid flow rates in RAHR systems, ensuring reliable performance in real-world applications [1].

This thesis focuses on evaluating the effectiveness of the temperature-based control method for RAHR units through laboratory tests. The study evaluates its ability to enhance heat recovery efficiency, system stability, and adaptability under varying ventilation conditions. Considering the increasing focus on energy efficiency and sustainability in building operations, this research is particularly relevant to organizations managing large-scale HVAC systems. The findings have the potential to inform the development of practical guidelines for integrating temperature-based control into existing RAHR installations, supporting efforts to optimize energy performance while ensuring operational reliability.

As energy regulations tighten and sustainability goals drive the adoption of advanced HVAC technologies, optimizing heat recovery through intelligent control mechanisms is essential for

reducing energy consumption in ventilation systems. The insights from this study can guide facility managers and HVAC designers in implementing more efficient and adaptive control strategies, ultimately contributing to improved energy performance and operational efficiency in buildings.

1.2 Aim of the thesis

The objective of this thesis is to evaluate the performance of a novel temperature-based control method for run-around heat recovery systems through laboratory experiments. The study aims to evaluate its effectiveness in optimizing liquid flow rates and enhancing heat recovery efficiency compared to conventional control strategies.

Additionally, the research analyses the system's stability, responsiveness, and efficiency under varying operational conditions and ventilation demands. The findings can contribute to understanding the feasibility of temperature-based control for real-world applications and its potential integration into existing run-around heat recovery system installations to improve energy efficiency and operational reliability.

1.3 Literature review

Buildings play a vital role in the global energy system, accounting for 30% of global final energy consumption and contributing approximately 26% of energy-related CO_2 emissions in 2022, according to the International Energy Agency [2,3]. A significant portion of these emissions results from space heating which alone accounts for around 12% of the total global energy demand and emissions, primarily due to the thermal and ventilation requirements of indoor environments [2,4]. Ensuring thermal comfort and maintaining good indoor air quality is essential, particularly in commercial and institutional buildings which require high ventilation airflows.

To reduce energy use while maintaining indoor air quality, buildings are increasingly integrating heat recovery systems that capture thermal energy from extract air and transfer it to incoming fresh air. Under typical operating conditions, up to 30% of the energy used in buildings can be lost through exhaust air, highlighting the importance of recovery systems as an effective energy-saving measure [2,5]. Commonly used heat recovery technologies in buildings include plate heat exchangers, rotary heat exchangers and run-around coil systems. Among these, the run-around heat recovery system is widely implemented for complex configurations or retrofit applications.

A run-around heat recovery system comprises two separate fin-and-tube heat exchangers located in the exhaust and supply air streams. These coils are thermally coupled through a working fluid, typically a mixture of water and glycol, circulated by a pump. In contrast to rotary or plate exchangers, the run-around system enables complete separation of air streams, effectively eliminating the risk of cross-contamination. This characteristic makes the system well-suited for retrofit projects, hospitals, and laboratories. It is particularly advantageous in buildings with space limitations, where supply and exhaust ducts are widely spaced or strict hygiene standards must be maintained [2,6].

In response to the COVID-19 pandemic, HVAC standards started recommending higher ventilation rates and extended operating hours to reduce airborne transmission risks. However, these measures unintentionally lead to increase energy consumption in ventilation systems. As a result, the integration of efficient heat recovery solutions, including run-around heat recovery

systems, is increasingly important for balancing indoor air quality with energy performance objectives [2,5,6].

Despite the practical advantages, several studies have indicated that RAHRS frequently underperforms compared to the theoretical design efficiency, particularly in demand-controlled ventilation systems. Factors such as coil fouling, suboptimal liquid quality, malfunctioning valves, and inappropriate antifreeze concentrations can significantly affect system performance [2,7]. Moreover, design challenges such as unfavourable flow rates, pressure drops and limited control optimization further reduce the actual heat transfer effectiveness which typically ranges between 45 - 65%, despite a regulatory requirement of at least 68% effectiveness for units placed on the EU market after 2018 [2].

In comparison, plate heat exchangers typically deliver 50 - 80% efficiency, and rotary heat exchangers can exceed 80%, although they carry a higher risk of cross contaminations [1,8]. To address the inherent performance limitations of RAHRS and to achieve regulatory compliance, optimizing design and control strategies are essential. As suggested by Nelson [9], improving system effectiveness may include using large coil surface areas, low-pressure drop designs, optimized antifreeze concentrations, variable-speed pumping, and smart control sequences that respond dynamically to varying operational conditions.

With the increasing focus on energy-efficient building retrofits driven by global climate objectives and the necessity of ensuring occupant health, there is an evident requirement to advance the study and development of innovative control strategies for RAHRS. This thesis focuses on evaluating a novel temperature-based control approach for RAHRS to determine its effectiveness in achieving optimal thermal performance. The analysis considers varying ventilation rates, typically observed in DCV systems, with the goal of maximizing heat recovery while minimizing energy consumption.

1.3.1 Air-to-air energy recovery equipment

Air-to-air energy recovery systems significantly contribute to enhancing energy efficiency and maintaining indoor environmental quality by enabling the exchange of heat and, in some systems, moisture between two airstreams with different temperature and humidity levels. These systems are particularly important in buildings where substantial energy is used to condition ventilation air, in this manner supporting sustainable building design. The integration of these systems contributes to global sustainability objectives, particularly the United Nations Sustainable Development Goals (SDGs) including goal 7 (affordable and clean energy) and goal 13 (climate action) [10], as well as the European Green Deal's goals to improve energy performance and reduce greenhouse gas emissions in the building sector [11].

These systems can recover energy in both sensible form (related to temperature) and latent form (related to moisture). Devices that recover only sensible energy are typically referred to as heat recovery ventilators (HRVs), while those that recover both sensible and latent energy are known as energy recovery ventilators (ERVs). Both types are widely available for residential, commercial, and industrial applications [12].

ERVs are particularly advantageous in hot and humid climates, where moisture management is a key concern. By transferring moisture from the incoming ventilation air to the outgoing exhaust air, ERVs reduce the latent cooling load, improving the dehumidification performance of conventional HVAC systems. This capability supports compliance with ventilation

requirements indicated in ASHRAE standards, while maintaining occupant health and comfort by reducing indoor humidity and limiting the growth of mold, bacteria and allergens [12].

Applications

Air-to-air energy recovery applications can be broadly categorized into three types that are comfort-to-comfort, process-to-comfort and process-to-process. Comfort-to-comfort applications include residential buildings, offices, classrooms, healthcare facilities and hospitality environments. In these cases, energy recovery devices are used to precondition incoming fresh air by recovering energy from exhaust air, reducing heating and cooling demands throughout the year.

In process-to-comfort systems, waste heat from industrial processes, such as furnaces, dryers or ovens, is used to preheat ventilation or makeup air for comfort spaces, especially during winter. However, in warmer conditions, this recovery must be modulated or bypassed to avoid overheating. Process-to-process systems involve transferring energy directly between process exhaust and supply air within the same industrial operation. These systems typically recover only sensible heat and are designed to handle high-temperature exhaust, avoiding moisture transfer that could interfere with process integrity [12].

Technical considerations

The performance of HRVs and ERVs is measured through several key parameters that reflect both thermal and operational efficiency. Effectiveness measures the ratio of recovered energy to the theoretical maximum possible, indicating how well the system performs under given conditions. The recovery efficiency ratio (RER) represents the ratio of useful recovered energy output to the energy input required to operate the system. Other important considerations include pressure drop which results from airflow resistance and affects fan or pumping energy requirements, and cross leakage, the unintended mixing of exhaust and supply air streams that may compromise indoor air quality. Additionally, frost control mechanisms are essential in colder climates to prevent freezing within the heat exchanger, ensuring reliable operation during low-temperature periods [12].

From an economic perspective, the feasibility of implementing air-to-air energy recovery systems depends on factors such as capital investment, ongoing maintenance requirements, and operational cost savings achieved through reduced heating and cooling demands. A comprehensive life cycle cost analysis that incorporates these elements is required for evaluating the system's cost-effectiveness and determining the expected payback period across various building applications.

Types of air-to-air heat exchangers

Air-to-air energy recovery systems utilize a variety of heat exchanger configurations, each designed to meet specific application requirements and design constraints. These systems are integral to improving indoor air quality and energy performance in modern HVAC applications, particularly in buildings with high ventilation demands [12].

Fixed-plate heat exchangers are among the most widely used configurations in HRVs and ERVs. These units consist of alternating layers of air channels that enable heat and, in some cases moisture, transfer between supply and exhaust air streams without any direct mixing. Their reliability, due to the absence of moving parts, makes them suitable for residential and commercial installations where durability and simplicity are priorities.

Rotary wheels, also known as enthalpy wheels, are porous rotating devices that transfer both sensible and latent heat. Due to their high thermal effectiveness and compact design, they are particularly well-suited for large-scale commercial HVAC systems. However, their moving components require regular maintenance and proper sealing to prevent cross-contamination between airflows.

Heat pipe heat exchangers operate passively, using the phase change and capillary action of a working fluid contained within a sealed pipe. They are most effective when the supply and exhaust airflows are closely located but not necessarily aligned. These systems offer moderate efficiency and are valued for their simplicity and lack of mechanical components.

Runaround coil loops use a circulating liquid, typically a glycol-water mixture, to transfer heat between two separate air-handling units. This configuration allows energy recovery even when the supply and exhaust airflows are physically separated, making it a flexible option for complex building layouts. Their modularity, design flexibility, and inherent frost resistance make them particularly suitable for retrofit applications and cold climates. This configuration is of specific relevance to the present thesis, which explores the control optimization of such systems.

Thermosiphons function similarly to heat pipes but depend on gravity-driven natural convection rather than capillary action. These systems are generally used in vertically aligned ductwork where gravitational flow can be maintained for effective heat transfer.

Fixed-bed regenerators store thermal energy in a solid medium that alternates between hot and cold air streams. This cyclical operation enables high heat recovery efficiency but may introduce complexity in control and system integration. These systems are typically used in industrial or process ventilation settings.

Liquid-desiccant cooling systems are designed primarily for dehumidification, utilizing hygroscopic solutions to remove moisture from incoming air. While not primarily heat exchangers, they represent a specialized class of air-to-air recovery systems used in climate-sensitive or humidity-critical environments.

An ideal air-to-air energy recovery system should aim to maximize the transfer of heat and moisture based on differences in temperature and vapor pressure, while minimizing pressure drop to reduce fan energy consumption. It should also prevent cross-contamination between air streams to maintain indoor air quality and ensure hygiene. Additionally, optimal systems are those that achieve a balance between thermal efficiency, physical size, maintenance needs, and cost-effectiveness, factors that are especially important when integrating recovery systems into existing buildings.

1.3.2 Optimizing run-around coil heat recovery systems

Basic system configuration and performance

A standard run-around coil (RAC) system consists of two or more finned tube heat exchanger coils [9]. One coil is positioned in the exhaust airstream and the other in the supply airstream. These coils are connected by insulated piping that circulates a working fluid, typically water or a water–glycol mixture, using a pump. Since the airflows remain completely separated, the system depends entirely on the heat transfer characteristics of the fluid. The system's overall performance is influenced by several factors, including fluid flow rate, pump operation, fluid properties, and the effectiveness of the control strategy.

One significant advantage of RAC systems is their ability to maintain efficient performance under varying load conditions. This is achieved using variable-speed pumps and advanced control mechanisms. This adaptability ensures consistent heat recovery performance while maintaining indoor air quality and preventing the risk of cross-contamination. Additionally, these systems can be installed in air handling units that are not aligned or are located apart from each other, which provides practical advantages in retrofit applications or in situations with spatial constraints.

The thermal effectiveness of RAC systems typically ranges from 30% to 60%, depending on the configuration of the coils, the layout of the piping loop and the implemented control approach. Although this is significantly lower than the efficiency achieved by rotary heat exchangers, RAC systems provide specific operational advantages. These include improved control adaptability and increased freeze protection, particularly when glycol solutions are used in combination with well-regulated control strategies [9].

Key design parameters influencing the performance of RAC systems

The performance of RAC systems depends on several key design parameters that influence thermal efficiency, energy use and operational reliability. The following eight factors are particularly important when optimizing RAC system performance across different applications.

1. Coil heat transfer characteristics

The heat transfer ability of a coil is primarily determined by the UA value, which is the product of the overall heat transfer coefficient and the coil surface area. High-efficiency coils typically demonstrate UA values in the range of 1000 to 3000 W/°C, depending on parameters including airflow rate, coil depth and fin density [9]. Increasing fin density or the number of tube rows can improve thermal performance. However, it also results in a higher airside pressure drop, leading to increased fan energy use. Therefore, an optimal design should achieve a balance between effective heat transfer and acceptable pressure losses.

2. Working fluid selection

Water is typically the most effective working fluid due to its high specific heat capacity and low viscosity, which contribute to excellent heat transfer performance. However, it is subject to freezing in colder climates. To mitigate this, glycol mixtures, commonly 20 to 40 percent by volume, are added to provide freeze resistance at temperatures as low as -20 °C. Although glycol reduces the risk of freezing, it can reduce heat transfer efficiency by 15 to 25 percent and increases pumping requirements due to its higher viscosity [1,2,9]. Therefore, the selection of a suitable working fluid involves a balance between freeze protection and system efficiency, particularly in variable-speed applications.

3. System fluid flow rate

The fluid flow rate through the system directly influences the amount of heat exchanged between the exhaust and supply coils. Optimal flow rates are typically within the range of 0.05 to 0.1 l/s per kilowatt of heat transfer [9]. Flow rates that are too high increase pump energy use without a corresponding improvement in thermal performance, while insufficient flow can result in underperformance and poor temperature regulation or coil freezing. Using variable-speed pumps allows for dynamic flow rate control to maintain optimal operation under varying thermal loads.

4. Coil surface area

Larger coil surface areas improve heat recovery by increasing the contact area between the air and the coil surfaces. This is typically achieved by using multiple coil rows, generally between four and eight, and high fin densities of up to twelve fins per inch [9]. However, increasing the coil surface area also introduces challenges including space limitations, higher material costs and increased airside pressure drop. Therefore, proper design is required to achieve optimal performance within practical constraints.

5. Coil air pressure drop

High airside pressure drop across the coil can substantially increase fan energy consumption. It is generally recommended to design for pressure drops in the range of 40 to 80 pascals per coil, depending on airflow rates and coil size. Strategies to reduce airflow resistance include optimizing coil geometry, using smooth airflow paths and applying anti-fouling surface treatments. Additionally, appropriate positioning within the AHU contributes to minimizing overall pressure losses [9].

6. Coil construction and material options

Specialized coil designs can incorporate features such as optimized fin profiles, corrosion-resistant coatings, and tailored tube wall thicknesses. Thin tube walls, typically less than 0.5 mm, enable efficient heat transfer but are less durable in high-pressure or corrosive environments. To enhance resistance in such conditions, materials including stainless steel or epoxy-coated copper are typically used, particularly in systems exposed to aggressive indoor or outdoor air conditions [9].

7. Control sequences

To prevent frost formation on the exhaust coil in run-around heat recovery systems, appropriate control strategies are required when coil surface temperatures approach freezing. Conventional methods use fixed fluid temperature setpoints, but more effective strategies regulate the supply fluid flow to maintain the coil's leaving air temperature just above the exhaust air dew point. In colder climates, defrost methods such as scheduled flow interruptions can be used. However, under typical operating conditions, maintaining a fixed exhaust air temperature provides an adequately reliable solution [9].

8. Variable speed pump implementation

Variable-speed pumps are essential for achieving energy-efficient operation in run-around coil systems. By adjusting pump speed in response to real-time thermal loads and temperature differences, they can significantly reduce auxiliary energy use compared to fixed-speed pumps. They also improve control accuracy, enhance part-load performance and contribute to system reliability by reducing mechanical stress. These pumps are particularly important in control strategies aimed at optimizing performance and reducing operational costs.

Coil selection

Coil selection is an important part of RAC system design, requiring a balance between thermal performance, physical constraints and long-term reliability. Important considerations include airflow rate, supply and exhaust air temperatures, allowable pressure drop and the available space within the AHU. A properly selected coil allows the system to achieve the required thermal

effectiveness without excessive fan energy use. To support the selection process, engineers generally use coil simulation tools or manufacturer-specific software to align coil performance with the specific demands of the application.

System design

The design of a RAC system should consider the overall system function. It is important to account for how the components operate together. Appropriate system design involves proper insulation of fluid pipes, hydraulic loop balancing and the use of bypass lines to support maintenance and reduce the risk of frost during low-temperature conditions. Major design aspects include pump sizing, coil orientation and AHU zoning. Minimizing piping lengths and selecting components with low flow resistance can improve overall system efficiency. Integrating temperature sensors and flow meters supports real-time monitoring and diagnostics, which enhances reliability and control.

Energy and economic analysis

Properly designed RAC systems can recover around 70 percent of the thermal energy from exhaust air, with actual performance depending on seasonal outdoor conditions, control methods and system configuration [9,20]. From an economic perspective, both capital expenses and operating costs must be evaluated. While systems with variable-speed pumps and sensor-based controls typically require higher initial investments, they generally offer lower operational energy costs, resulting in an acceptable payback period of approximately three to five years. A comprehensive life-cycle cost analysis should include considerations of energy savings, maintenance requirements, system reliability, and the reduction of risks related to coil freezing and air contamination [9].

1.3.3 Fluid flow rate optimization

Optimizing the fluid flow rate in run-around heat recovery systems is necessary to achieve high thermal effectiveness while minimizing auxiliary energy use. Earlier research primarily explored the relationship between the characteristics of the coupling fluid flow and overall system performance. More recently, studies have examined the effects of variable operating conditions, including changes in airflow rate, working fluid composition, and coil configuration, on optimal flow parameters. The following subsection provides an overview of both foundational studies and recent contributions to the understanding of fluid flow rate optimization in run-around heat recovery systems.

Previous studies on Run-around heat recovery systems

One of the earliest significant contributions was made by Holmberg [2,13], who extended the theoretical framework established by Kays and London [2,14]. Holmberg developed an analytical expression to determine the optimum capacity flow rate of the coupling liquid, treating fluid velocity as an independent variable. His analysis concluded that thermal effectiveness is maximized when the capacity flow rate of the coupling fluid equals that of the air. Holmberg also emphasized that systems designed for higher thermal effectiveness tend to be more sensitive to deviations from this optimal flow rate.

Further insights were provided by Forsyth and Besant [2,15], who examined the influence of various coil parameters on system effectiveness. Their study revealed that liquid flow rate and

tube diameter have a substantial impact on performance, while fin spacing and fin thickness have comparatively minor effects. Particularly, field data demonstrated that the maximum thermal effectiveness does not always occur at a capacity flow ratio of one, challenging earlier assumptions. In a follow-up study [2,16], the authors validated the theoretical predictions of Kays and London by comparing them with experimental data, finding deviations within ±5%. They also emphasized the importance of ensuring turbulent flow in the coil's liquid-side passing to enhance heat transfer performance.

One of the studies, Zeng [2,17] introduced the consideration of temperature-dependent fluid properties in modelling RAHRS. Their findings indicated that ignoring these variations can significantly reduce model accuracy. Conversely, Balen [2,14], through experiments involving two coil configurations with different fin pitches and thicknesses, observed that changes in fluid temperature did not significantly influence thermal effectiveness. Despite contradicting Zeng's conclusions, their results were consistent with earlier work by Holmberg and Kays and London, confirming that effectiveness typically peaks when the capacity flow ratio is close unity.

However, a frequent limitation in earlier studies is the absence of validated models that consider the use of various glycol-water mixtures when determining optimal flow rates. In addition, previous research did not examine the effect of variable air volume (VAV) conditions on system performance when using water-ethylene glycol solutions, particularly under laminar flow conditions on the liquid side. This gap in understanding was recently addressed by Mahmoud [2], whose work is outlined in the following subsection.

Latest studies on Run-around heat recovery systems and fluid flow rate optimization

Recent research on the modelling and simulation of RAHRS, particularly the work by Mahmoud [2], has contributed valuable knowledge on how operating conditions and coupling fluid properties affect thermal effectiveness. The developed detailed simulation model incorporates variable air volume conditions and accounts for the temperature-dependent properties of the coupling liquid, allowing for a more accurate evaluation of system performance under realistic scenarios.

In these simulations, a 37% ethylene glycol–water mixture was used as the coupling fluid. The results showed that as the airflow rate increased, the maximum effectiveness of the system decreased, primarily due to a decline in the number of thermal transfer units (NTU), as illustrated in Figure 1. At lower airflow rates (0.3 and 0.5 m^3/s), the coupling liquid remained within the laminar flow regime, and maximum effectiveness was also achieved under these conditions [2].

Importantly, the study found that maximum effectiveness did not always occur at a capacity flow ratio of one. Instead, the optimal flow ratio varied depending on the airflow rate, contradicting earlier research findings that consistently associate the best performance with a unity capacity flow ratio. These results highlight the need for dynamic control strategies that adjust fluid flow rates in response to real-time airflow conditions, particularly in systems operating under VAV control [2].

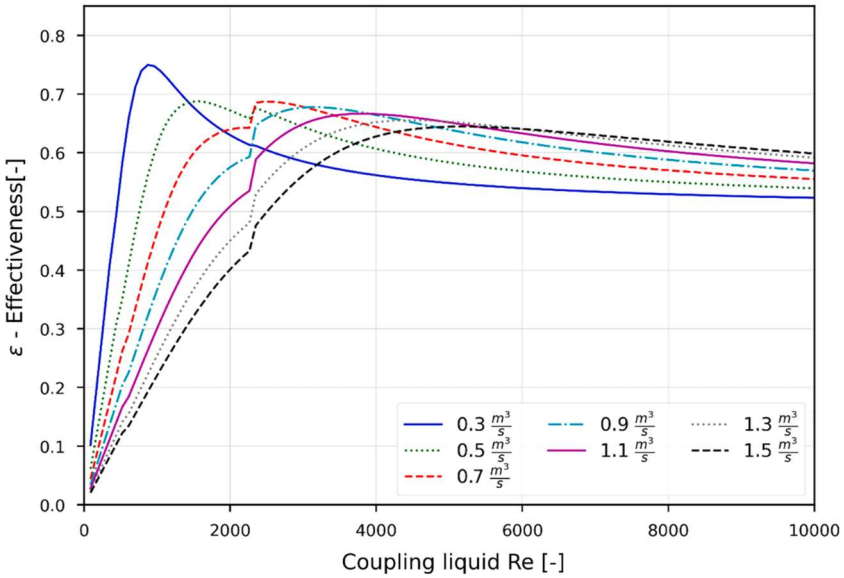

Figure 1: The effectiveness related to the coupling liquid Reynold number with 37% ethylene glycol.
(Source, Mohammad Mahmoud (2022) [1])

As shown in Figure 2, the overall thermal conductance of the coil (UA-value) increases with the Reynolds number of the coupling fluid, with a significant increase occurring around a Reynolds number of 2300, which marks the transition from laminar to turbulent flow. However, the increase in UA-value was not always sufficient to compensate for the higher heat capacity flow rate when it exceeded a ratio of one. At these elevated flow rates, the temperature difference between the coil inlet and outlet was reduced, resulting in decreased heat transfer effectiveness [2].

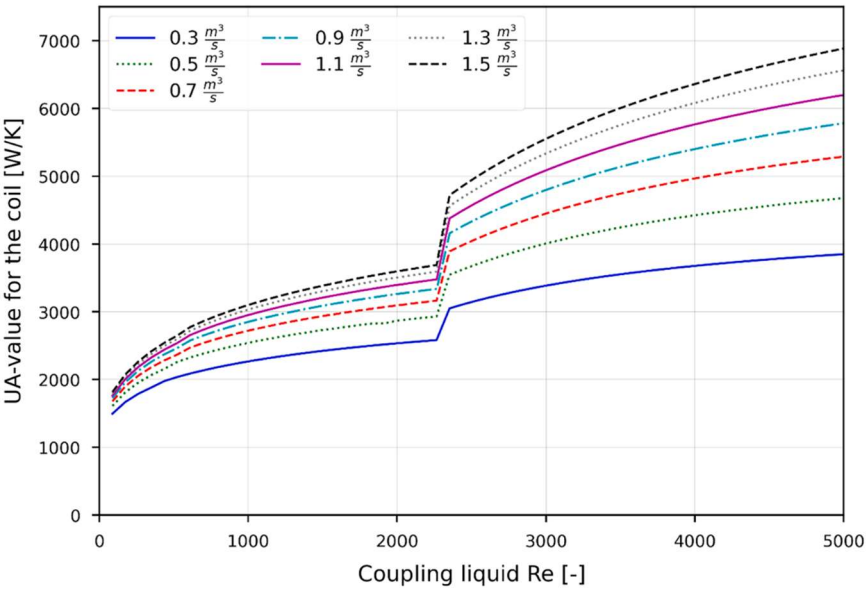

Figure 2: The UA-value for the coil at different air flow rates and Reynold number with 37% ethylene glycol.
(Source, Mohammad Mahmoud (2022) [1])

The study also investigated the effect of glycol concentration on system effectiveness. The results, presented in Table 1 of the referenced paper [2], indicated that higher glycol concentrations tended to reduce the maximum effectiveness. This reduction was more evident at certain airflow rates, particularly around 0.5 m³/s. At lower concentrations, such as 10%, the variation of effectiveness with respect to the capacity flow ratio became more steady, and the optimal flow ratio approached unity. In comparison, increasing the glycol concentration to 30% or 40% moved the optimal capacity flow ratio further away from unity. These trends are illustrated in Figure 3, which reproduce the results from Appendix A of the study [2].

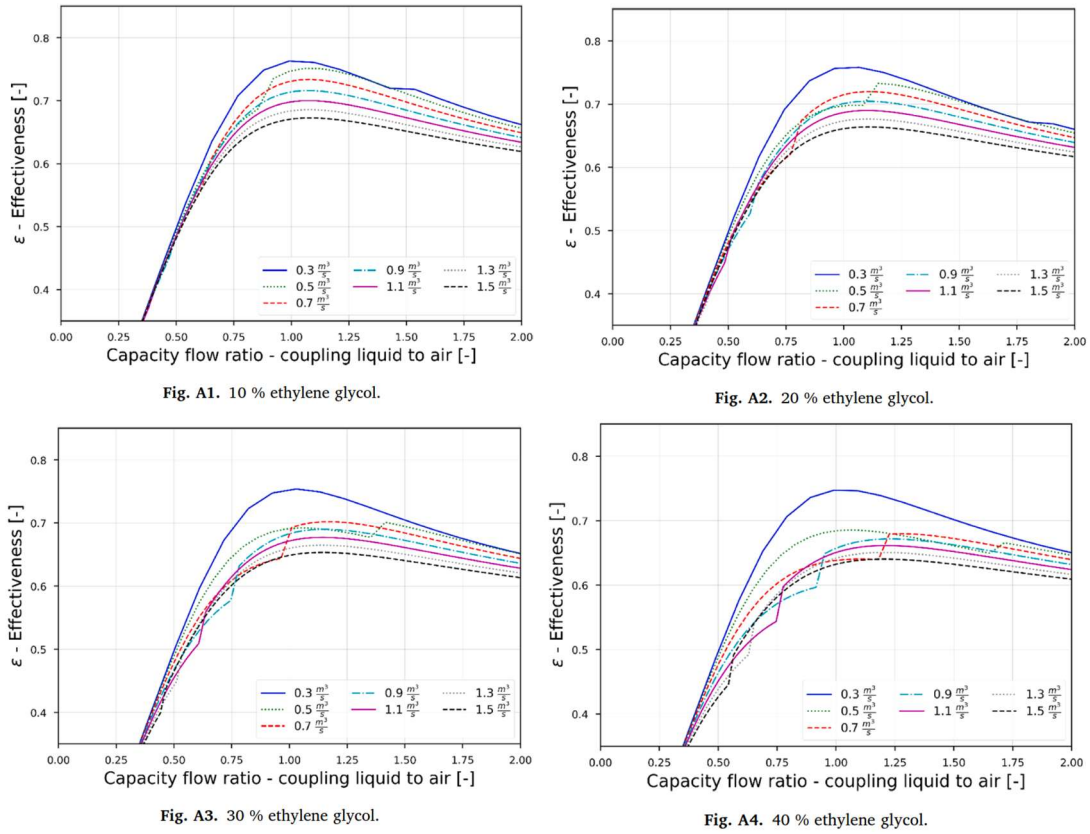

Fig. A1. 10 % ethylene glycol.

Fig. A2. 20 % ethylene glycol.

Fig. A3. 30 % ethylene glycol.

Fig. A4. 40 % ethylene glycol.

Figure 3: Effectiveness as a function of capacity flow ratio for different ethylene glycol concentrations.
(Source, Mohammad Mahmoud (2022) [1])

Another important variable examined in the study was the coupling liquid velocity, which was modified by changing the number of coil circuits. Reducing the number of circuits decreased the flow area, leading to an increase in both the velocity and Reynolds number of the coupling fluid. This change results in an earlier transition from laminar to turbulent flow, enhancing heat transfer. As a result, systems with fewer circuits achieved higher maximum effectiveness, as shown in Table 2 and Figures 10 and 11 of the referenced paper [2]. This trend was further confirmed by Appendix B, which presents the influence of circuit number on effectiveness across different capacity flow ratios [2].

Additionally, the study concluded that achieving turbulent flow does not always result in the highest effectiveness. Instead, there is an optimal balance between fluid velocity, flow rate and the resulting thermal gradients. These findings extend and add to earlier research by Holmberg [13], Forsyth and Besant [15,16], and Balen [18], highlighting that maximum effectiveness can be achieved within the laminar flow regime under certain conditions, particularly when using glycol-water mixtures and operating under VAV systems.

Furthermore, the study concluded that no single capacity flow ratio is universally optimal. The ideal ratio depends on the interaction between airflow rate, coupling liquid composition, and coil circuit design [2]. These insights make a significant contribution to fluid flow optimization in RAHRS and provide a strong foundation for future experimental and control-oriented studies.

1.3.4 Liquid flow rate control

Effective control of the liquid flow rate in run-around heat recovery systems is essential for optimizing system performance, particularly under varying operational conditions such as temperature fluctuations, changes in fluid properties and variations in airflow rates. This section reviews prevailing control methods, presents the governing equations used in existing systems, discusses their limitations and introduces a novel temperature-based control method proposed in recent studies [1].

Conventional methods of liquid flow rate control

Conventionally, liquid flow rate control in RAHRS involves matching the liquid-side heat capacity rate with the air-side heat capacity rate, a concept referred to as balanced heat capacity. This approach requires measuring various parameters, including the volumetric flow rates of both air and liquid, along with their respective densities and specific heat capacities. The liquid-side flow rate is typically determined by measuring the pressure drop across one of the HX coils or an orifice plate and correlating it with the flow rate using calibration curves or models [1].

However, this method is subjected to significant uncertainty. The thermophysical properties of heat transfer fluids, particularly glycol-water mixtures, vary with temperature and glycol concentration. For instance, increasing the glycol concentration or lowering the fluid temperature decreases specific heat capacity and increases viscosity. This creates a paradox [1]: while the system requires a higher flow rate to maintain thermal performance, the increased viscosity raises the pressure drop, which the control system may incorrectly interpret as higher flow. As a result, the pump speed is reduced, leading to a lower actual flow rate.

The selection of glycol type (e.g., ethylene glycol for colder climates due to its lower freezing point and propylene glycol for warmer environments due to its non-toxicity) and its concentration significantly influence fluid behaviour. For instance, at 20°C, ethylene glycol shows a 35% increase in dynamic viscosity when the concentration rises from 30% to 40% [1]. This change must be considered in control strategies to prevent performance degradation.

Another critical factor is the freezing point of the fluid, which depends on the glycol concentration. While several guidelines recommend adjusting the glycol concentration based on the burst temperature to prevent system damage during stagnation, others emphasize avoiding operational issues, such as slush formation, during sub-zero active conditions [1].

Equations for control methods

Prevailing control strategies typically use a pump control approach based on a heat balance method. A balanced heat capacity rate is achieved when the heat capacity ratio (denoted as Xv) equals one. This ratio is determined by the specific heat and mass flow rate (determined using volumetric flow and density) of both the liquid and supply air sides.

$$X_V = \frac{V_a \ \rho_a \ Cp_a}{V_l \ \rho_l \ Cp_l}$$

Drawbacks of conventional control methods

Prevailing flow-based control systems are subjected to performance degradation, particularly when changes in glycol concentration are not properly considered. The study by P. Filipsson [1] demonstrated that increasing the ethylene glycol concentration from 30% to 50% without adjusting the control parameters resulted in a series of significant issues. The first issue was a reduction in heat transfer efficiency, caused by an increase in viscosity and a decrease in the thermal conductivity of the glycol mixture. This hindered the system's ability to transfer heat effectively.

The second issue was an increase in the required liquid flow rate, which resulted from the decreased specific heat capacity of the glycol. Despite this, the control system misinterpreted the increased pressure drop, caused by higher viscosity, as an indication of higher flow. Consequently, the system reduced the pump speed, resulting in a lower actual flow rate. Simulation results indicated that failing to account for viscosity increases could lead to significant reductions in heat recovery efficiency. While minor decreases in effectiveness may be acceptable when the heat capacity balance is not perfectly maintained, the largest losses occurred when the system failed to recognize and adjust to changes in fluid properties [1].

Proposed control method based on temperature measurements

In response to the limitations of conventional methods, a novel control strategy was proposed by P. Filipsson [1], based exclusively on temperature measurements. This approach determines the heat capacity ratio by measuring the terminal temperature differences across one or both coils, eliminating the need for pressure or flow measurements and the associated uncertainties.

When air flow rates are balanced, temperature measurements from only one coil are sufficient (denoted as Xt). However, when air flow rates are unbalanced, temperature measurements from both the supply and exhaust air coils are required. The average temperature ratio across both coils (denoted as Xt,2) offers a more comprehensive indication of the RAHRU thermal balance [1].

This method offers several advantages:

- It automatically compensates for changes in fluid properties such as viscosity and specific heat capacity.
- It can adapt to latent heat transfer scenarios, where condensation on the exhaust air coil increases heat recovery potential.
- It enables performance monitoring by detecting deviations indicative of fouling or coil imbalance.
- It identifies unintended air flow imbalances that could degrade system performance.

The simulation study validated the robustness of this approach under varying air flow rates and glycol concentrations, demonstrating its ability to maintain near-optimal heat transfer effectiveness, where conventional methods could be less effective [1].

The new control system

Developing on the temperature-based approach, the new control system incorporates real-time temperature monitoring at the coil inlets and outlets, using primary heat transfer equations to guide pump control. This reduces dependence on fluid-specific measurements and minimizes the impact of sensor uncertainty and calibration drift.

This system represents a significant advancement in RAHRS control by shifting from rigid, flow-based methods that depend on multiple parameters to a more adaptive, temperature-based approach with fewer data requirements. This transition enables the integration of fault detection, automatic balancing, and energy efficiency improvements through intelligent control algorithms based on directly measured thermal performance instead of indirectly inferred fluid behaviour [1].

1.3.5 Variation of properties of ethylene glycol with temperature and concentration

As discussed in the previous subsection, conventional liquid flow rate control methods are significantly influenced by the thermophysical properties of the working fluid, typically an ethylene glycol and water solution, which vary with both glycol concentration and temperature. The most relevant properties for optimizing run-around heat recovery systems include density, viscosity, thermal conductivity, and specific heat capacity. Among these, thermal conductivity and viscosity directly affect the effectiveness of heat transfer and the regulation of liquid flow rate, respectively. In addition, density and specific heat capacity determine the liquid-side heat capacity rate, which must be appropriately matched to the air-side in order to optimize overall heat recovery performance.

The relevant thermophysical properties of ethylene glycol, a commonly used working fluid in cold climates, are presented in Figures 4 to 7 for three different average temperatures representative of this environmental context. The property data used to generate these figures were obtained from the ASHRAE Handbook (2021) [19].

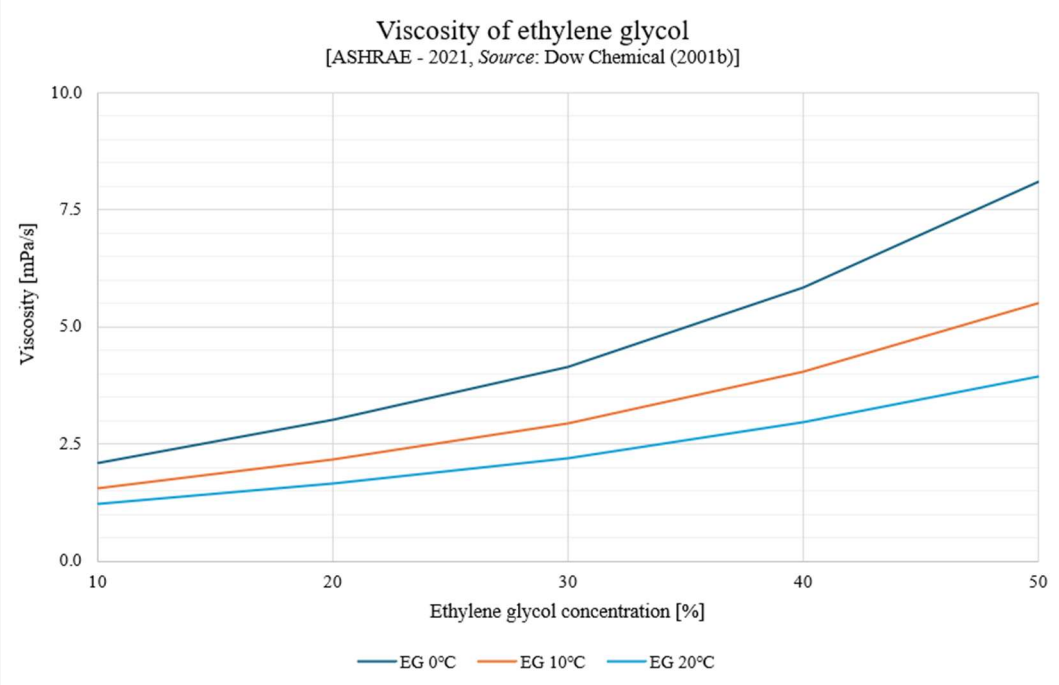

Figure 4: Viscosity of ethylene glycol at three different temperatures as a function of concentration.

According to the Figure 4, the viscosity of the ethylene glycol solution increases with higher glycol concentration, and this effect becomes more pronounced at lower temperatures. Conversely, as temperature increases, the viscosity of the solution decreases.

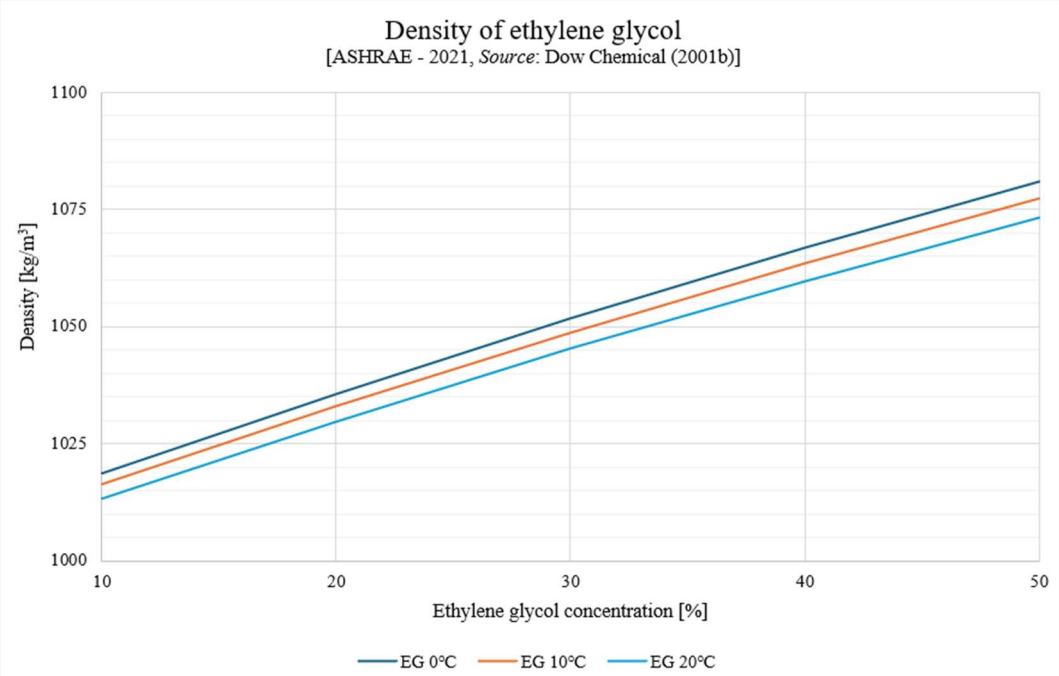

Figure 5: Density of ethylene glycol at three different temperatures as a function of concentration.

According to Figure 5, the density of the ethylene glycol solution increases with higher glycol concentration. However, unlike viscosity, this increase is relatively moderate. Conversely, as temperature rises, the density of the solution decreases.

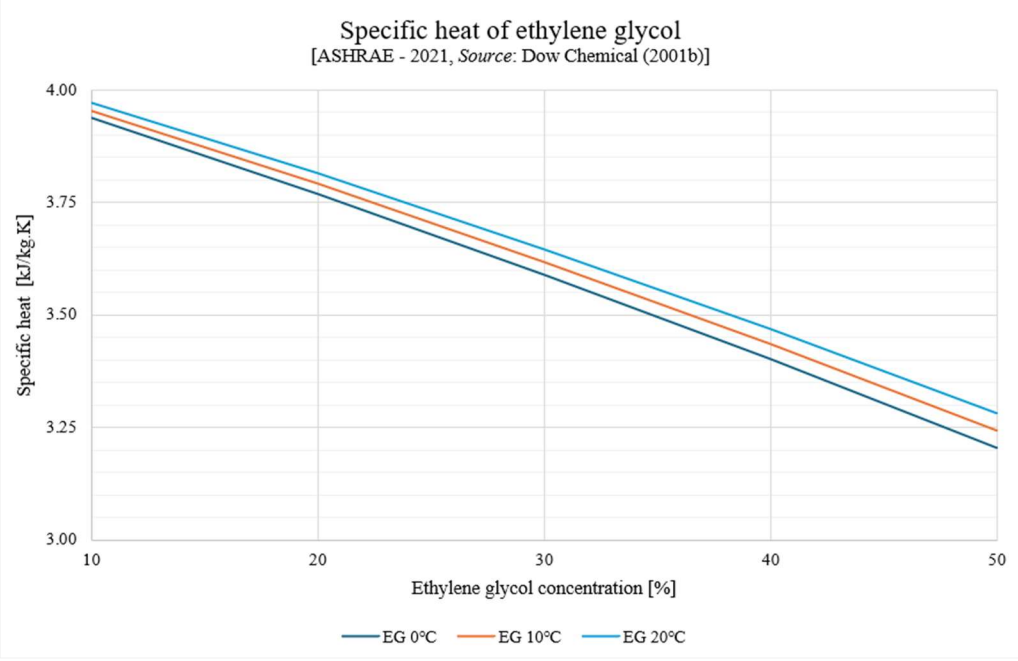

Figure 6: Specific heat of ethylene glycol at three different temperatures as a function of concentration.

According to Figure 6, the specific heat capacity of the ethylene glycol solution decreases significantly with increasing glycol concentration. In contrast, as temperature rises, the specific heat capacity increases moderately.

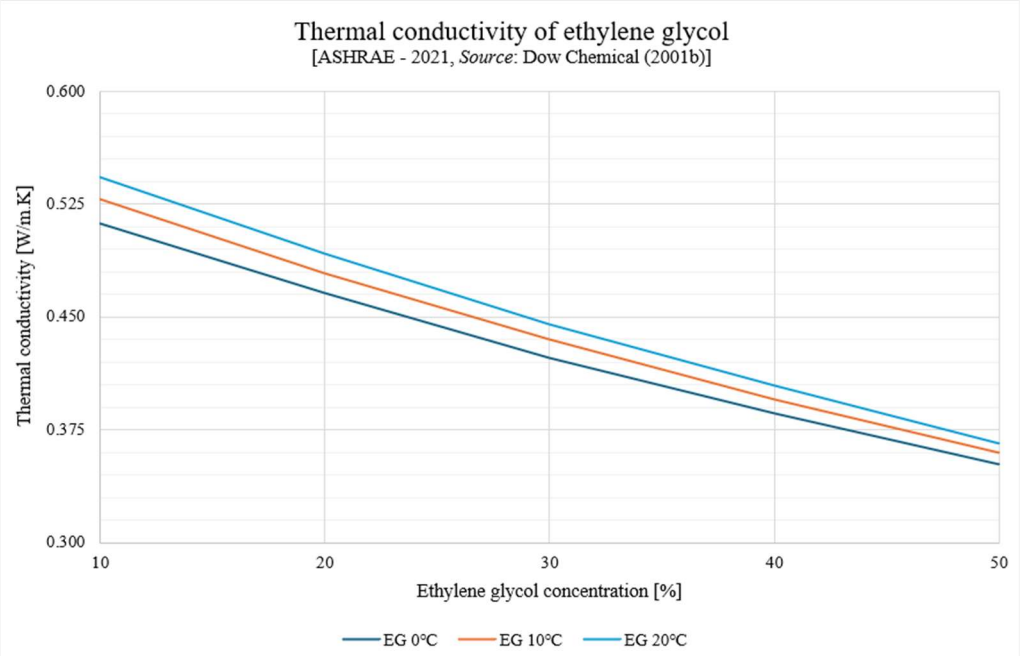

Figure 7: Thermal conductivity of ethylene glycol at three different temperatures as a function of concentration.

According to Figure 7, the thermal conductivity of the ethylene glycol solution decreases significantly with increasing glycol concentration. Meanwhile, as temperature increases, the thermal conductivity demonstrates a slight increase.

2. Laboratory Unit

2.1 Lab test rig

The ventilation test rig used to evaluate the novel temperature-based control system of the run-around heat recovery unit is a double-deck (two-tier) AHU. The rated airflow capacity of each air stream is 1.0 m³/s (1000 l/s), with static pressure drops of 580 Pa in the supply stream and 520 Pa in the extract stream, in accordance with the standard components.

The general arrangement of the AHU, indicating its main components, is presented in Figure 8 below.

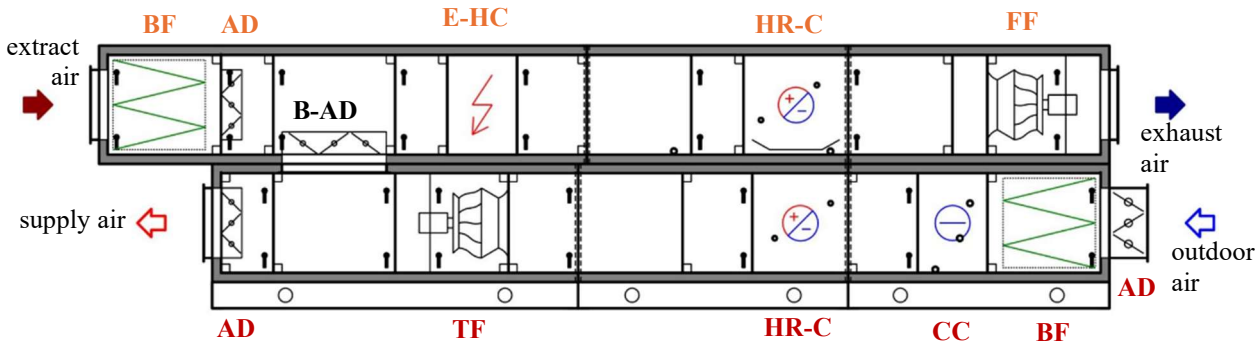

AD	: air damper	E-HC	: electric heater coil
B-AD	: bypass air damper	FF	: exhaust air fan
BF	: bag filter (air filter)	HR-C	: heat recovery coil
CC	: cooling coil	TF	: supply air fan

Figure 8: General arrangement of the AHU used for lab testing.
(Source, Product data sheet of AHU eQ, FläktGroup, 2020 [20])

The supply air stream deck of the AHU consists of the following components in sequence; outdoor air intake, outdoor air damper, air filter assembly, cooling coil, heat recovery coil, supply air fan, and supply air damper, with a flange connection at the supply air delivery end. Similarly, the extract air stream deck includes the following components; extract air intake, air filter assembly, air damper, electric heater coil, heat recovery coil, extract air fan, and a flange connection at the exhaust air delivery end. Additionally, a horizontal bypass air damper, labelled as B-AD in Figure 8, is installed between the supply and extract air decks. This damper allows the supply air to bypass directly into the extract air stream when required for experimental purposes, ensuring that test air temperatures do not negatively impact the laboratory indoor environment.

The overall dimensions of the AHU are 5.8 m in length, 1.2 m in width, and 1.5 m in height. Photos taken in the laboratory AHU are presented in Figure 9 below.

Figure 9: Test tig photos taken in the laboratory.

Supply and extract fans:

Both the supply air fan and extract air fan are equipped with variable frequency drive (VFD) electric motors, allowing for adjustable airflow rates in both streams based on experimental requirements. The rated airflow capacity of each fan is 1000 l/s, in accordance with the standard components mentioned above.

Additionally, the fan assembly is designed for high electrical efficiency, with a specific fan power (SFP) of 1.49 kW/(m^3/s) at the rated airflow rate.

However, the airflow rate of both the supply and extract fans can be adjusted between 0 l/s and 1500 l/s using the VFD unit, allowing for greater flexibility in experimental conditions.

Cooling coil:

A cooling coil with a capacity of 16.5 kW and a four-pass configuration is installed at the outdoor air intake to cool the incoming air before it passes through the heat recovery unit (HRU), as required for experimental purposes.

However, during the evaluation of the novel control system, the cooling coil was not utilized, as the outdoor air temperatures during the test period reflected average winter conditions, making its operation unnecessary.

Run-around heat recovery unit:

As shown in Figure 8, both air streams are equipped with heat exchange (HX) coils. The heat transfer capacity of the unit is 26 kW with a fluid flow rate of 0.36 l/s (1296 l/h) using a 30% ethylene glycol solution. The pressure drop across the HX coil at this rated fluid flow is approximately 125 kPa. Under these flow conditions, the rated efficiency of the RAHR unit is 67.1%.

Each HX coil consists of 64 fluid paths, constructed from 25 mm copper tubes with aluminium fins spaced at a 2 mm pitch. The liquid volume of each coil is 26 liters.

Electric air heater coil:

A step-controlled electric heater with a capacity of 24 kW is installed in the extract air stream to increase the extract air temperature. It ensures that the air reaches the required temperature range before entering the HX coil, in accordance with the set values. This allows for the adjustment of the extract air temperature according to indoor conditions, ensuring accurate simulation of different test conditions.

Pumping system of the RAHR unit:

The pumping system used to circulate the 30% ethylene glycol solution between the two heat exchangers consists of insulated copper pipes, a VFD driven vertical inline circulation pump, a pressure vessel, pressure gauges, thermometers, an automatic 3-way valve, a manual 3-way valve, a smart flow meter, and valves for purging, draining, and refilling. Figure 10 illustrates the pumping system installed in the laboratory.

Figure 10: Pumping system of the RAHRU, photos taken in the laboratory.

The circulation pump has a rated capacity of 3.0 m³/h (0.83 l/s) at a head of 38.3 m, with an efficiency of 57.3%. Equipped with a variable frequency drive, the pump allows for precise regulation of the liquid flow rate based on system requirements and control signals.

However, the liquid flow rate in the novel control unit is automatically adjusted based on the updated tuning parameters. The flow rate varies between a minimum of approximately 0.1 l/s and a maximum of 0.5 l/s, depending on the control signal from the new controller.

2.2 Arrangement of sensors and devices in the Novel control setup

Figure 11 illustrates the general arrangement of the sensors used for measurement and control, along with their locations within the RAHR system for the novel control setup.

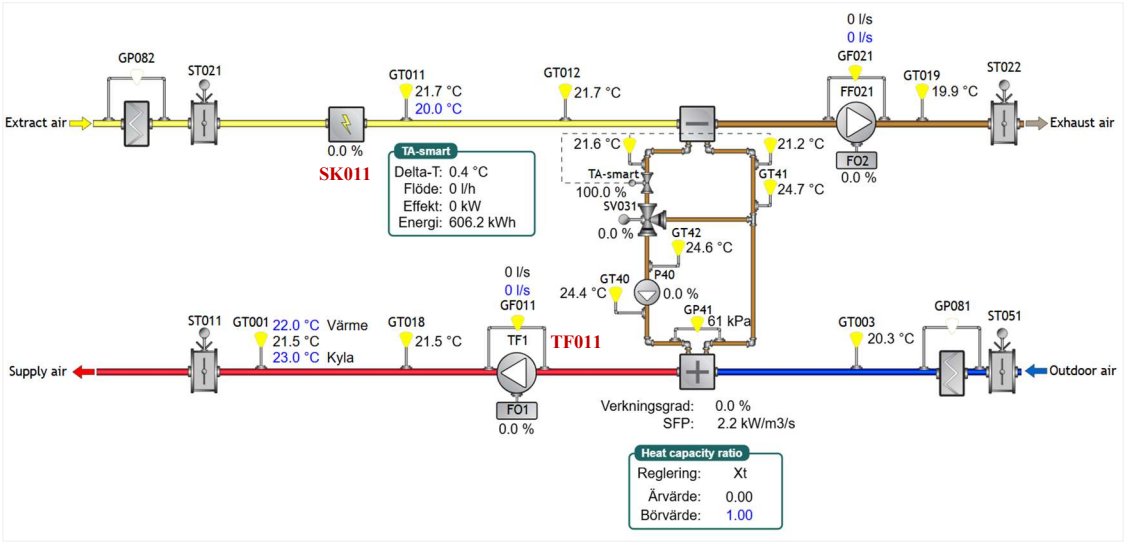

Figure 11: General arrangement of novel control setup.

Table 1 below provides a detailed list of sensors, including their labels, locations, functions, and relevant remarks regarding the novel control system of the RAHR unit.

Table 1: List of sensors and their functions.

Label	**Type / description**	**Location**	**Function and remarks**
FF021	extract air fan	inside extract air deck, between heat exchange (HX) coil and exhaust air damper	flow rate can be varied from 0 l/s to 1500 l/s
TF011 (TF1)	supply air fan	inside supply air deck, between HX coil and supply air damper	flow rate can be varied from 0 l/s to 1500 l/s
FO1	VFD drive supply air fan	inside the control panel	regulate the frequency based on the control signal
FO2	VFD drive extract air fan	inside the control panel	regulate the frequency based on the control signal
SK011	electric air heater	on extract air deck, between extract air damper and HX coil	regulate extract air temperature before entering to HX coil
P40	circulation pump VFD	on hydronic pipe circuit in warm water side, between the extract HX coil and supply HX coil	circulated the liquid flow and flowrate varies based on control signal
TA smart	2-way control valve with integrated ultrasonic flow meter	on liquid circulation pipe, in between extract heat exchanger and circulation pump	measure liquid flow rate and recovered energy (flow rate can be regulated)
GT018 (GT001)	temperature sensor (supply air)	inside supply air deck, between supply air damper and supply air fan	measure supply air temperature after fan
GT003	temperature sensor (outdoor air)	inside supply air deck, between filter assembly and HX coil	measure outdoor air temperature

Label	Type / description	Location	Function and remarks
GT011	temperature sensor (extract air after heater)	inside extract air deck, after heater coil	measure extract air temperature after heater coil
GT012	temperature sensor (extract air before HX coil)	inside extract air deck, between electric heater coil and HX coil closer to HX coil	measure extract air temperature before HX coil
GT019	temperature sensor (exhaust air after fan)	inside extract air deck, after extract air fan (between extract fan and exhaust air damper)	measure exhaust air temperature after fan
GT40	liquid temperature sensor (warm side)	on hydronic pipe after circulation pump (P40)	measure warm water temperature before entering to the supply air HX coil
GT41	liquid temperature sensor (cool side)	on hydronic pipe after supply air HX coil	measure cool water temperature after supply air HX coil
GT42	liquid temperature sensor (warm side)	on hydronic pipe after extract air HX coil	measure warm water temperature after extract air HX coil
GF011	differential pressure sensor (supply fan)	in supply air deck, across the supply air fan (TF011)	measure diff. air pressure across the supply air fan and control the supply air flow rate
GF021	differential pressure sensor (extract fan)	in extract air deck, across the extract air fan (FF021)	measure diff. air pressure across the extract air fan and control the extract air flow rate
GP41	differential pressure sensor (liquid)	on hydronic pipe system, across the supply air HX coil	measure diff. air pressure across the supply air HX coil
GP081	differential pressure sensor (air filter)	in supply air deck, across the supply air filter (F7 bag filter)	measure diff. air pressure across the supply air filter
GP082	differential pressure sensor (air filter)	in extract air deck, across the extract air filter (F7 bag filter)	measure diff. air pressure across the extract air filter
ST011	on-off damper actuator (supply air)	in supply air deck, on supply air damper	open-close control: supply air damper
ST021	on-off damper actuator (extract air)	in extract air deck, on extract air damper	open-close control: extract air damper
ST022	manual damper (exhaust air)	in extract air deck, at exhaust air end	manually open-close: exhaust air damper
ST051	on-off damper actuator (outdoor air)	in supply air deck, on outdoor air damper	open-close control: outdoor air damper
SV031	automatic 3-way valve (bypass water-glycol from warm side to cool side)	on hydronic pipe system as indicated, from warm side to cool side	in this experiment not used bypass (0% bypass)

The control system of the RAHR unit integrates various sensors and control devices to monitor and regulate airflow, temperature, pressure, and fluid flows, ensuring optimal system performance.

Fan control:

The airflow control is managed through the supply air fan (TF011) and extract air fan (FF021), both of which have variable flow rate capabilities ranging from 0 l/s to 1500 l/s. The operation of these fans is controlled by variable frequency drives (FO1 and FO2), which regulate their speed based on the system's airflow requirements. To ensure precise control of airflow, differential pressure sensors (GF011 and GF021) are installed across the supply and extract fans, respectively, providing real-time feedback for maintaining the desired air flow rates.

Hydronic circulation system:

The hydronic system is responsible for circulating a 30% ethylene glycol solution between the heat exchangers to facilitate heat recovery. A variable frequency-driven circulation pump (P40) regulates the liquid flow rate based on control signals. The system includes liquid temperature sensors (GT40, GT41, and GT42) to monitor the water-glycol temperature at critical points: GT40 measures the warm-side temperature before entering the supply air heat exchanger, GT2 measures the temperature after the extract air heat exchanger, and GT41 measures the cooled liquid temperature after passing through the supply air heat exchanger. Additionally, a differential pressure sensor (GP41) is positioned across the supply air heat exchanger to evaluate hydronic performance, while a smart flow meter (TA smart) continuously measures the water-glycol flow rate within the circuit.

TA Smart flow measuring device:

The TA smart is an ultrasonic flow measurement device that provides accurate flow measurements, even at low flow rates. Accurate monitoring of the ethylene glycol solution's flow rate is essential for evaluating heat recovery performance, and the TA Smart ensures reliable data collection for effective system assessment. This precision ensures the RAHR unit operates efficiently across varying ventilation rates.

In addition to flow measurement, the TA Smart continuously monitors valve position, temperature differences using sensors installed around the extract heat exchanger unit, and the recovered heating power and energy across the extract heat exchanger. This comprehensive data collection offers valuable insights into system performance.

Further, the TA smart allows for manual adjustments to the flow rate when necessary, providing flexibility under various testing conditions.

Temperature measurement and control:

Air temperature regulation is a key aspect of the RAHR system's control strategy. Several temperature sensors are installed at different locations to monitor air temperatures throughout the process. GT018 (GT001) measures the supply air temperature before it enters the room or extract stream (measures the supply air temperature immediately after the fan). Similarly, the GT019 sensor tracks the exhaust air temperature after the extract fan. To monitor the outdoor air conditions before entering the system, GT003 is installed at the inlet of the supply air deck, just before the heat exchanger coil.

Extract air temperature is monitored by GT011 and GT012, both of which are positioned downstream of the electrical heater (SK011). GT011 is installed immediately after the heater to measure the temperature increase due to heating, while GT012 is placed closer to the heat exchanger coil to track the extract air temperature before it enters the heat recovery unit. These

sensors ensure that the extract air temperature is maintained within the desired range according to the control setpoints.

This comprehensive sensor integration, as detailed in Table 1 and depicted in Figure 11, ensures precise control of airflow rates, temperature regulation, and fluid circulation, enabling an effective evaluation of the novel control strategy under varying experimental conditions.

2.3 Control methods used in the run-around heat recovery unit

As indicated in section 1.2 (Literature review), the conventional method for controlling the liquid flow rate in a run-around heat recovery unit is based on the thermophysical properties and flow rates of both the air and liquid media, along with the pressure drop across the liquid side. The control strategy aims to balance the heat capacity flow rates of the air and liquid streams to optimize the heat recovery effectiveness of the system. This is typically achieved by adjusting the pump speed through a variable frequency drive (VFD) based on the following heat capacity equation [1] .

Equation 1

$$V_l = \frac{V_a \ \rho_a \ Cp_a}{\rho_l \ Cp_l}$$

Based on equation 1, the liquid flow rate V_l is determined to regulate the pump speed. The parameters in this equation are defined as follows: V_a is airflow rate, ρ_a is air density, Cp_a is specific heat capacity of air, ρ_l is liquid media density and Cp_l is specific heat capacity of the liquid media.

Equation 1 assumes a balanced heat capacity rate, with a heat capacity ratio equal to one. Accordingly, the heat capacity ratio based on flow rates, denoted as *Xv*, is expressed in Equation 2 below.

Equation 2

$$X_V = \frac{V_a \ \rho_a \ Cp_a}{V_l \ \rho_l \ Cp_l}$$

For the supply air heat exchange coil, the heat balance equation can be written as equation 3 below.

Equation 3

$$V_a \ \rho_a \ Cp_a \ (t_{sa} - t_{oa}) = V_l \ \rho_l \ Cp_l \ (t_{l,w,2} - t_{l,c})$$

The parameters in above equation are defined as follows: t_{sa} is supply air temperature, t_{oa} is outdoor air temperature and $t_{l,w,2}$ is warm side liquid temperature after the pump, and $t_{l,c}$ is cold side liquid temperature.

Considering Equations 2 and 3, for a balanced ventilation system, the heat capacity ratio based on temperature, *Xt* can be expressed as Equation 4 below.

Equation 4

$$X_t = \frac{t_{sa} - t_{oa}}{t_{l,w,2} - t_{l,c}}$$

Accordingly, Xv and Xt represent the same heat capacity ratio, however, their calculation approaches differ. Xv is determined using the flow rates and thermophysical properties of both air and liquid media, while Xt is derived entirely from temperature measurements. Based on Equation 4, Xt can be calculated without the need for flow rate or thermophysical property data. In dynamic systems, accurately capturing these properties is challenging. Additionally, reliable flow measurement requires precision flow meters, which are expensive [1].

Using Xt for control provides a more practical and robust approach, as it avoids dependence on variable fluid properties and eliminates the need for a precision flow meter. Considering these advantages, the implemented novel control unit regulates the RAHR system based on Xt, using temperature-based heat capacity ratio regulation.

2.4 Novel control system

The proposed novel control system is designed based on temperature measurements in air streams and liquid media, in contrast to the previous control approach, which depend on thermophysical properties and flow rates.

In the new control system, the flow rate of the working fluid (30% ethylene glycol) is adjusted to achieve optimal system effectiveness based on the heat capacity ratio, Xt, which is calculated from temperature measurements. This ratio is derived from the measured temperature difference between the air stream and the liquid medium across the supply air heat exchanger coil. The control method incorporates predefined set values that consider airflow rates. A single-line closed-loop control diagram representing the Xt-based regulation is shown in Figure 12 below.

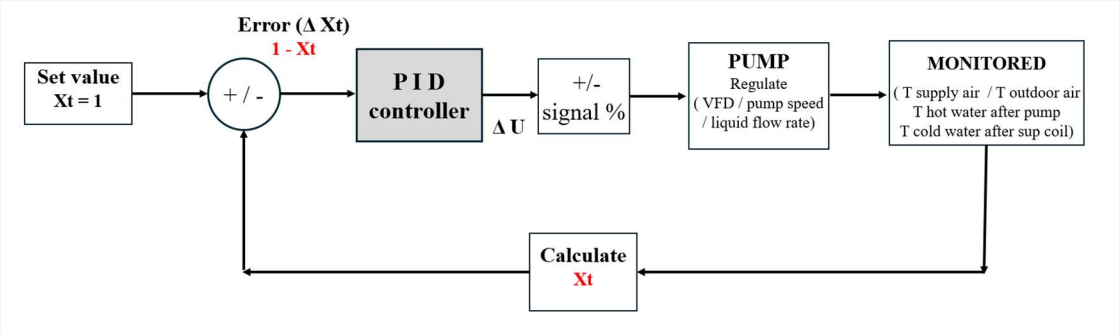

Figure 12: Control diagram of the Xt-based regulation system.

The heat capacity ratio, Xt, is calculated based on the temperatures measured around the supply air heat exchanger, as defined in Equation 4. If Xt exceeds the setpoint value of 1 (Xt = 1), the controller adjusts the system to reduce the liquid flow rate. Conversely, if Xt is below the setpoint, the controller increases the liquid flow rate.

This novel control system continuously monitors and regulates parameters based on experimental requirements. The system is managed through a web-based application developed specifically for this control approach by Sustainable Intelligence (SI).

New control unit:

A new control unit, together with the necessary devices and accessories, was installed within the existing control panel and integrated with the AHU and RAHR system panels and the field devices.

The installed controller is the REGIN EXOcompact Ardo, model XCA283W-4. This compact controller features 28 I/O points, an external display unit, and supports multiple communication protocols, including EXOline, Modbus, BACnet, and EFX. It also provides web server access, enabling remote monitoring and control. Field photos of the controller and its display unit are shown in Figure 13 below.

Figure 13: Field photos of the controller and its display unit.

Web application for remote access, monitoring and controlling:

The web application for remote access, monitoring, and control of the novel control unit is provided by Sustainable Intelligence (SI). It integrates with the ARRIGO BMS to enable the operation of the run-around heat recovery unit through a web-based interface.

The following Figures 14 to 16 present screenshots of the Windows web application, including the dashboard, the RAHR unit monitoring and control panel, and the trend analysis interface.

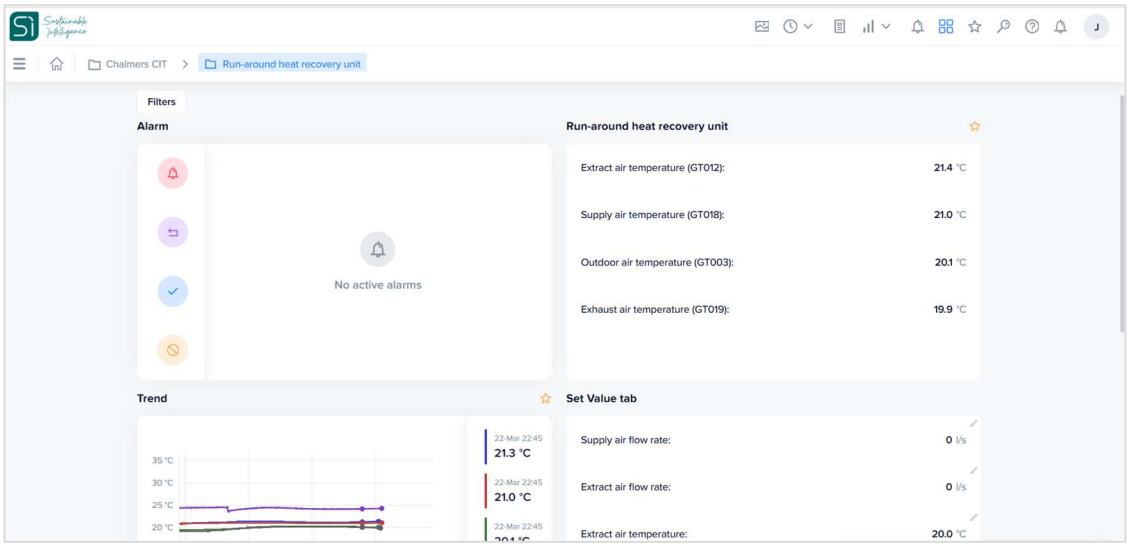

Figure 14: Dashboard interface of the web application.

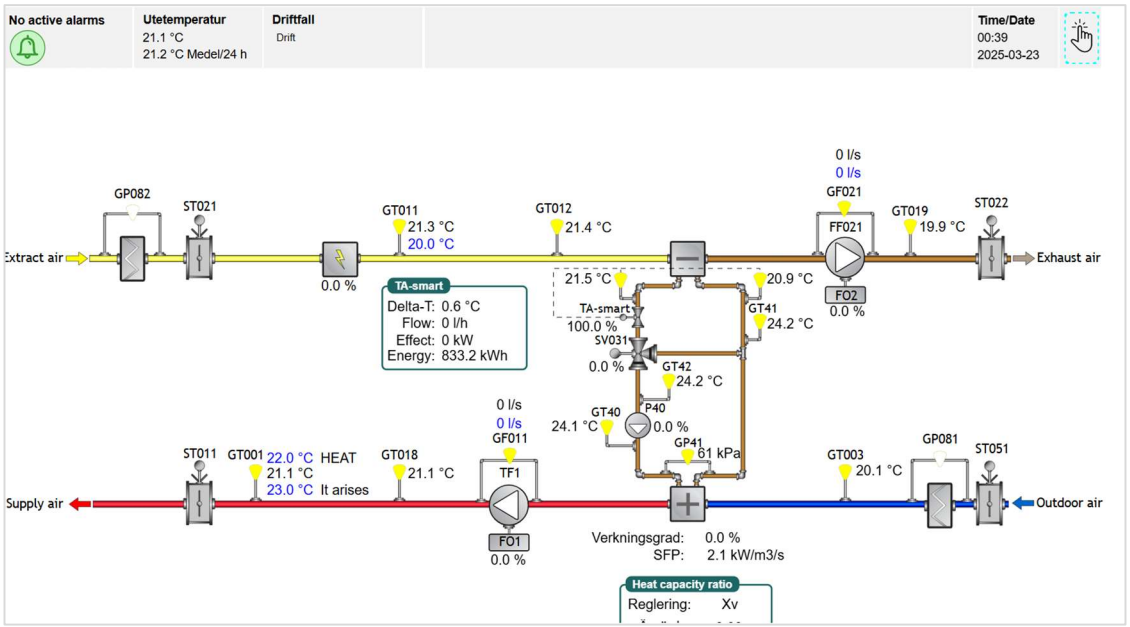

Figure 15: Web application interface for monitoring and control of the run-around heat recovery unit.

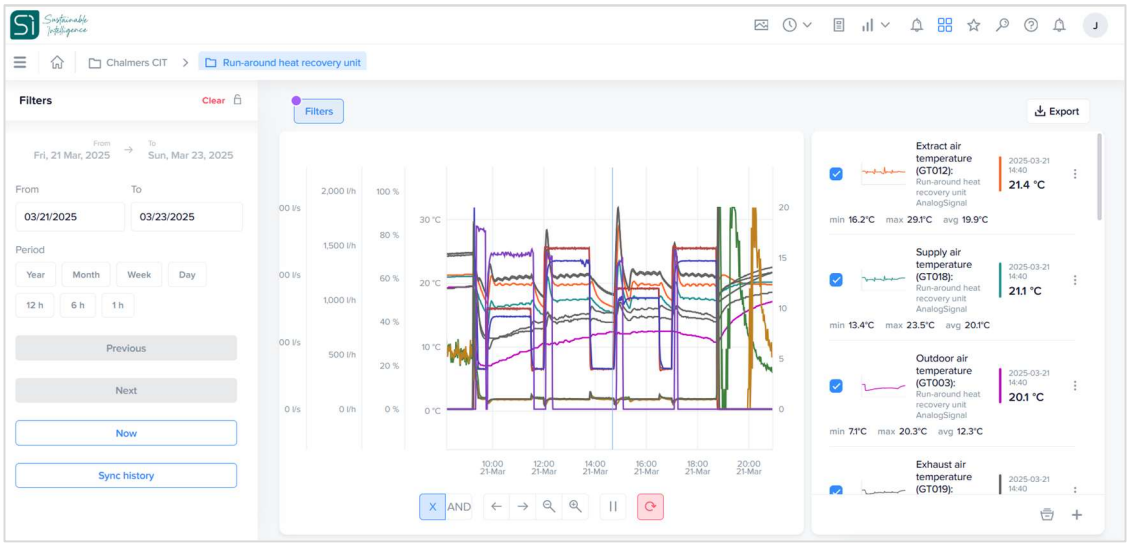

Figure 16: Web application interface for the trend analysis window.

Controllable parameters:

Figure 17 below shows the controllable parameters, highlighted in light blue, on the web application's monitoring and control interface. These parameters can be adjusted according to different test requirements.

The primary controllable parameters used in the testing include the supply and extract air flow rates, extract air temperature (adjusted using electrical heater coil), and the parameters within the heat capacity ratio window. Further details regarding heat capacity ratio window are discussed below, along with the relevant figures.

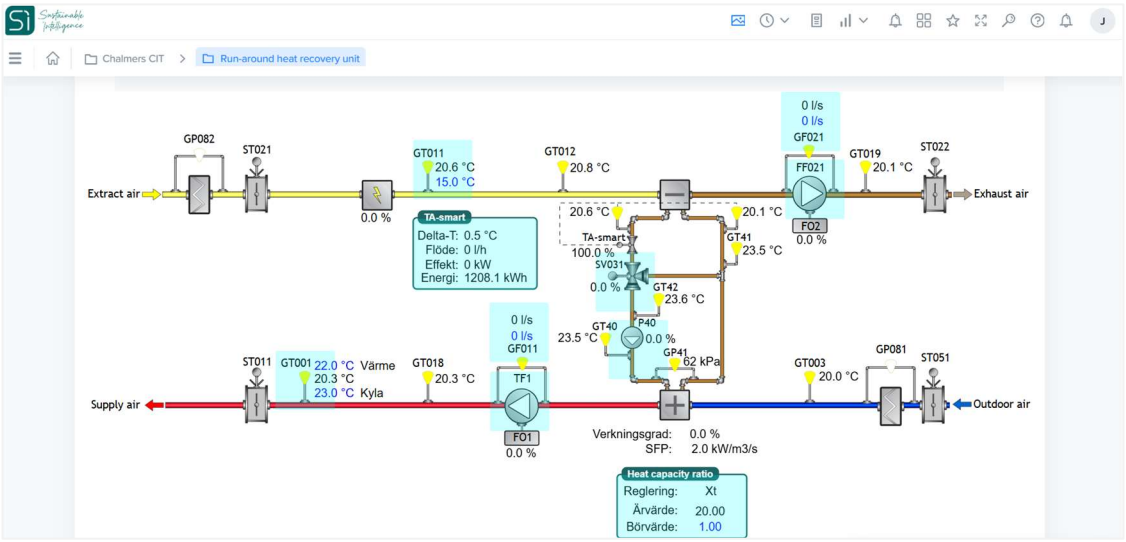

Figure 17: Controllable parameters on the web application's monitoring and control interface.

Additionally, the output of the TA valve, specifically the valve opening position (expressed as a percentage), can be manually adjusted using set points. During the tests conducted in this thesis, the valve opening was set to 100%, and the fluid flow rate in the circulation system was entirely controlled by the circulation pump, based on control signals from the selected regulation method.

Heat capacity ratio window:

Figure 18 illustrates the heat capacity ratio window, which includes the main parameter selection tabs required for regulating the novel control unit.

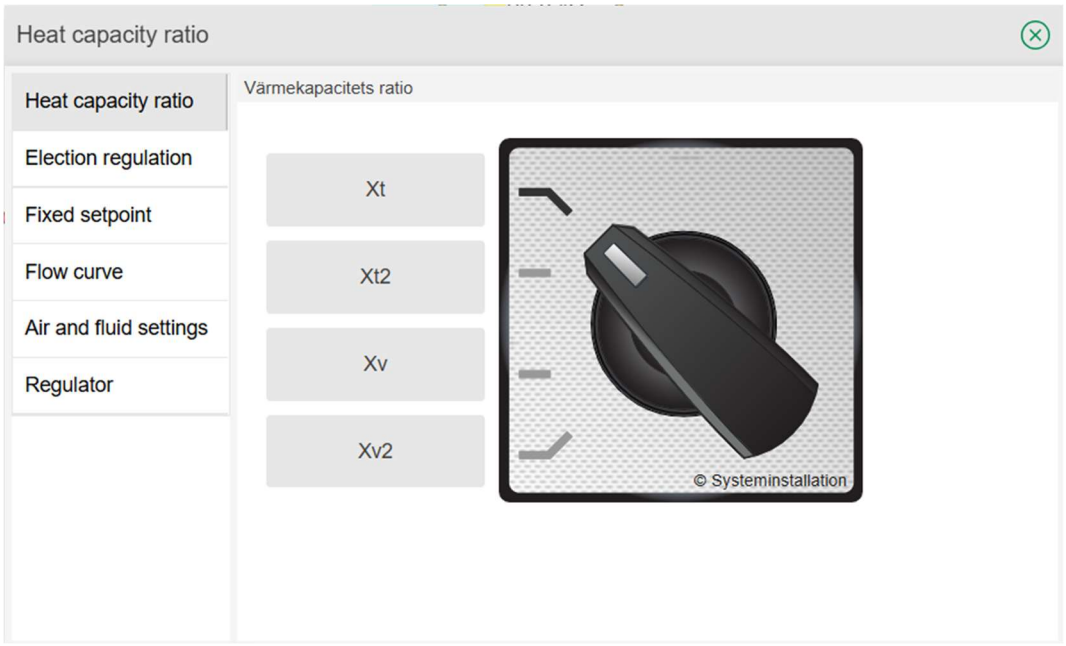

Figure 18: Heat capacity ratio window on the web application interface.

The heat capacity ratio window includes several key tabs for configuring the control system. These tabs consist of the heat capacity ratio selection tab, the setpoint input tab, and the air and fluid settings tab, where the thermophysical properties of the air and liquid are entered,

particularly important for flow-rate-based regulation (Xv). Additionally, the regulator tab allows the input of appropriate PID values, based on the selected regulation method and airflow rates. These tabs are illustrated in Figures 19 to 21 below.

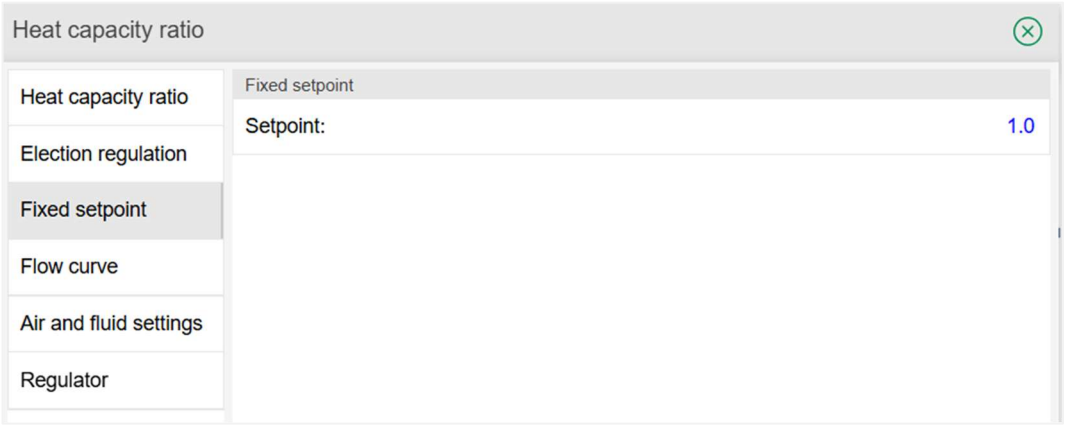

Figure 19: Fixed setpoint tab on the web application interface.

The fixed setpoint tab is used to define the desired value for the selected regulation option. This setpoint represents the heat capacity ratio and is typically set to 1 to achieve maximum system effectiveness. However, it can be adjusted to other positive values depending on the specific requirements of the test.

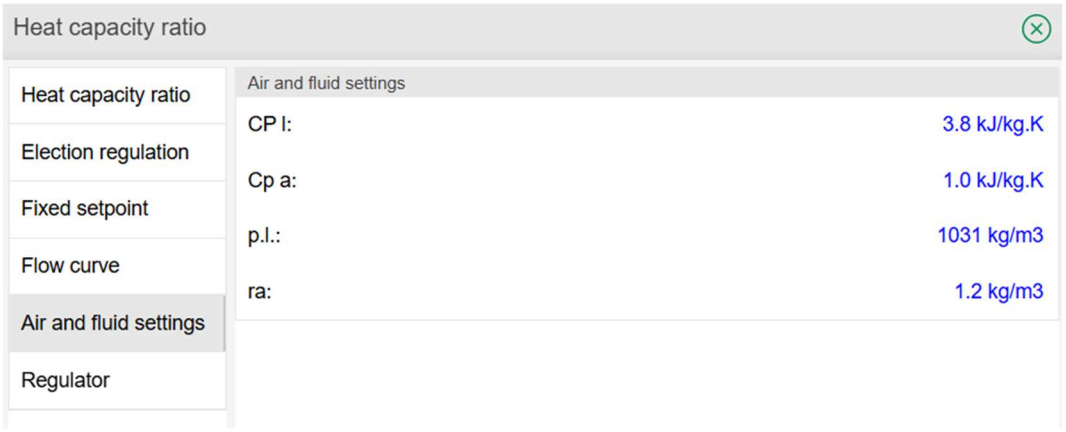

Figure 20: Air and fluid properties tab on the web application interface.

The air and fluid properties setting tab enables the input of the average thermophysical properties of the air and working fluid media. These properties are determined based on the average temperature observed during the testing phase. This information is essential when selecting flow-rate-based regulation methods, Xv and Xv2, as it ensures accurate control of the system in relation to the fluid media properties.

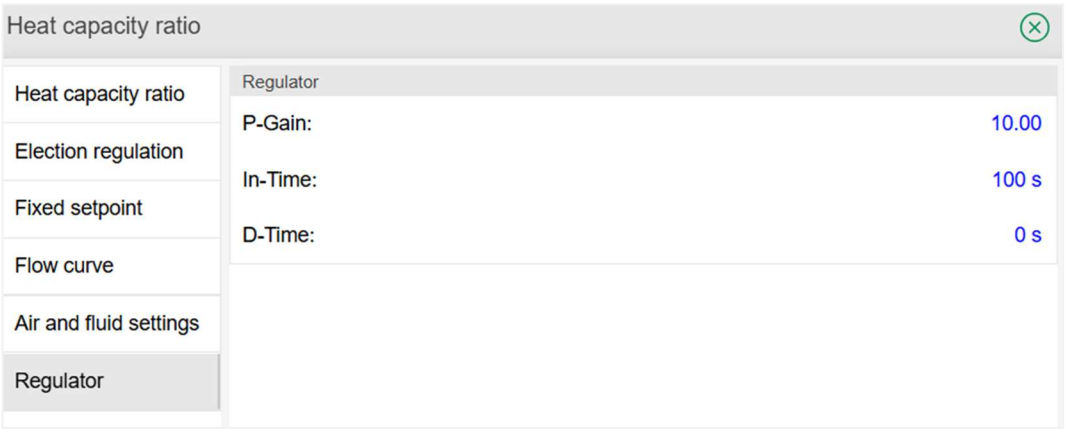

Figure 21: Regulator tab used set the PID value.

The regulator tab allows for the input of PID values, which are essential for optimal system performance. As the derivative (D) value is always set to 0 due to inherent signal noise, it is crucial to select appropriate proportional (P) and integral (I) values. These PI values vary for each test, depending on the selected regulation method and air flow rates. Additionally, the PI values must be manually entered for different test scenarios.

Regulation options:

As illustrated in Figure 18 above, the heat capacity ratio window presents four different regulation options, each designed to control the operation of the novel control unit under different system conditions. The primary regulation option, referred to as Xt, is based on temperature measurements obtained from the supply HX coil. This regulation method is specifically designed for systems with balanced air flow rates. It aims to optimize the performance of the RAHR system by maintaining an optimal heat capacity ratio, based on the measured temperature differences.

In addition to Xt, the system includes Xt2, which is designed for conditions with unbalanced airflows. As Xt, Xt2 is also based on temperature measurements, but it accounts for differences in airflow rates between the supply and exhaust air streams. Xt2 is developed by considering the average heat recovery effectiveness of both the supply and exhaust heat exchanger coils.

The third and fourth regulation options, Xv and Xv2, are developed based on flow-rate methods, focusing on adjusting the liquid flow rate to maintain a balanced heat capacity ratio. Xv is used for systems with balanced ventilation systems. In contrast, Xv2 is specifically designed for systems with unbalanced ventilation.

Each of these regulation options is governed by specific equations, which are essential for calculating the heat capacity ratio and determining the corresponding control actions. The following section presents the detailed equations used for each regulation method.

Equation used in each regulation method:

The equation used to calculate Xt based on temperature measurements is presented above as Equation 4. This calculation requires four temperature measurements across the supply air heat exchanger coil. The method is specifically designed for balanced ventilation systems, where the supply and exhaust airflow rates are equal. The corresponding control diagram is illustrated in Figure 12 above.

For Xt2 regulation, the equation used to calculate Xt2 based on temperature measurements is presented below as Equation 6. This regulation method is specifically designed for unbalanced ventilation systems. Accordingly, the Xt2 calculation requires seven temperature measurements across both the supply and extract air heat exchanger coils. The corresponding control diagram for the Xt2 regulation method is illustrated in Figure 22 below.

Equation 6

$$X_{t2} = \frac{(t_{ea} - t_{eha}) + (t_{sa} - t_{oa})}{t_{l,w,1} + t_{l,w,2} - 2t_{l,c}}$$

The parameters in above Equation 6 are defined as follows: t_{sa} is supply air temperature, t_{oa} is outdoor air temperature, t_{ea} is extract air temperature, t_{eha} is exhaust air temperature, $t_{l,w,1}$ is warm side liquid temperature before the pump, $t_{l,w,2}$ is warm side liquid temperature after the pump, and $t_{l,c}$ is cold side liquid temperature.

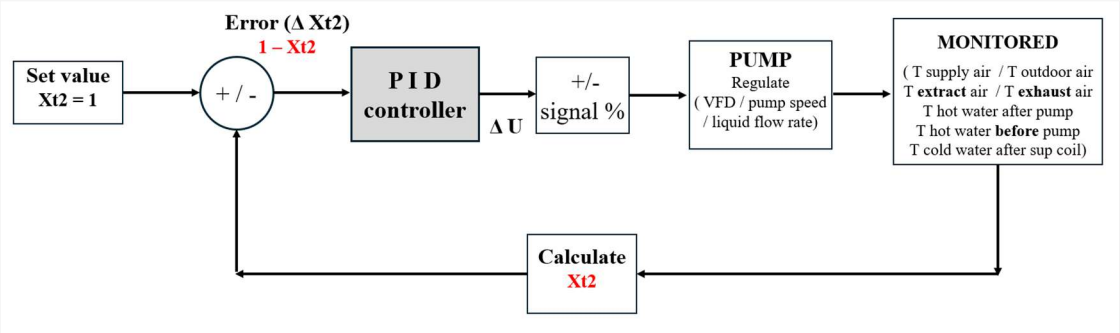

Figure 22: Control diagram for the Xt2 - based regulation system.

For Xv regulation, the equation used to calculate Xv based on flow rate measurements is presented below as Equation 7. This calculation requires two flow rate measurements across the supply air heat exchanger coil: the liquid flow rate and the supply air flow rate, as this regulation method is designed for balanced ventilation systems. Additionally, the thermophysical properties of the air and liquid media, determined based on the average operating temperature of the run-around heat recovery unit, are required. These properties are manually entered into the control unit, considering the test conditions. The corresponding control diagram is illustrated in Figure 23 below.

Equation 7

$$X_V = \frac{V_l \ \rho_l \ Cp_l}{V_{sa} \ \rho_a \ Cp_a}$$

The parameters used in Equations 7 and 8 are defined as follows: V_l is liquid flowrate, V_{sa} is supply air flowrate, V_{ea} is extract air flowrate ρ_a is air density, Cp_a is specific heat capacity of air, ρ_l is liquid media density and Cp_l is specific heat capacity of the liquid media.

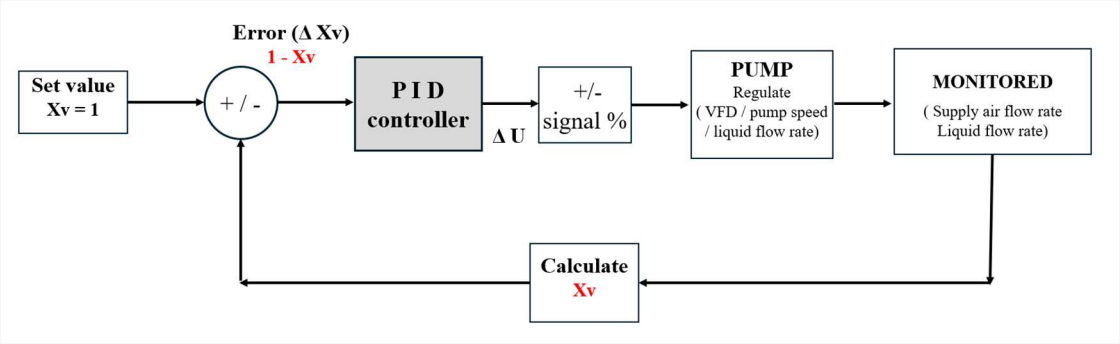

Figure 23: Control diagram for the Xv - based regulation system.

For Xv2 regulation, the equation used to calculate Xv2 based on flow rate measurements is presented below as Equation 8. This regulation method is specifically designed for unbalanced ventilation systems. Therefore, the Xv2 calculation requires three flow rate measurements: supply air flow rate, extract air flow rate, and liquid flow rate. Additionally, the thermophysical properties of the fluid are also required, considering the test conditions. The corresponding control diagram for the Xv2 regulation method is illustrated in Figure 24 below.

Equation 8

$$X_{V2} = \frac{V_l \ \rho_l \ Cp_l}{\frac{(V_{sa}+V_{ea})}{2} \ \rho_a \ Cp_a}$$

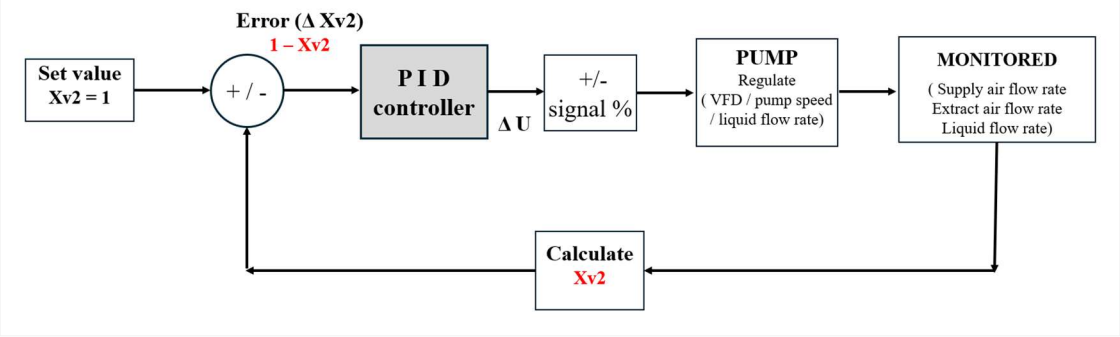

Figure 24: Control diagram for the Xv2 - based regulation system.

3. Methodology

This chapter presents the methodological framework used to evaluate the performance of a novel control system developed for a run-around heat recovery unit. The evaluation is carried out through a series of controlled laboratory experiments using newly implemented regulation strategies under varying airflow conditions. The primary objective is to evaluate the effectiveness of both temperature-based (Xt and Xt2) and flow rate-based (Xv and Xv2) approaches in regulating the RAHRU, particularly under conditions relevant to modern demand-controlled ventilation systems with balanced and unbalanced airflow configurations.

The methodology includes a detailed description of the method of evaluation, limitations associated with the laboratory tests, performance metrics, evaluation approach, test measurements and the accuracy of the recorded data.

3.1 Method of evaluation

The evaluation of the novel control system is structured into two main parts. The first part focuses on verifying the unit's performance by comparing the results obtained using the new control system with those from previous laboratory tests and simulation models. The second part assesses the control performance of the system under conditions representative of DCV systems. These two components provide the basis for evaluating the effectiveness and practical applicability of the proposed control strategies and are described in detail in the followings.

Unit performance verification:

To evaluate and verify the performance of the RAHRU under the novel control system, a comparative approach is considered. The evaluation begins by referring to test results obtained from earlier manual measurements conducted in the previous laboratory setup. Although the setup has been relocated, the same test rig and RAHRU were used, ensuring consistency. In addition, relevant simulation results and manufacturer established standard performance data for the RAHRU are reviewed and compiled.

Based on this information, performance curves, specifically RAHRU efficiency as a function of liquid flow rate across varying airflows, are identified and prepared. Key performance indicators, including maximum efficiency points with corresponding liquid flow rates, are also established from this baseline data.

Afterwards, laboratory tests are carried out using the novel control system, using regulation methods based on both temperature and flow rate measurements. These tests are designed to cover a representative range of airflow conditions. The resulting data are recorded, and corresponding graphs of heat recovery efficiency versus air and fluid flow rates (with 30% glycol) are prepared, together with tabulated results.

Finally, the performance results under the novel control system are analysed and compared with the reference data. The findings are documented in the results section for further evaluation.

Control performance:

To evaluate and verify the control performance of the novel control unit under real-world conditions, the control unit is tested within the context of a modern DCV system. Both balanced

and unbalanced ventilation scenarios are considered to reflect typical operating conditions in building ventilation systems.

A suitable DCV application is selected, together with an appropriate control schedule and a range of airflow settings, based on the limitations of the laboratory test rig. These selections are described in the evaluation approach and Laboratory test rig limitation sections in the below.

Tests are first carried out using temperature-based control (Xt regulations). This includes balanced ventilation scenarios using Xt and unbalanced scenarios using Xt2. All relevant data are recorded, and the results are presented in the graphs and tables for further analysis.

In parallel, tests are conducted using heat capacity-based control (flow rate-based regulation, Xv). Balanced ventilation is evaluated using Xv regulation, while unbalanced conditions are tested using Xv2. The collected data are compiled into both graphical and tabular formats.

In addition to the above, further tests are performed by using Xt and Xv regulations separately to the previously tested unbalanced scenarios. These additional tests aim to identify and compare the performance differences between Xt2 and Xt, as well as between Xv2 and Xv, under identical unbalanced airflow conditions. The results are compiled and formatted for comparison and analysis.

Finally, the control performance of the novel system is evaluated under both temperature-based (Xt/Xt2) and flow rate-based (Xv/Xv2) control strategies. Key performance aspect, including consistency, stability, and responsiveness to variations in airflow, are evaluated. The findings are summarized and discussed in the results section for further explanation.

3.2 Limitations of the laboratory tests

This section provides the primary limitations associated with the laboratory testing conducted during the evaluation of the novel control system. These limitations guide the selection of test airflow ranges, DCV schedules, as well as the analysis of performance results.

Airflow rate limitations:

The rated air flowrate used in the laboratory test rig is 1000 l/s, based on standard components and pressure drop as described in the laboratory equipment section. Both supply and extract fans are equipped with VFDs, allowing airflow to be adjusted between 0 (zero) and a maximum of approximately 1500 l/s. However, this upper limit is defined by the physical capacity of the AHU fans. These constraints restrict the simulation of higher airflow scenarios.

Liquid flow rate limitations with pump control:

The liquid flow rate is controlled via signals sent to the circulation pump. Under all regulation modes, temperature-based (Xt) and flow rate-based (Xv), the pump operates in automatic control mode.

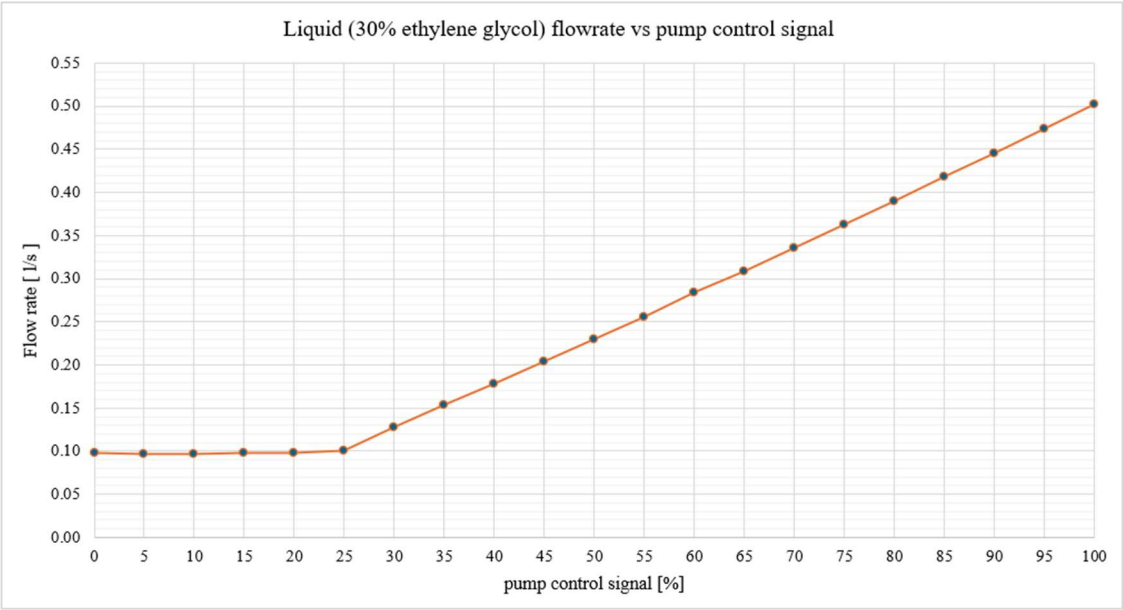

Figure 25: Variations of liquid flowrates with the pump control signal percentage.

As shown in Figure 25, the flowrate shows a non-linear response to control signals. Pump flowrate remains at a minimum of approximately 0.1 l/s between 0% and 25% signal and then increases closely linearly up to a maximum of about 0.5 l/s at 100% signal. This non-linearity limits the precision of flow control at lower signal levels, which restricts the ability to conduct stable tests at lower airflow rates, for example 250 l/s.

Working fluid type:

The working fluid used throughout the tests is a 30% ethylene glycol solution, widely used in RAHR systems for buildings in cold climates including Sweden. While this selection reflects typical real-world applications, the evaluation is limited to a 30% ethylene glycol considering the time constraints of the thesis work. Therefore, this evaluation of novel control system is limited to the working fluid type of 30 % ethylene glycol.

PI control parameters:

The proportional-integral (PI) control parameters, particularly the proportional gain (P), are manually adjusted for each test depending on airflow conditions and the type of regulation (Xt or Xv) applied. Automated tuning or adaptive PI parameter selection is not implemented in the current control setup. This manual tuning approach may lead to slight variations in the controller's responsiveness, stabilization time, and consistency across tests, which could affect the comparability of control performance results.

3.3 Performance evaluation metrics

The primary performance metric used in this study is the overall effectiveness, also referred to as the temperature efficiency, of the RAHR system. This is followed by several additional parameters that facilitate evaluate the performance of the control system. These include liquid flow rate (l/s), supply and extract airflow rates (l/s) and heat capacity ratio (dimensionless).

The heat capacity ratio (X) is one of the most important parameters used in evaluating the control strategies. Four different types of heat capacity ratios listed below are defined and implemented within the controller, depending on the airflow condition and measurement type.

- Xt is based on temperature measurements under balanced airflow conditions
- Xt2 is based on temperature measurements under unbalanced airflow conditions
- Xv is based on flow rate measurements under balanced airflow conditions
- Xv2 is based on flow rate measurements under unbalanced airflow conditions

3.4 Evaluation approach

Implementation of regulation strategies in the novel control system

In the initial phase of the evaluation, the functionality of the newly implemented control system was tested using a temperature-based regulation method. These preliminary tests confirmed that the regulation using Xt, a heat capacity ratio based on temperature measurements around the supply air heat exchanger under balanced airflow conditions, functioned as intended.

Developing upon this, the control logic was extended to manage unbalanced airflow systems. This led to the development and implementation of Xt2, which calculates the heat capacity ratio using temperature readings from both the supply and extract air heat exchangers. The integration of Xt2 enabled the system to respond effectively to unbalanced conditions, which are typical in real-world ventilation applications.

As the work progressed, additional regulation strategies were introduced. Particularly, Xv and Xv2 were developed as flow rate-based alternatives to Xt and Xt2, respectively. These strategies use measured airflow and liquid flow rates to compute the heat capacity ratio, enabling the control system to manage both balanced and unbalanced ventilation conditions.

With all four regulation strategies, Xt, Xt2, Xv, and Xv2, successfully implemented, the control system enhanced capable of operating under diverse ventilation conditions. This multi-regulation configuration laid the base for a structured evaluation approach.

Novel control unit evaluation approach

The performance and applicability of the control system are evaluated through a structured, stepwise evaluation approach. This approach includes four key stages, each addressing specific objectives related to control performance, comparative analysis and real-world applicability.

Step 1 - controller tuning and verification:

The first step focuses on verifying the effectiveness of the control system in achieving the desired regulation performance using the implemented strategies. The main aim is to determine whether the system can reach the setpoint quickly and maintain stable operation across various regulation modes.

This requires the tuning of the proportional (P) and integral (I) parameters for each regulation method (Xt, Xt2, Xv, and Xv2). The P and I values are determined through iterative testing based on system response, using a trial-and-error approach informed by control theory principles

and expert input. Ensuring appropriate controller tuning is essential for the stability and responsiveness of the RAHR unit under dynamic ventilation conditions.

Step 2 - comparative analysis with existing data and model predictions:

In the second step, the performance of the novel control system is evaluated against both previously collected experimental data and results from a validated simulation model. The earlier experimental data are compiled originate from research conducted on the same test rig and are published in the paper titled *"Liquid flow rate control in run-around heat recovery system"* by Peter Filipsson [1].

This comparative analysis is performed under balanced airflow conditions at supply and extract airflows of 500 l/s, 750 l/s, and 1000 l/s. Key performance indicators include the heat transfer effectiveness as a function of the liquid flow rate and the heat capacity ratio, derived using both temperature-based (Xt) and flow rate-based (Xv) regulations.

The evaluation also incorporates simulation results for various liquid flow rates using a 30% ethylene glycol solution and further compares these with the rated effectiveness values provided by the manufacturer for rated conditions. These comparisons alleviate to assess the maximum achievable effectiveness, as well as the effectiveness at the specific points where Xt = 1 and Xv = 1, under each airflow scenario. This step provides valuable insight into how closely the experimental results obtained using the novel control unit align with theoretical expectations and previously validated performance data.

Step 3 - evaluation under dynamic demand-controlled ventilation (DCV) conditions:

The third step evaluates the performance of the control system in DCV scenarios, which involve both balanced and unbalanced airflow conditions. A representative real-world application, a lecture hall operating from 07:30 AM to 17:00 PM, is selected to simulate a realistic DCV schedule. Corresponding balanced and unbalanced airflow profiles are developed based on typical occupancy and ventilation demand patterns.

Initially, the control system is tested under balanced airflow using the temperature-based Xt regulation, followed by similar tests using the flow rate-based Xv regulation. These tests are intended to evaluate how each method responds to variable airflow demands and varying environmental conditions.

The same DCV application is then tested under unbalanced airflow conditions, using Xt2 and Xv2 regulations. These experiments assess the system's capacity to maintain heat recovery effectiveness when the supply and extract airflows are not equal, which is a common condition in actual DCV operation.

This stage of the evaluation provides critical insights into the system's behaviour in practical applications and supports a performance comparison between regulation strategies under both steady and variable operating conditions.

Step 4 - sensitivity assessment of fluid properties on Xv regulation:

The final step in the evaluation approach focuses on assessing the sensitivity of the Xv regulation method to variations in fluid and air properties. While the initial tests were conducted using the thermophysical properties of a 30% ethylene glycol (EG) solution, three additional tests were performed using the same fluid but with thermophysical data corresponding to different EG concentrations that are 20% EG (ASHRAE), 30% EG (ASHRAE), and 40% EG (ASHRAE).

These property sets, established by ASHRAE, were selected to examine the potential impact of applying incorrect or non-matching fluid parameters in the control unit.

The purpose of this analysis is to investigate how changes in key thermophysical properties, specifically, specific heat capacity and density, within a typical operational temperature range affect the calculated heat capacity ratio and the overall performance of the system. This evaluation is essential to understanding the reliability and robustness of the flow-based regulation method under variable operational conditions, including seasonal variations or deviations from design specifications.

Together, these four steps provide a comprehensive evaluation approach for assessing the performance of the novel RAHR control system. The approach combines laboratory testing, model validation, and real-world DCV application scenarios, covering both temperature-based and flow rate-based regulation strategies under balanced and unbalanced airflow conditions.

The insights gained from each step of the evaluation are presented and analysed in the following chapters, where the performance of each regulation method is critically examined and compared.

3.5 Measurements and accuracy

The schematic diagram of the run-around heat recovery system used in this study is shown in Figure 26 below.

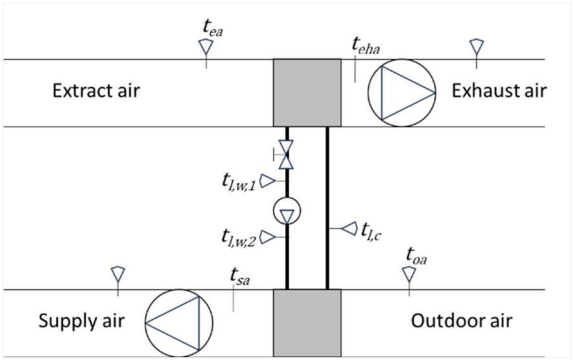

Figure 26: Schematic diagram of the run-around heat recovery test setup.
(Source, Peter Filipsson, 2024 [1])

The measurements were carried out in the laboratory test rig following scientific procedures to evaluate the overall effectiveness of the run-around heat recovery unit using the novel control system. The evaluation included various airflow rates, different heat capacity ratios achieved through changes in the working fluid flow rate, and both balanced and unbalanced DCV schedules. A 30% ethylene glycol solution was used as the working fluid in the RAHR system.

The supply and exhaust air fans are equipped with VFDs, allowing the airflow rates to be adjusted according to the test requirements. During the unit performance evaluation phase, three airflow rates were tested: 500 l/s, 750 l/s, and 1000 l/s. In the control performance evaluation phase, several airflow rates were tested based on the selected demand-controlled ventilation schedule, incorporating both balanced and unbalanced ventilation scenarios. The tested airflow rates in this phase were 240 l/s, 300 l/s, 600 l/s, 720 l/s, 750 l/s, 900 l/s, 960 l/s, and 1200 l/s. Airflow rates were measured using the built-in measurement system of the AHU, which calculates flow based on the pressure difference across the air fans.

The working fluid, a 30% ethylene glycol solution, was circulated by a pump equipped with a variable frequency drive, allowing the liquid flow rate to be adjusted according to the control

signal based on the selected regulation method. The flow rate was measured using a control valve identified as TA-Smart, as shown in Figure 27, which illustrates the control and monitoring interface of the RAHR unit.

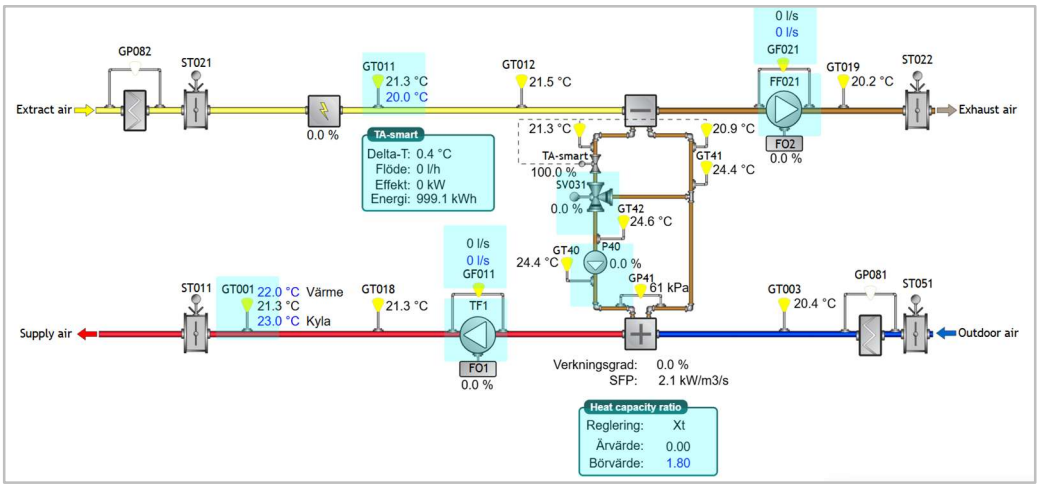

Figure 27: Control and monitoring interface of the run-around heat recovery unit.

The TA-smart control valve (IMI TA-Smart PN 25) is an ultrasonic flow-measuring valve with an uncertainty of ±3% when used with a 30% ethylene glycol solution. Throughout all tests, the TA-Smart valve remained fully open (100%), and the liquid flow rate was regulated based on the pump's control signal.

Thermocouples were used to measure the coupling liquid temperatures at the inlet and outlet of the heat recovery coils, as well as the air temperatures around the supply and extract air coils in the air streams. The temperature sensors, PT-100 for both air and liquid measurements, were calibrated using an ice-bath method against a Dostmann P600 reference sensor with an uncertainty of ±0.1% for water. As shown in Figure 27, the temperature between the supply air coil and the fan in the supply air stream was not directly measured in the test rig. Therefore, the heat contribution from the supply air fan was measured separately and accounted for in the analysis.

To evaluate the unit performance, several tests were conducted using different regulation methods under balanced airflow conditions for three airflow rates: 500 l/s, 750 l/s, and 1000 l/s. The coupling liquid flow rate was varied between 0.1 l/s and 0.5 l/s, depending on the set value of the heat capacity ratio according to the selected regulation method. This setup was used to assess the effectiveness of the system under different heat capacity ratios and the corresponding liquid flow rates. The outdoor air temperature was changed within a range from 3 °C below zero to 10 °C. The extract air temperature was varied between 14 °C and 26 °C by using an electric heater installed in the extract air stream.

For each change in airflow rate or heat capacity ratio setting, the test rig was operated for at least 30 minutes and 15 minutes respectively, or until steady-state conditions were achieved, before starting data collection. All sensors in the test rig were connected to the SI web-based application, where the measured data were continuously recorded and stored for further analysis.

To evaluate the control performance using a demand-controlled ventilation schedule, several tests were also carried out under both balanced and unbalanced airflow conditions. These tests followed a full daily schedule from 7:30 in the morning to 5:00 in the evening. All data from these tests were recorded in the SI web-based application and later downloaded for detailed evaluation.

4. Results and Analysis

This section presents the evaluation and performance assessment of the novel control unit developed for the run-around heat recovery system. The analysis is structured into three main parts: (1) the performance of Xt and Xv regulation methods, (2) the evaluation of the system under demand-controlled ventilation operation, and (3) a sensitivity analysis related to the selection of thermophysical properties in Xv regulation. Each subsection provides a detailed investigation based on experimental test results, simulation comparisons, and technical evaluations.

The first part, focusing on Xt and Xv regulation performance, commences with a comparison of the maximum effectiveness achieved using these methods against the manufacturer's specified rated effectiveness, allowing to validate the novel control unit's performance. This is followed by an in-depth evaluation of the controller under Xt regulation, including a detailed performance profile across various operating conditions. Additionally, the test results from the novel controller are compared with relevant simulation outcomes to assess model accuracy and control reliability. Finally, a comprehensive comparison between the novel regulation strategies (Xt and Xv) and previous laboratory test results is presented. This includes performance assessments at different airflow rates (500, 750, and 1000 l/s), shown both individually and collectively to demonstrate consistency and performance improvements.

This second part of the results section examines the performance of the novel control unit under demand-controlled ventilation operation. It begins with an evaluation of the heat recovery system operating under balanced airflow conditions using both Xt and Xv regulation strategies. The subsequent analysis focuses on the system's performance under unbalanced ventilation scenarios, which are commonly encountered in real-world DCV applications. Additionally, a comparative study assesses the effectiveness of applying the standard Xt and Xv regulations, based on supply air measurements, instead of the dedicated Xt2 and Xv2 approaches specifically designed for unbalanced conditions. The findings provide valuable insights into the control system's robustness and adaptability across varying airflow profiles.

The final section presents a sensitivity analysis evaluating how variations in the thermophysical properties of the heat transfer fluid influence the performance of the Xv regulation method. By examining multiple ethylene glycol concentrations, this analysis highlights the significance of accurate property selection in maintaining reliable and efficient system control, especially under demand-based airflow variations.

4.1 Results of Xt and Xv regulations

This section presents the results of the Xt and Xv regulations, comparing them with the manufacturer's rated effectiveness for the RAHR unit, the findings from the simulation model, and the results from previous lab tests.

4.1.1 Comparison with the manufacturer's specified rated effectiveness

Figure 28 shows the results of the Xt and Xv regulations, along with the previous lab test results, for an air flow rate of 1000 l/s. The manufacturer's rated effectiveness value is also indicated on the same figure.

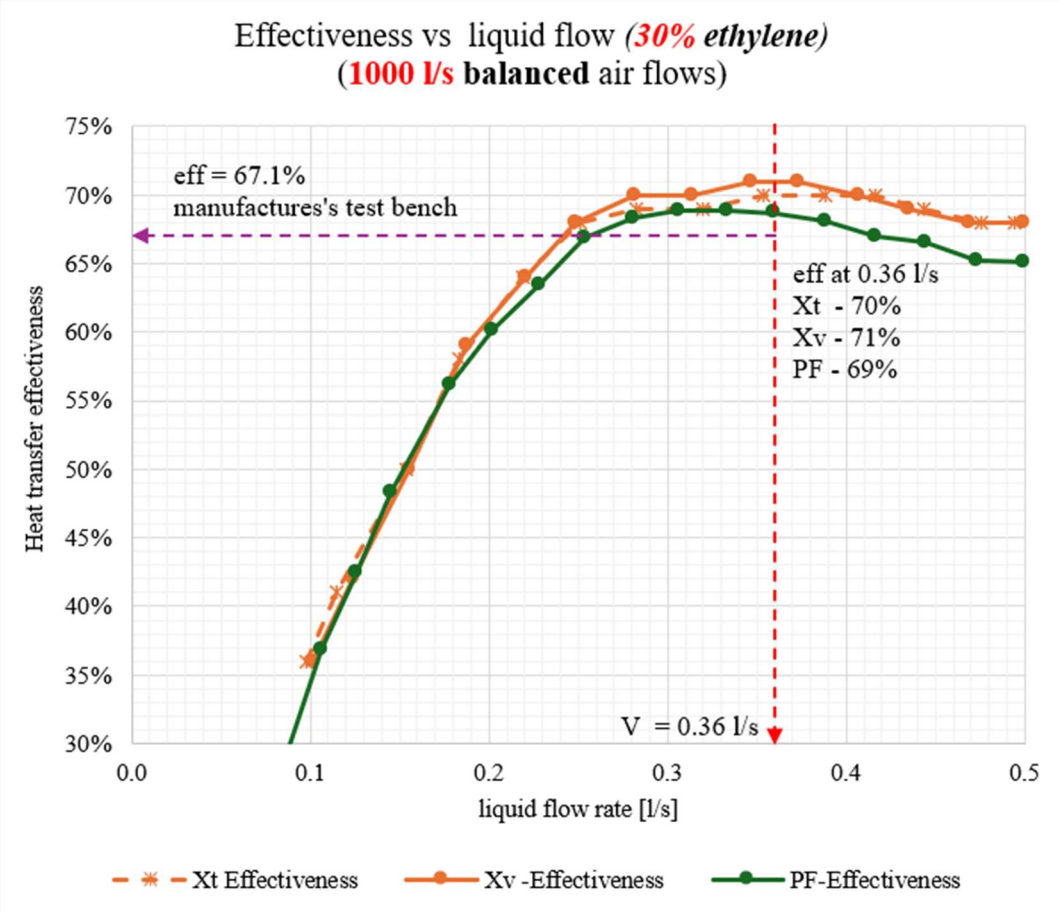

Figure 28: Effectiveness as a function of liquid flow rate at an airflow rate of 1000 l/s for the novel control regulations (Xt and Xv) and the previous lab test results.

According to Figure 28, the test results obtained using the new controller with both Xt and Xv regulations at a liquid flow rate of 0.36 l/s and the rated AHU flow rate of 1000 l/s show good agreement with the manufacturer's test bench results. However, the effectiveness values obtained from Xt and Xv regulations are slightly higher, exceeding the manufacturer's established effectiveness of 67% by 4% and 6%, respectively. Additionally, the old lab test results align closely with those of the novel control system, showing an effectiveness that is 3% higher than the manufacturer's specified value.

4.1.2 Performance of the novel control unit : Xt regulation

The variation in heat transfer effectiveness as a function of liquid flow rate (V_l) and heat capacity ratio (Xt) under Xt regulation for three ventilation rates (500 l/s, 750 l/s, and 1000 l/s) is presented in Figures 29 to 31. These figures highlight key points, including the effectiveness at Xt = 1 and the maximum achievable effectiveness when using 30% ethylene glycol as the working fluid.

Balanced ventilation rate : 500 l/s

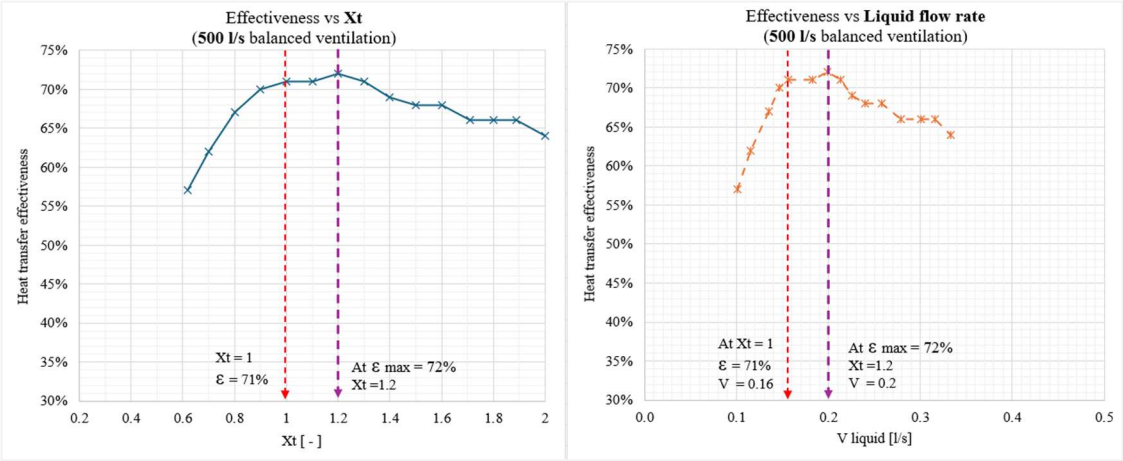

Figure 29: Heat transfer effectiveness as a function of Xt and liquid flow rate for 500 l/s air flow rate using 30% EG.

Figure 29 illustrates the heat transfer effectiveness at a ventilation airflow rate of 500 l/s. At Xt = 1, the effectiveness reaches 71% with a liquid flow rate of 0.16 l/s. The maximum effectiveness of 72% is achieved at Xt = 1.2, where the liquid flow rate increases to 0.2 l/s. These results are consistent with established knowledge, showing that maximum effectiveness is influenced by the concentration of ethylene glycol and its impact on the thermophysical properties of the fluid.

Balanced ventilation rate : 750 l/s

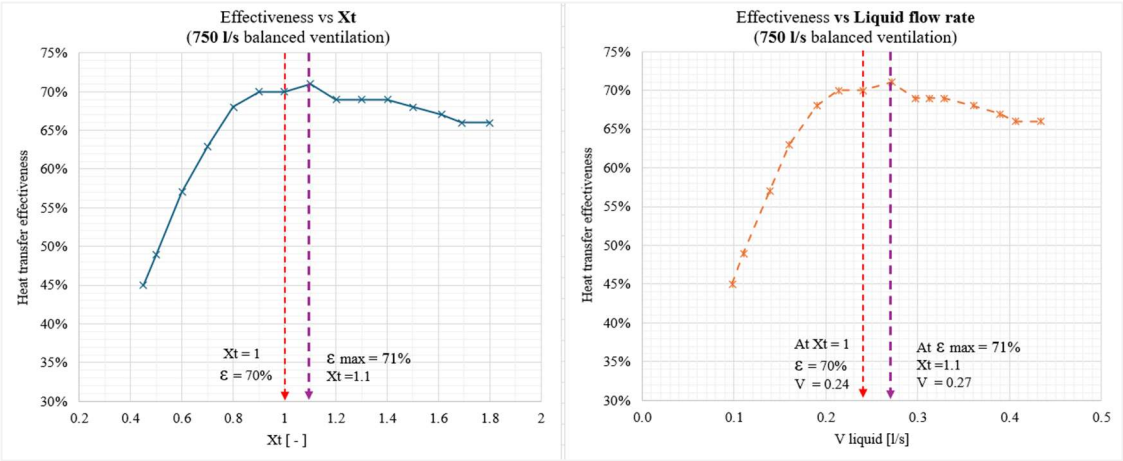

Figure 30: Heat transfer effectiveness as a function of Xt and liquid flow rate for 750 l/s air flow rate using 30% EG.

Figure 30 illustrates the heat transfer effectiveness for a ventilation airflow rate of 750 l/s. At Xt = 1, an effectiveness of 70% is achieved with a liquid flow rate of 0.24 l/s. The maximum effectiveness of 71% occurs at Xt = 1.1, where the liquid flow rate increases to 0.27 l/s. These results follow a similar trend to the 500 l/s airflow case. Additionally, the liquid flow rates at critical performance points increase as the airflow rate increases. This observation is consistent with previously established knowledge.

Balanced ventilation rate : 1000 l/s

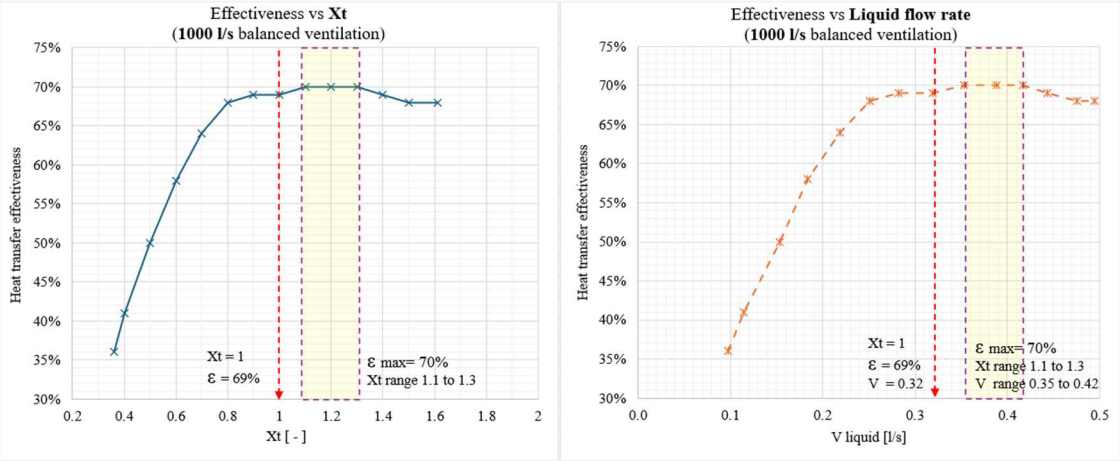

Figure 31: Heat transfer effectiveness as a function of Xt and liquid flow rate for 1000 l/s air flow rate using 30% EG.

Figure 31 illustrates the heat transfer effectiveness for a ventilation airflow rate of 1000 l/s. At Xt = 1, an effectiveness of 69% is achieved with a liquid flow rate of 0.32 l/s. For this higher airflow rate, the maximum effectiveness of 70% is observed within the Xt range of 1.1 to 1.3, corresponding to a liquid flow rate increase from 0.35 to 0.42 l/s. These results follow a similar trend to the lower airflow cases, except that the maximum effectiveness occurs over a range of liquid flow rates rather than at a single point. This observation is consistent with previously established test and simulation results.

4.1.3 Comparison with simulation results

In this section, the results obtained from the novel control unit using Xt regulation, as presented in the previous section, are compared with the corresponding simulated results for 30% EG, published by P. Filipsson [1].

The liquid flow rates at key performance points, Xt =1 and the point of maximum effectiveness, are mapped onto the corresponding simulated graphs. The mapped points for each airflow rate, 1000 l/s, 750 l/s and 500 l/s, are illustrated in Figures 32 to 34 , respectively.

Figure 32 illustrates the key performance points, liquid flow rates and corresponding effectiveness values for the 1000 l/s airflow rate, as discussed above. The mapped points show that the liquid flow rates and effectiveness values obtained from Xt regulation are in good agreement with the simulated results using 30% EG.

Similarly, in Figure 33, for the 750 l/s airflow rate, the liquid flow rates at the key points of Xt regulation align with the simulated results. The effectiveness values from Xt regulation are slightly higher than the simulated results, with a difference of approximately 2% at both key points.

In Figure 34, for the 500 l/s airflow rate, the liquid flow rates at the key points for Xt regulation also align with the simulated results. The Xt effectiveness values are again slightly higher than the simulated results, with a difference of about 3% to 4% at both key points.

Based on the comparison above, the overall results obtained using the novel control unit with Xt regulation show good agreement with the simulated results using 30% EG as the liquid media.

Balanced ventilation rate : 1000 l/s

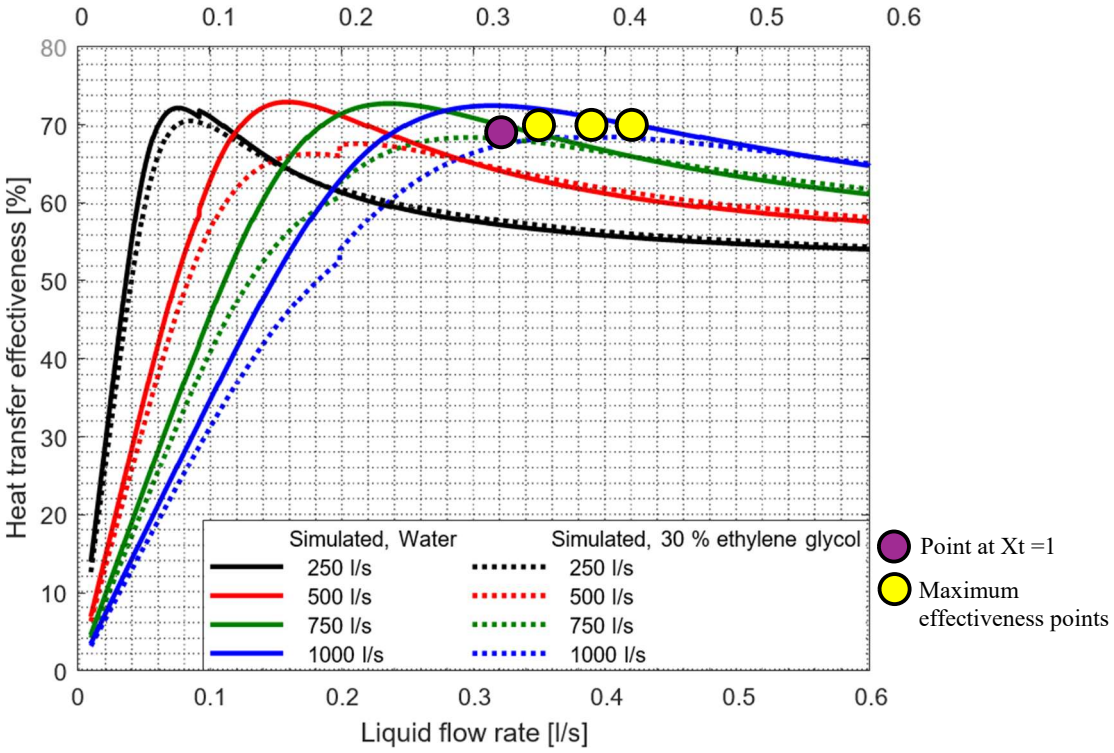

Figure 32: Comparison of effectiveness and liquid flow rate for 1000 l/s air flow rate.

Balanced ventilation rate : 750 l/s

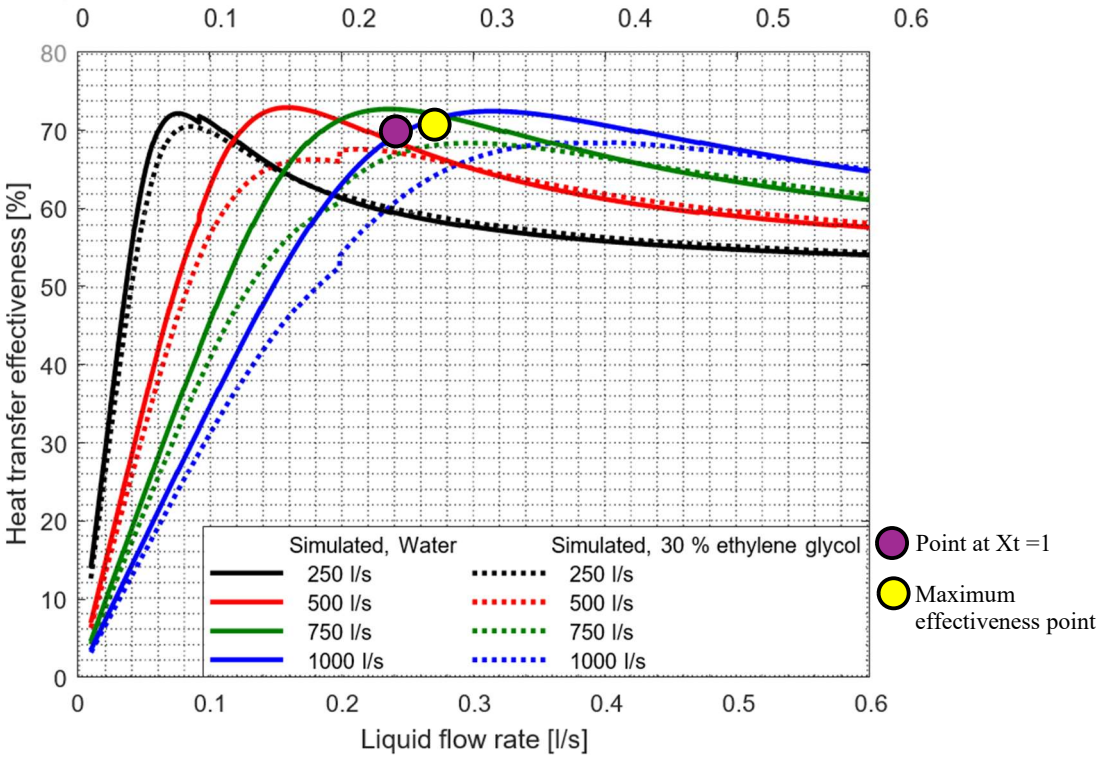

Figure 33: Comparison of effectiveness and liquid flow rate for 750 l/s air flow rate.

Balanced ventilation rate : 500 l/s

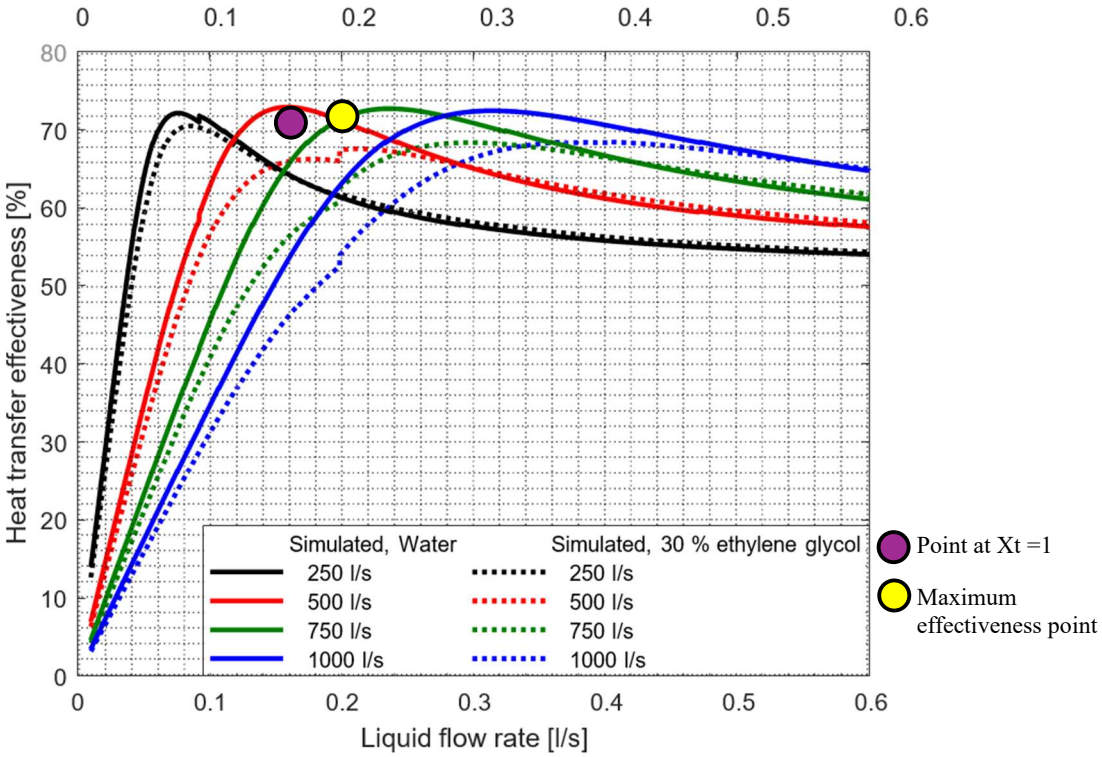

Figure 34: Comparison of effectiveness and liquid flow rate for 500 l/s air flow rate.

4.1.4 Comparison of novel control unit (Xt and Xv) with previous lab test results

This section compares the results obtained from the novel control unit, using both Xt (temperature-based regulation) and Xv (flow rate-based regulation), with the results from earlier laboratory tests conducted using a 30% EG solution.

Comparison of three airflow rates in combined and separate graphs for Xt, Xv, and old lab test results:

The heat recovery effectiveness as a function of liquid flow rate for different airflow rates is illustrated in Figures 35 to 37, corresponding to Xt regulation, Xv regulation, and the old lab test, respectively.

The comparison evaluates the performance trends for three airflow rates: 500 l/s, 750 l/s, and 1000 l/s, using 30% EG as the working fluid. A summary of the key performance metrics, including the maximum effectiveness and the corresponding liquid flow rates, is presented in Table 2.

Table 2: Maximum effectiveness and corresponding liquid flow rates for three air flow rates.

Air flowrate (l/s)	**Xt** regulation		**Xv** regulation		**Old lab** (manual test)	
	Max Eff %	Liquid flow (l/s)	Max Eff %	Liquid flow (l/s)	Max Eff %	Liquid flow (l/s)
500	72	0.20	72	0.19	70	0.16
750	71	0.27	72	0.26	69.5	0.23
1000	70	0.35 to 0.42	71	0.35 to 0.37	69	0.33

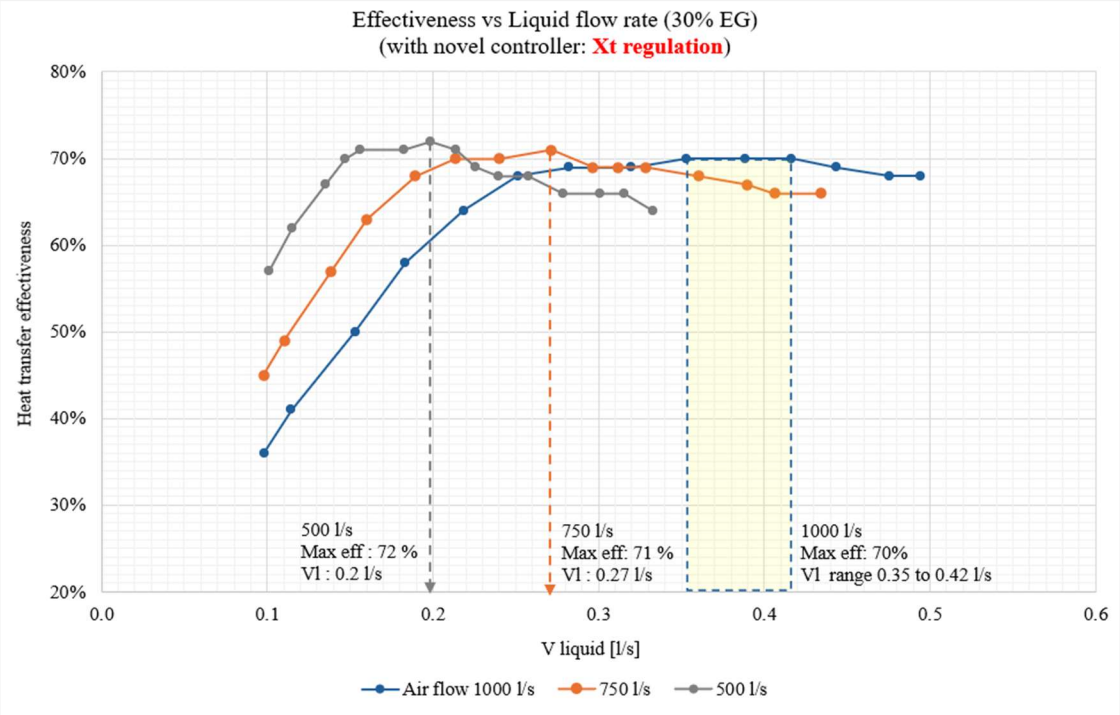

Figure 35: Xt regulation, effectiveness as a function of liquid flow rate for different air flow rates.

Based on Table 2 and Figures 35 to 37, the main observations are summarized below:

- The maximum effectiveness achieved using both Xt and Xv regulations is nearly identical across all airflow rates. Specifically, the Xv regulation results in effectiveness values approximately 1% higher than those obtained with Xt regulation.
- In comparison to the old lab test results, both Xt and Xv regulations produce slightly higher maximum effectiveness values. Specifically, the old lab results are approximately 2% lower than the Xt regulation results across all airflow rates.
- For both novel control methods (Xt and Xv), the liquid flow rates at the critical performance points are nearly identical. However, the Xv regulation consistently results in slightly lower liquid flow rate values compared to the Xt regulation.
- The old lab tests also show lower liquid flow rate values compared to those obtained with the Xt regulation.

The performance data obtained from the novel control unit using both temperature-based Xt and flow rate-based Xv regulations show a high level of consistency with each other and with the old lab test results conducted using a 30% EG. Although there are minor differences, the Xv

regulation achieves approximately 1% higher effectiveness and slightly lower liquid flow rates, while the old lab tests show around 2% lower effectiveness and slightly lower flow rates. However, the overall trends of the new control regulations and the old lab test results are in strong agreement.

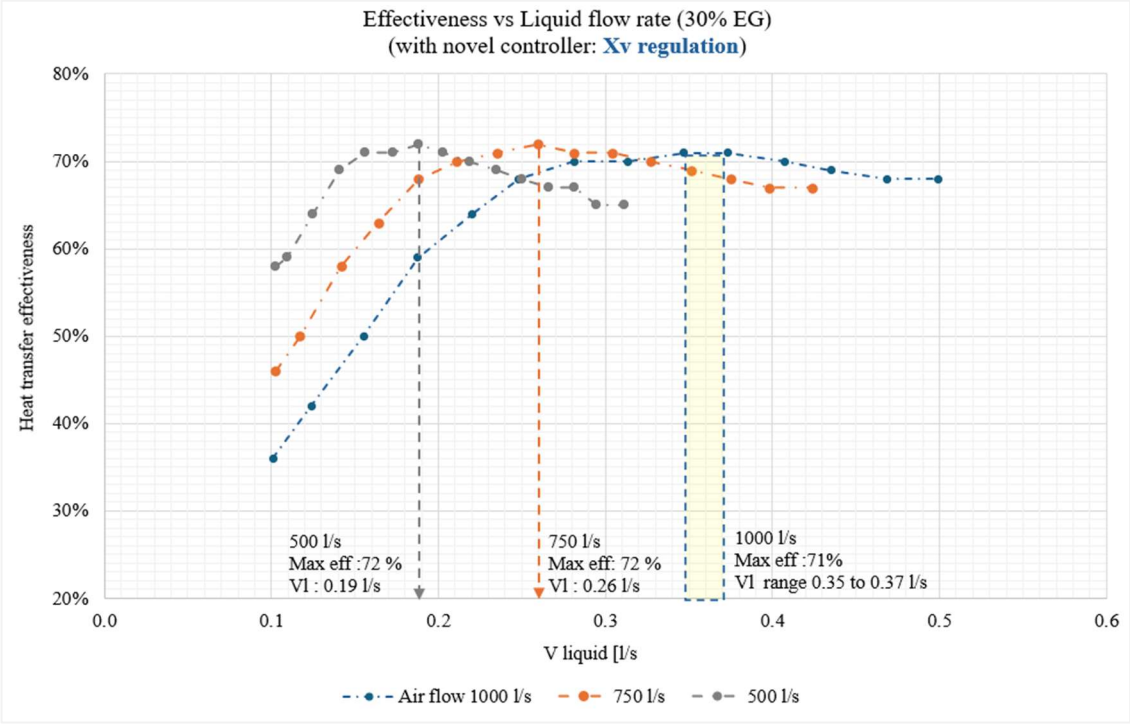

Figure 36: Xv regulation, effectiveness as a function of liquid flow rate for different air flow rates.

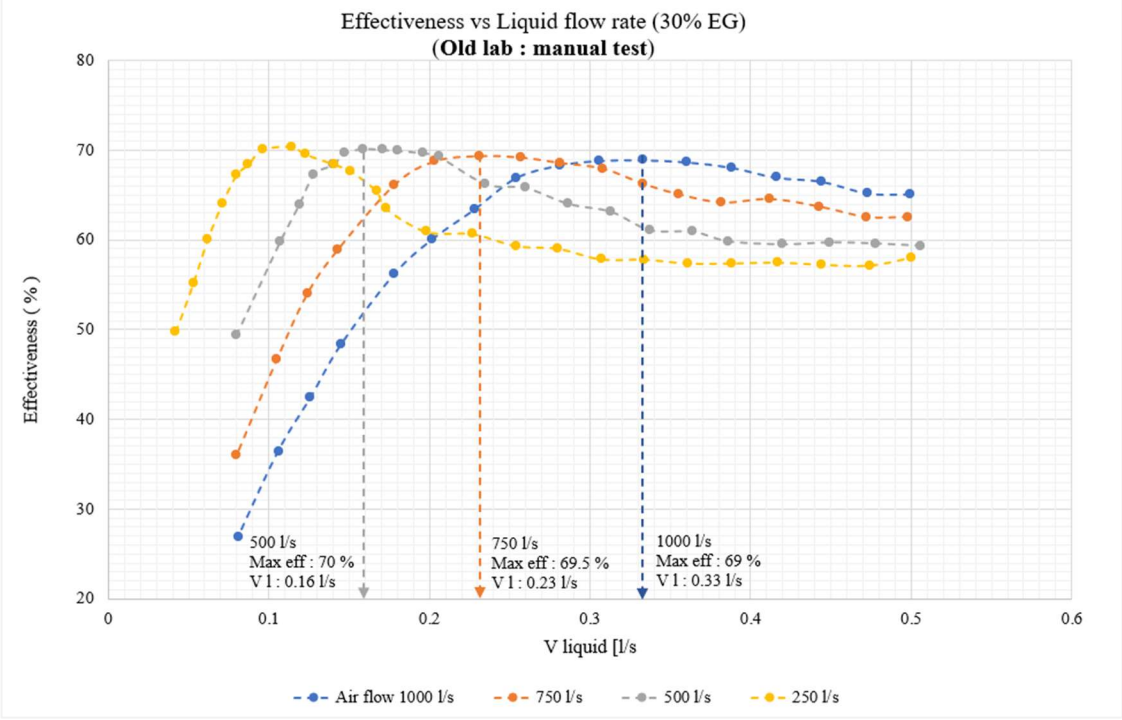

Figure 37: Old lab test, effectiveness as a function of liquid flow rate for different air flow rates.

Comparison of different airflow rates (500 l/s, 750 l/s and 1000 l/s)

To closely monitor the behaviour of the new controller, the results obtained from Xt and Xv regulations, along with the old lab manual test results, are illustrated in Figures 38 to 40 for airflow rates of 500 l/s, 750 l/s, and 1000 l/s, respectively.

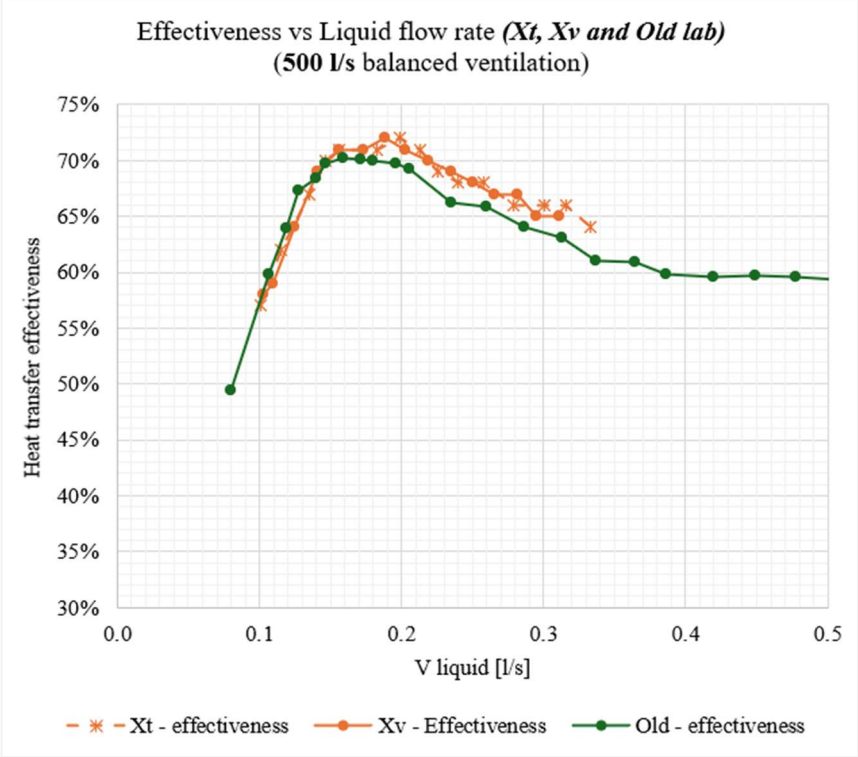

Figure 38: Comparison of Xt, Xv and Old lab results for 500 l/s air flowrate.

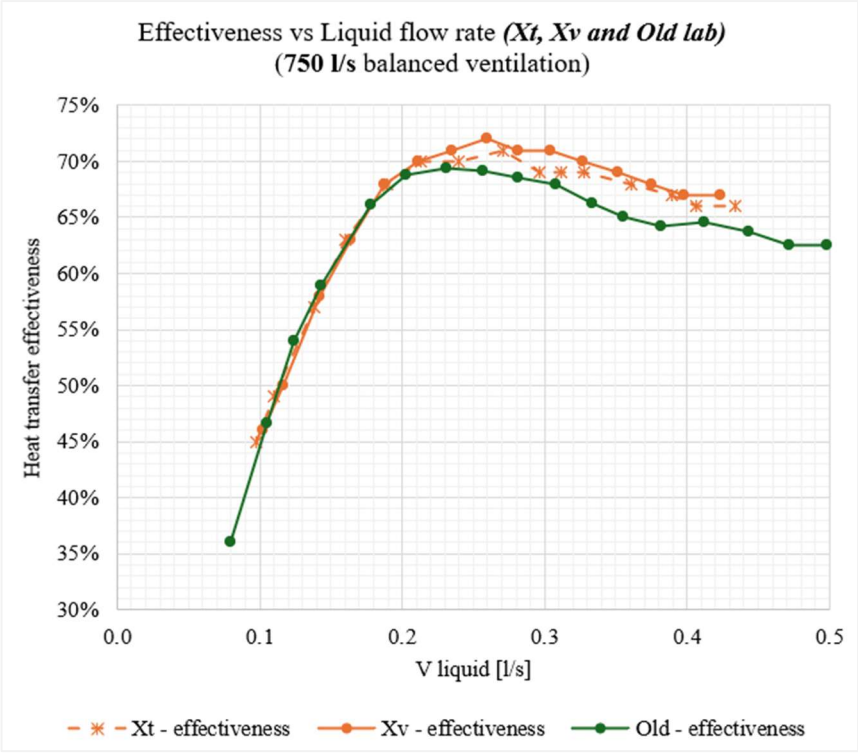

Figure 39: Comparison of Xt, Xv and Old lab results for 750 l/s air flowrate.

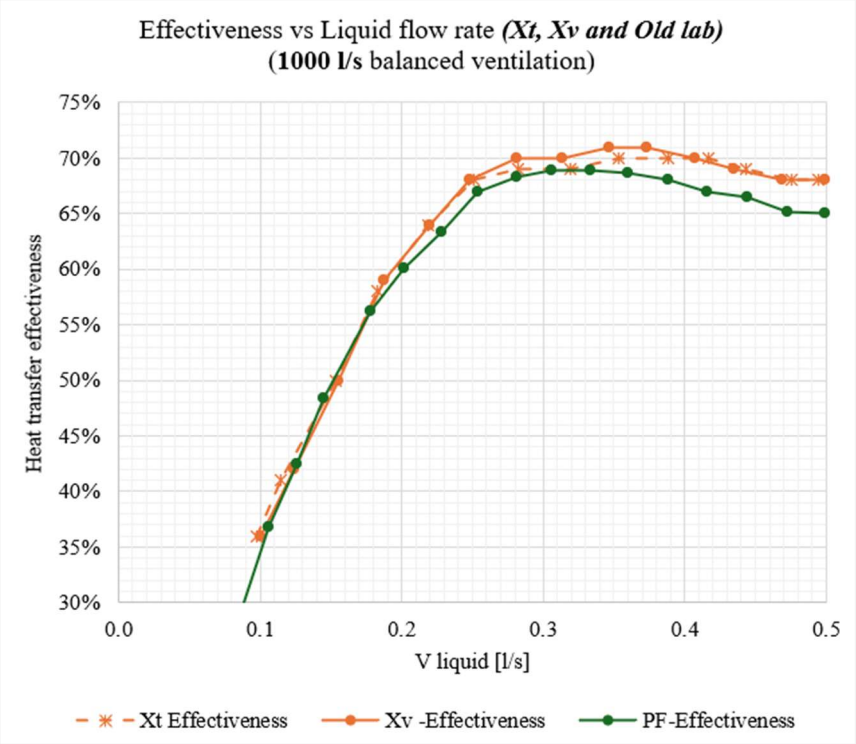

Figure 40: Comparison of Xt, Xv and Old lab results for 1000 l/s air flowrate.

According to the trends observed across the evaluated airflow rates, both Xt and Xv regulations demonstrate similar performance, with only minor deviations in effectiveness after reaching their respective maximum effectiveness. Compared to the old lab test results, the maximum effectiveness in the old tests is achieved at lower liquid flow rates, and the effectiveness values are consistently 2% to 3% lower than those obtained with Xt regulation. Furthermore, beyond the point of maximum effectiveness, the decline in effectiveness in the old lab tests is slightly steeper than in the results from the new controller (Xt and Xv). Accordingly, the difference in effectiveness between the old lab tests and Xt and Xv regulations becomes more noticeable beyond the maximum effectiveness point.

However, despite these differences, the overall behaviour of the Xt, Xv, and old lab manual control methods follows a similar trend across all tested airflow rates. This consistency indicates that both Xt and Xv regulations are effective in optimizing heat recovery performance across the full range of airflow rates.

4.2 Performance evaluation of demand control ventilation (DCV) systems

The following figures illustrate the behaviour of the novel control system under different regulation methods used in a demand-controlled ventilation system for a lecture hall application. The system was tested in the laboratory test rig under both balanced and unbalanced ventilation conditions, simulating lecture hall operation from 7:30 AM to 5:00 PM.

Figures 41 to 43 present the performance of the novel control unit in a balanced ventilation system, with Figure 41 showing Xt regulation, Figure 42 showing Xv regulation, and Figure 43 illustrating a comparison of both Xt and Xv regulations.

For unbalanced ventilation, Figures 44 and 45 demonstrate the performance of the system with Xt2 and Xv2 regulations, respectively.

Figures 46 and 47 compare the performance of novel control unit across both balanced and unbalanced ventilation conditions. Figure 46 presents the effectiveness of Xt and Xt2 regulations, while Figure 47 shows the results for Xv and Xv2 regulations.

The simulated lecture hall application, designed with a ventilation rate of 1500 l/s, along with its corresponding schedule, is presented in Tables 3 and 4 for the balanced and unbalanced ventilation systems, respectively.

Table 3: Lecture hall - DCV schedule for balanced ventilation.

	Schedule	Time / Period		DCV %	Air flow rate (l/s)
		Time	Period		
1	Start	07:30	00:30	20%	300
2	Lecture 1	08:00	01:45	50%	750
3	Break 1	09:45	00:30	20%	300
4	Lecture 2	10:15	01:45	80%	1200
5	Lunch break	12:00	01:00	20%	300
6	Lecture 3	13:00	01:45	60%	900
7	Break 2	14:45	00:30	20%	300
8	Lecture 4	15:15	01:45	80%	1200
9	End	17:00			

Table 4: Lecture hall - DCV schedule for unbalanced ventilation with a 20% reduction in extract airflow.

	Schedule	Time / Period		DCV %	Air flow rate (l/s)	
		From	Period		Supply	Extract
1	Start	07:30	00:30	20%	300	240
2	Lecture 1	08:00	01:45	50%	750	600
3	Break 1	09:45	00:30	20%	300	240
4	Lecture 2	10:15	01:45	80%	1200	960
5	Lunch break	12:00	01:00	20%	300	240
6	Lecture 3	13:00	01:45	60%	900	720
7	Break 2	14:45	00:30	20%	300	240
8	Lecture 4	15:15	01:45	80%	1200	960
9	End	17:00				

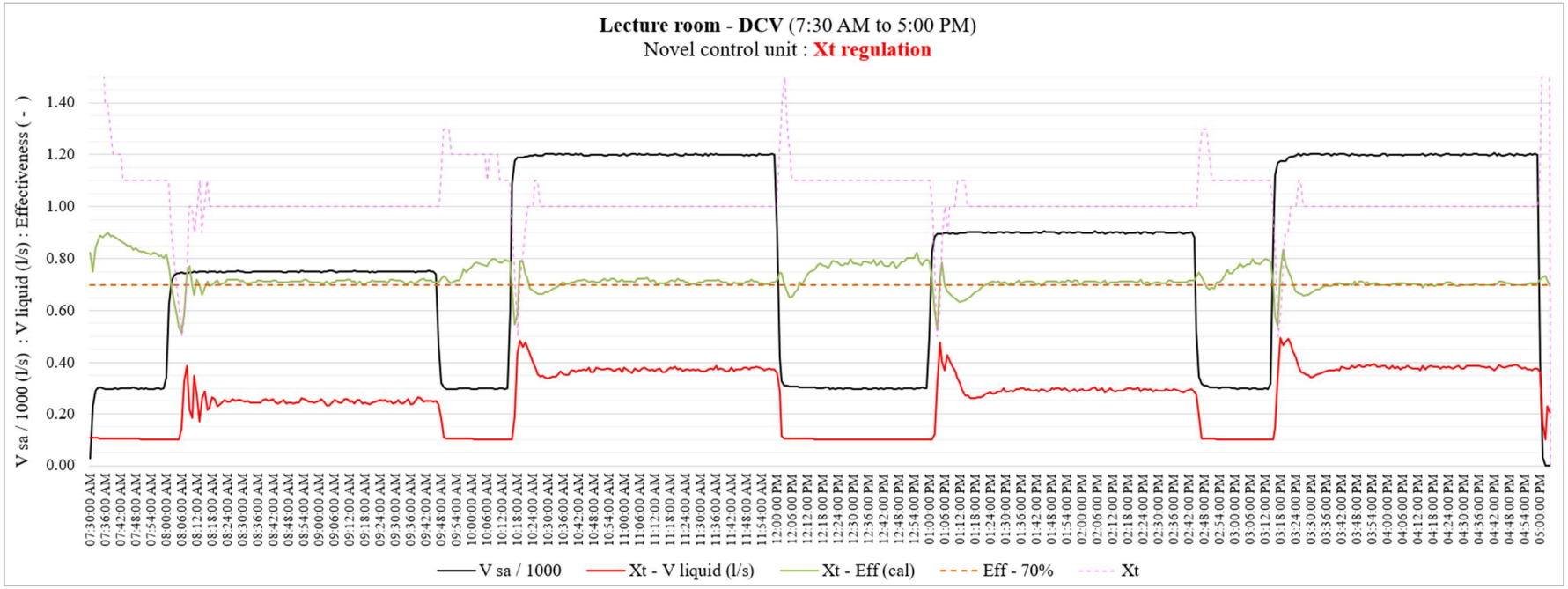

Figure 41: Novel control unit utilizing Xt regulation for a demand-controlled ventilation (DCV) system in a lecture hall application.

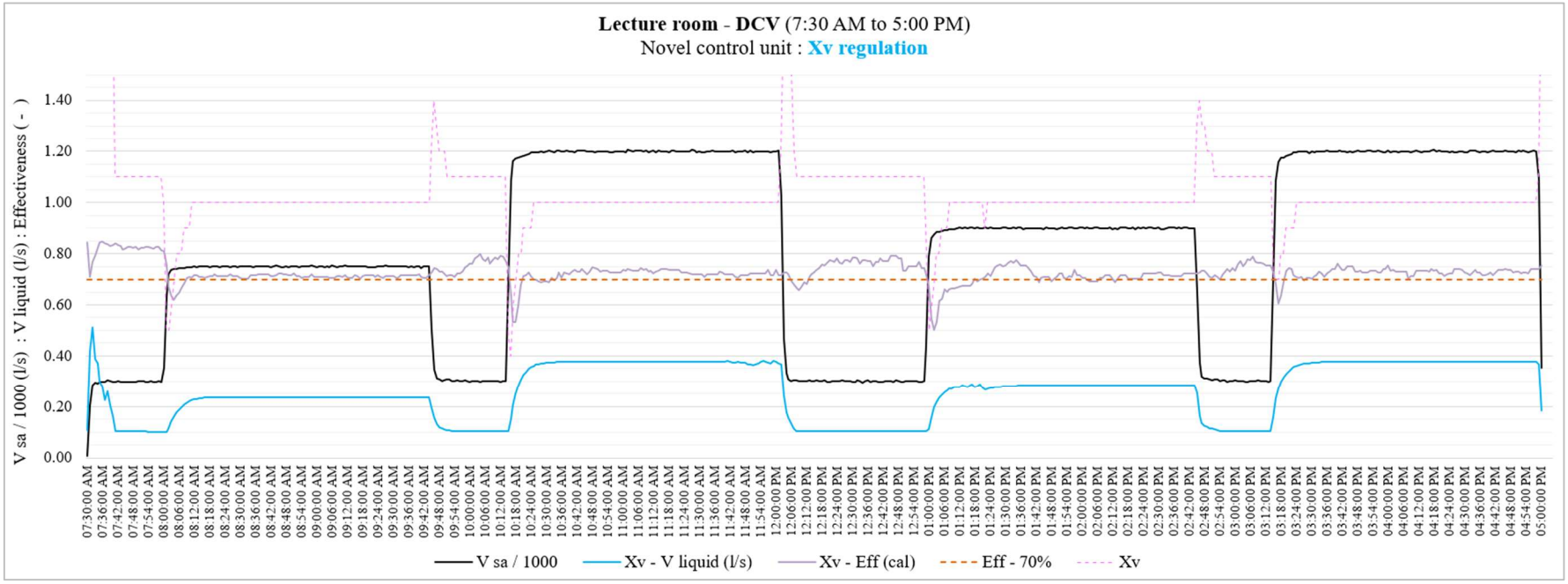

Figure 42: Novel control unit utilizing Xv regulation for a demand-controlled ventilation (DCV) system in a lecture hall application.

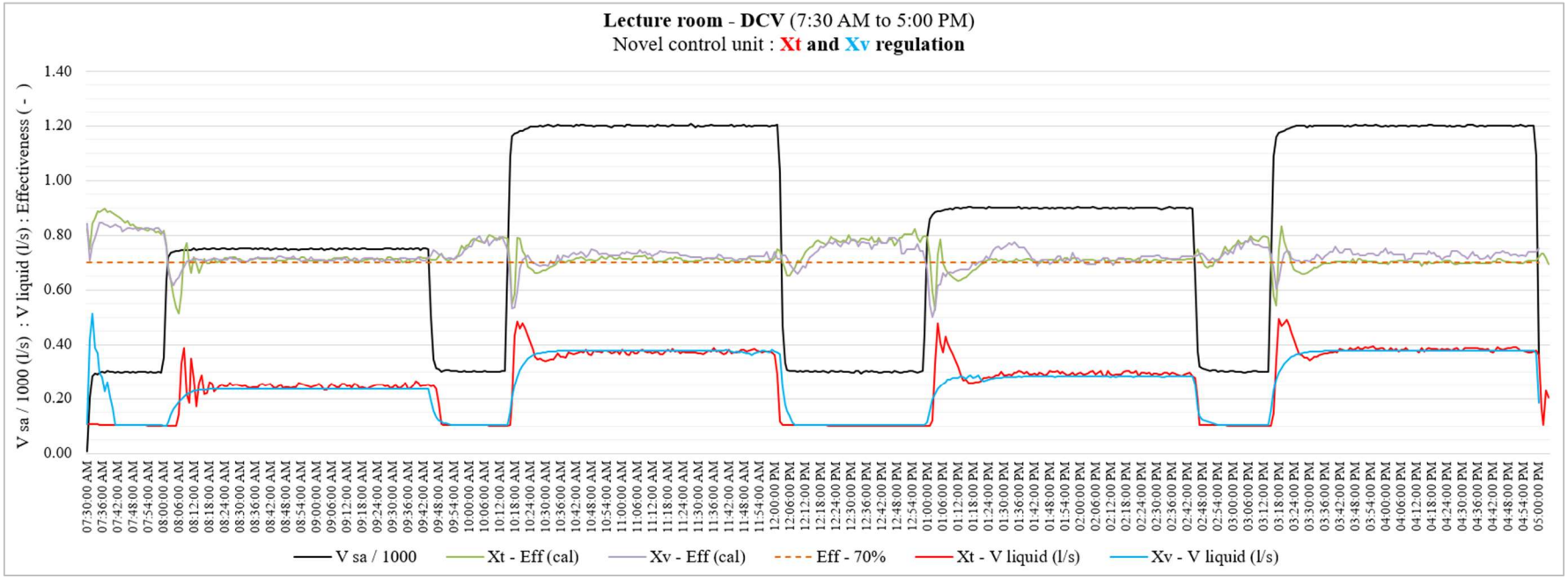

Figure 43: Comparison of Xt and Xv regulations for a demand-controlled ventilation (DCV) system in a lecture hall application.

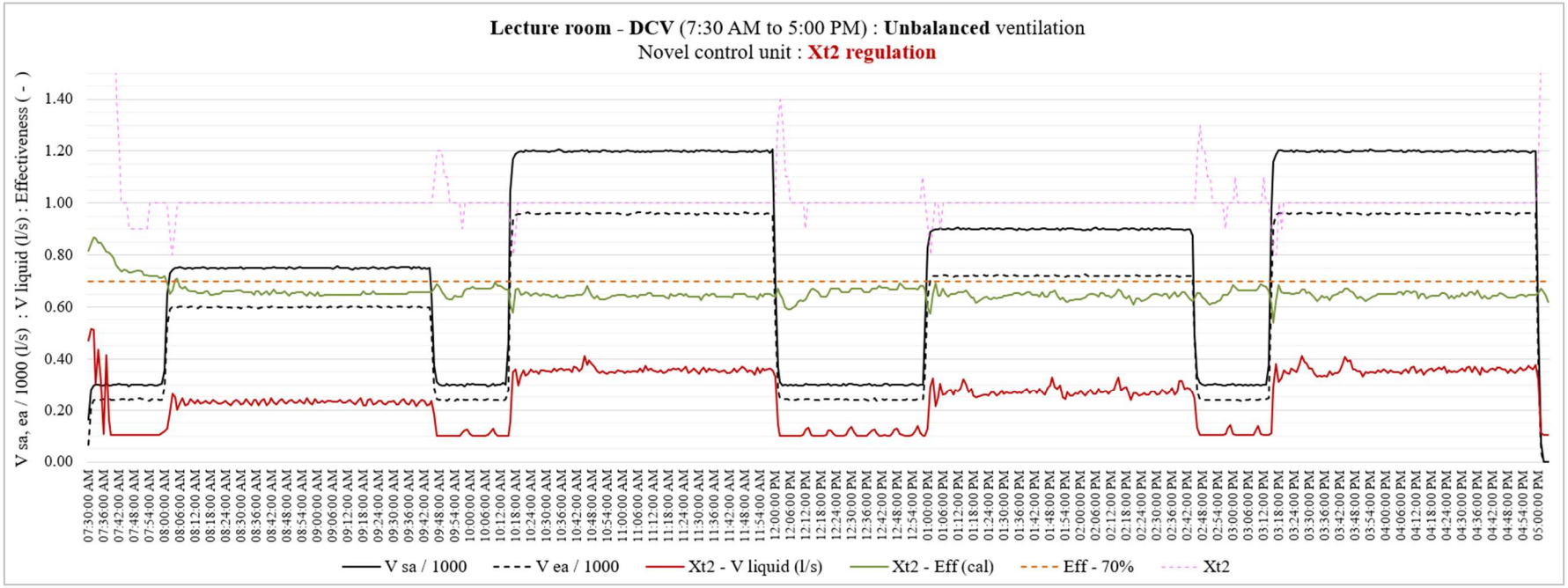

Figure 44: Novel control unit utilizing Xt2 regulation for an unbalanced demand-controlled ventilation (DCV) system in a lecture hall application.

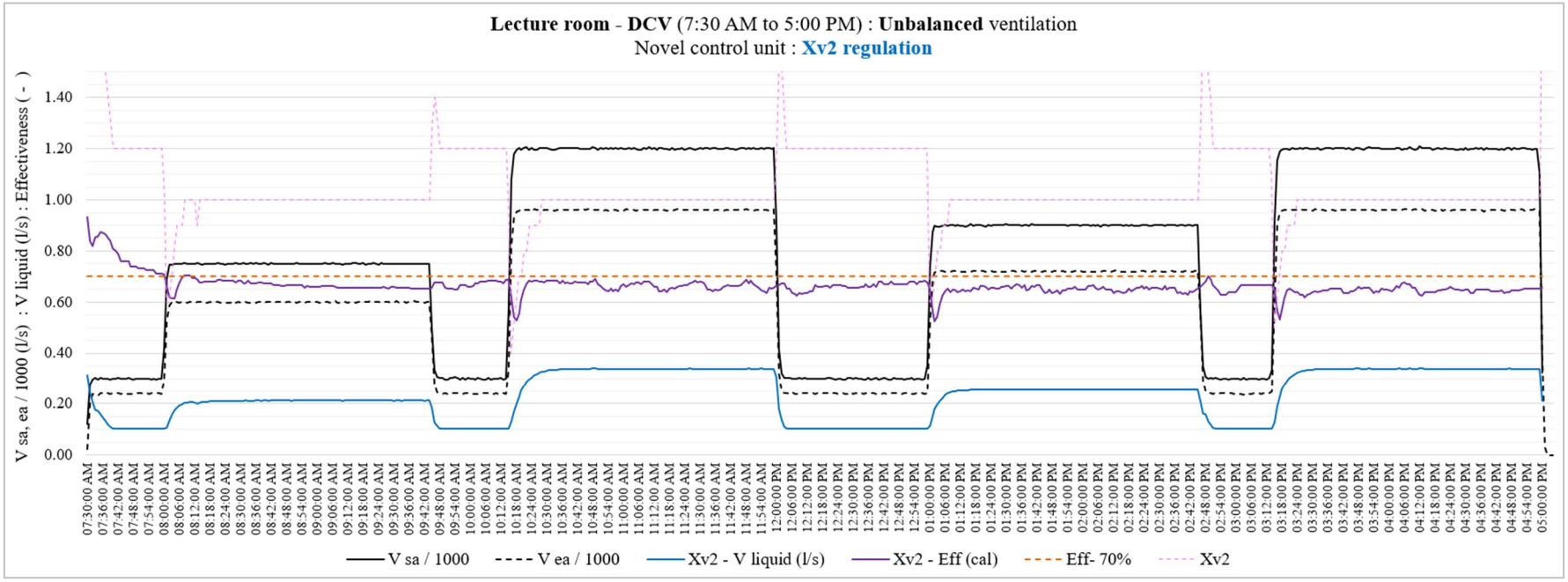

Figure 45: Novel control unit utilizing Xv2 regulation for an unbalanced demand-controlled ventilation (DCV) system in a lecture hall application.

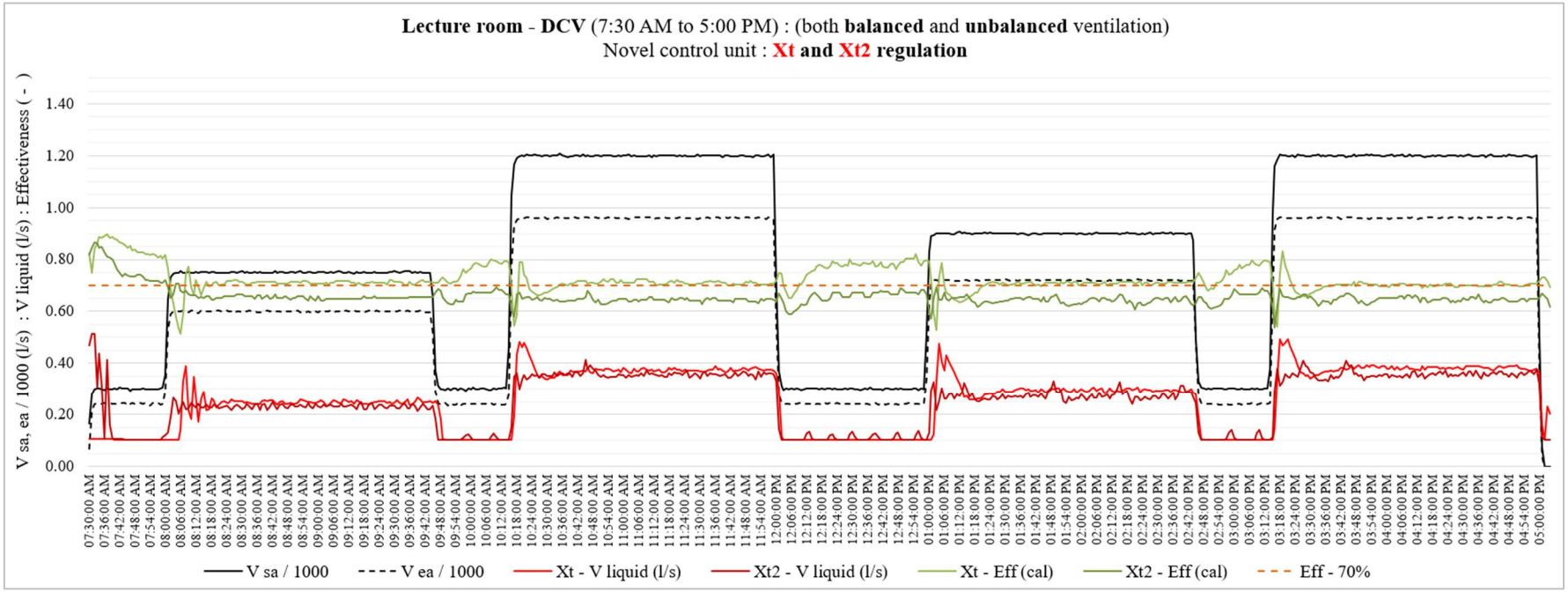

Figure 46: Comparison of Xt and Xt2 regulations for a demand control ventilation (DCV) system (both balanced and unbalanced) in a lecture hall application.

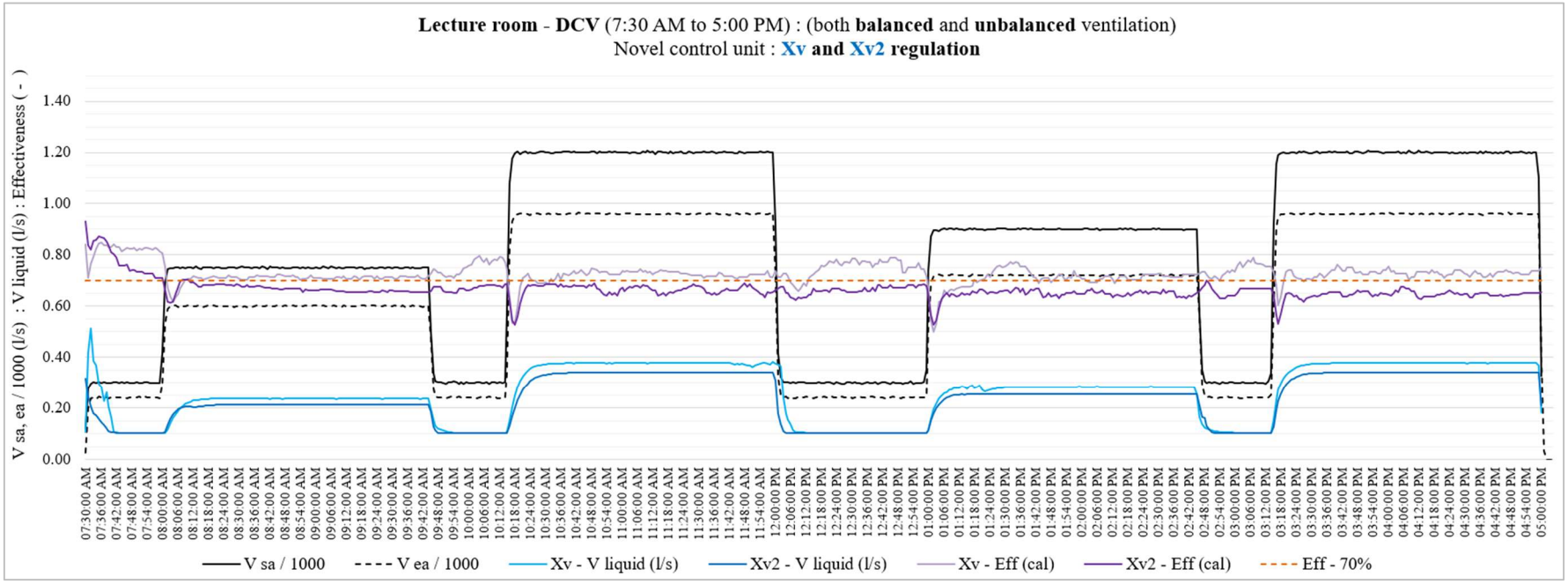

Figure 47: Comparison of Xv and Xv2 regulations for a demand control ventilation (DCV) system (both balanced and unbalanced) in a lecture hall application.

4.2.1 DCV with balanced ventilation system

In addition to the balanced ventilation results shown in Figures 41 and 42 for Xt and Xv regulation, the average effectiveness and average liquid flow rate for each time period are compared and presented in Table 5 below.

Table 5: Comparison of average effectiveness and fluid flow rates for different time periods under Xt and Xv control regulations.

Schedule	Balanced ventilation (l/s)		**Xt** =1, regulation		**Xv** =1, regulation	
	supply air	extract air	effectiveness (average)	liquid flow (l/s) (average)	effectiveness (average)	liquid flow (l/s) (average)
Start	300	same	84%	0.10	82%	0.17
Lecture 1	750	same	71%	0.24	71%	0.23
Break 1	300	same	75%	0.12	75%	0.11
Lecture 2	1200	same	71%	0.37	72%	0.37
Lunch break	300	same	76%	0.11	75%	0.12
Lecture 3	900	same	70%	0.29	70%	0.28
Break 2	300	same	75%	0.11	74%	0.11
Lecture 4	1200	same	70%	0.38	73%	0.37

Average effectiveness and liquid flow:

According to Table 5, both Xt and Xv regulations in the DCV operation of the lecture hall application demonstrate comparable effectiveness values and corresponding liquid flow rates for each time period, with slight deviations.

During lecture periods, when the DCV percentage is 50% or higher, both Xt and Xv regulation maintain an average effectiveness of 70% to 73%, with liquid flow rates appropriately adjusted to the corresponding airflow rates. The average effectiveness of Xv is either equal to or slightly higher than that of Xt. Additionally, the average liquid flow rate maintained by Xv is generally similar to Xt or slightly lower than the corresponding Xt value.

During break periods, when the DCV operates at the lowest airflow rate of 20% (except for the initial startup period), both Xt and Xv provide similar average effectiveness and airflow rates, with slight deviations. However, both Xt and Xv maintain a higher average effectiveness of approximately 75% and a heat capacity ratio of 1.1 or above, as shown in Figures 41 and 42. Additionally, during periods of minimal airflow, the liquid flow rate approaches the minimum operating limit of the circulation pump.

Comparison of balanced ventilation flow rate at 750 l/s:

The average effectiveness and corresponding liquid flow rate for both Xt and Xv regulation align with the results shown in Figures 30 and 39, which illustrate effectiveness as a function of the heat capacity ratio and liquid flow rates for the balanced 750 l/s airflow.

Xt and Xv balanced ventilation - Figures 41, 42, and 43:

A comparison of the effectiveness and liquid flow rate profiles for both Xt and Xv regulation in Figures 41, 42, and 43 further highlights the previously discussed trends. Both regulation methods maintain acceptable effectiveness and liquid flow rate levels throughout the entire DCV operation, except for slight deviations during transitions in the DCV rate.

The liquid flow rate profile of the Xv regulation demonstrates a smoother transition between DCV rate changes and maintains a more consistent liquid flow rate compared to Xt regulation. This difference is recognized to the PID controller settings, where the proportional gain (P-value) varies between Xt and Xv. Additionally, Xt regulation utilizes four temperature measurements for system control, while Xv regulation depends on two flowrate measurements.

4.2.2: DCV with unbalanced ventilation

In addition to the unbalanced ventilation results shown in Figures 44 and 45 for Xt2 and Xv2 regulation, the average effectiveness and average liquid flow rate for each time period are compared and summarized in Table 6 below.

Table 6: Comparison of average effectiveness and fluid flow rates for different time periods under Xt2 and Xv2 control regulations.

Schedule	Unbalanced ventilation (l/s)		**Xt2** =1, regulation		**Xv2** =1, regulation	
	Supply air	Extract air	Effectiveness (Ave)	liquid flow (l/s) (Ave)	Effectiveness (Ave)	liquid flow (l/s) (Ave)
Start	300	240	77%	0.18	78%	0.13
Lecture 1	750	600	66%	0.23	67%	0.21
Break 1	300	240	66%	0.11	67%	0.11
Lecture 2	1200	960	64%	0.35	66%	0.33
Lunch break	300	240	66%	0.11	66%	0.11
Lecture 3	900	720	64%	0.27	65%	0.25
Break 2	300	240	65%	0.11	66%	0.12
Lecture 4	1200	960	65%	0.35	64%	0.33

Average effectiveness and liquid flow:

According to Table 6, both Xt2 and Xv2 regulations in the DCV operation of the lecture hall application produce comparable effectiveness values with corresponding liquid flow rates for each period, with only minor deviations.

Throughout all periods, except for the initial phase, both Xt2 and Xv2 regulation maintain an average effectiveness of 64% to 67%, with liquid flow rates appropriately adjusted to match the corresponding airflow rates. The average effectiveness of Xv2 is generally equal to or slightly higher than that of Xt2, except during the final lecture period, where it is 1% lower than Xt2. Additionally, the average liquid flow rate maintained by Xv2 is typically similar to or slightly lower than the corresponding Xt2 value.

Comparison of unbalanced ventilation flow rate at 750 l/s airflow *(supply 750 l/s and extract 600 l/s):*

To further evaluate the performance of Xt2 regulation, an additional test was conducted under unbalanced ventilation conditions, where the supply airflow was set to 750 l/s and the extract airflow was reduced by 20% to 600 l/s. The results are illustrated in Figure 48.

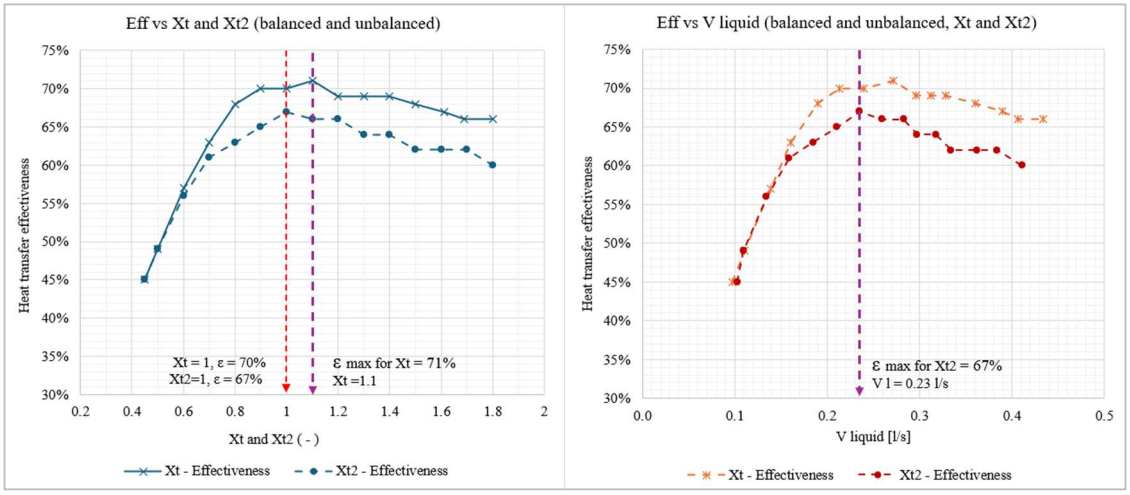

Figure 48: Xt and Xt2 regulation for balance airflow of 750 l/s and unbalanced airflow of 750/600 l/s.

Figure 48 presents the relationship between effectiveness and both Xt2 and Xt, as well as the relationship between effectiveness and liquid flow rate under Xt2 and Xt regulations for both balanced and unbalanced ventilation, enabling a direct comparison within the same figure.

Under unbalanced ventilation conditions with Xt2 regulation, the maximum effectiveness achieved is 67% at a liquid flow rate of 0.23 l/s. A comparison of effectiveness and liquid flow rates for Xt2 regulation shows that at an unbalanced airflow of 750/600 l/s, the system operates within an acceptable range, demonstrating the controller's reliability under dynamic unbalanced DCV conditions

Xt2 and Xv2 Unbalanced Ventilation (Figures 44 and 45):

As shown in Figures 44 and 45, while the heat capacity ratio of Xt2 remains close to 1 throughout the entire DCV period, Xv2 maintains a ratio of 1.2 or higher during periods of minimal unbalanced airflow, break periods. Additionally, during these break periods, the liquid flow rate for both Xt2 and Xv2 approaches the minimum operating limit of the circulation pump.

A comparison of the effectiveness and liquid flow rate profiles for Xt2 and Xv2 regulation in Figures 44 and 45 further highlights the previously discussed trends. Both regulation methods maintain acceptable effectiveness and liquid flow rate levels throughout the entire unbalanced DCV operation, with only slight deviations during DCV rate transitions.

The liquid flow rate profile of Xv2 regulation demonstrates a smoother transition between DCV rate changes and maintains a more consistent liquid flow rate compared to Xt2 regulation. This difference is recognized to the PID controller settings, where the P-value differs between Xt2 and Xv2. Furthermore, Xt2 regulation uses seven temperature measurements for system control, while Xv2 regulation relies only on three flowrate measurements.

Balanced and Unbalanced DCV Comparison (Figures 46 and 47):

Figures 46 and 47 clearly show that the effectiveness values for unbalanced DCV are approximately 5% lower than those for balanced ventilation DCV, with a slight reduction in the corresponding liquid flow rates.

According to Figure 46, a comparison between Xt and Xt2 reveals that Xt2 regulation provides a smoother transition compared to Xt. This behaviour is recognized to the different P-values used in the control settings, with P = 10 for Xt and P = 15 for Xt2.

Furthermore, Figure 47 confirms the smooth operation of both Xv and Xv2 regulation in balanced and unbalanced DCV conditions. This consistency is achieved by maintaining the same P values for Xv and Xv2, in addition to the factors discussed in the previous section.

4.2.3: Unbalanced DCV using Xt and Xv regulations

To evaluate the impact of using Xt and Xv regulation in a DCV system with unbalanced airflow, two full test cycles were conducted based on a lecture hall application. The tests followed the operational schedule outlined in Table 4 above. Unlike the previous tests, which applied Xt2 and Xv2 regulation methods for unbalanced ventilation scenarios, these tests used the base Xt and Xv regulation approach. This method, which is commonly applied in real-world scenarios where control is typically based on the supply air side, was used to evaluate performance under typical unbalanced ventilation conditions.

Figures 49 and 50 illustrate the performance of the novel control unit in an unbalanced DCV ventilation system for the lecture hall application, using Xt and Xv regulation methods, respectively. Figure 51 presents a comparison between Xt and Xt2 temperature-based regulation methods under the same unbalanced conditions. Additionally, Figure 52 compares the performance of Xv and Xv2 flow-based regulation methods for the unbalanced DCV system.

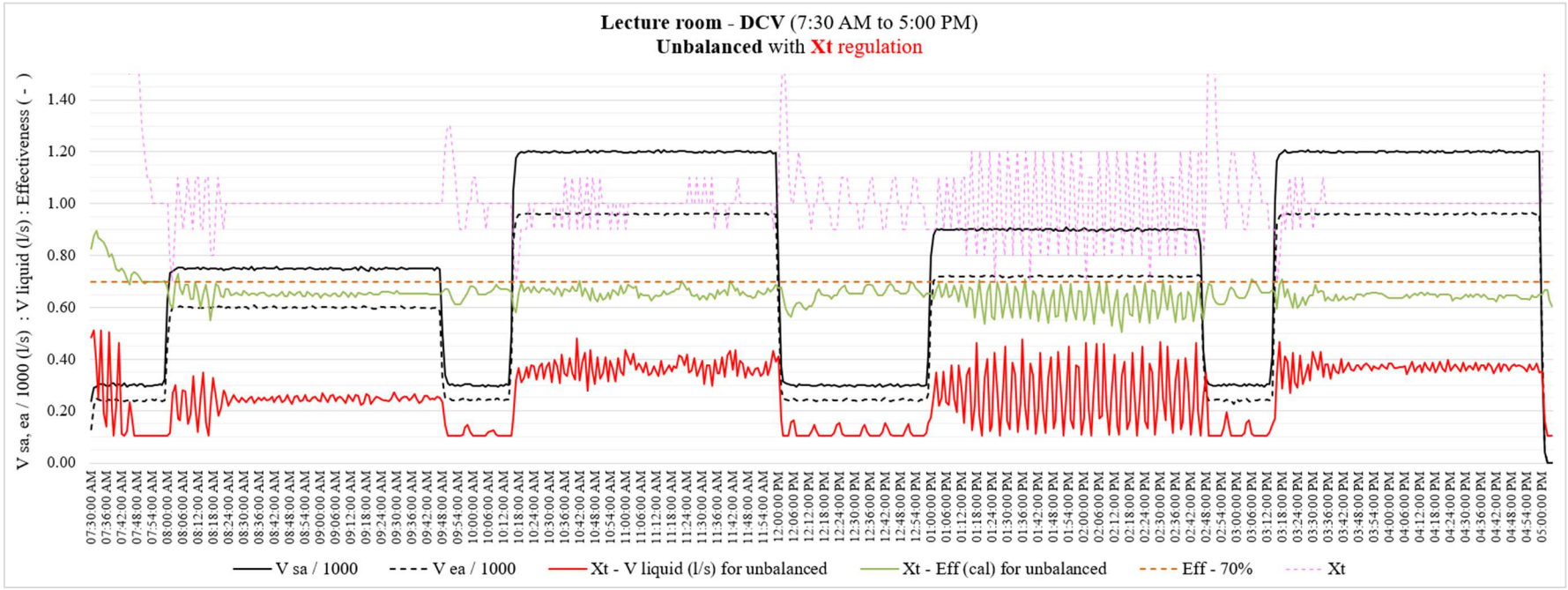

Figure 49: Novel control unit utilizing Xt regulation for an unbalanced demand-controlled ventilation (DCV) system in a lecture hall application.

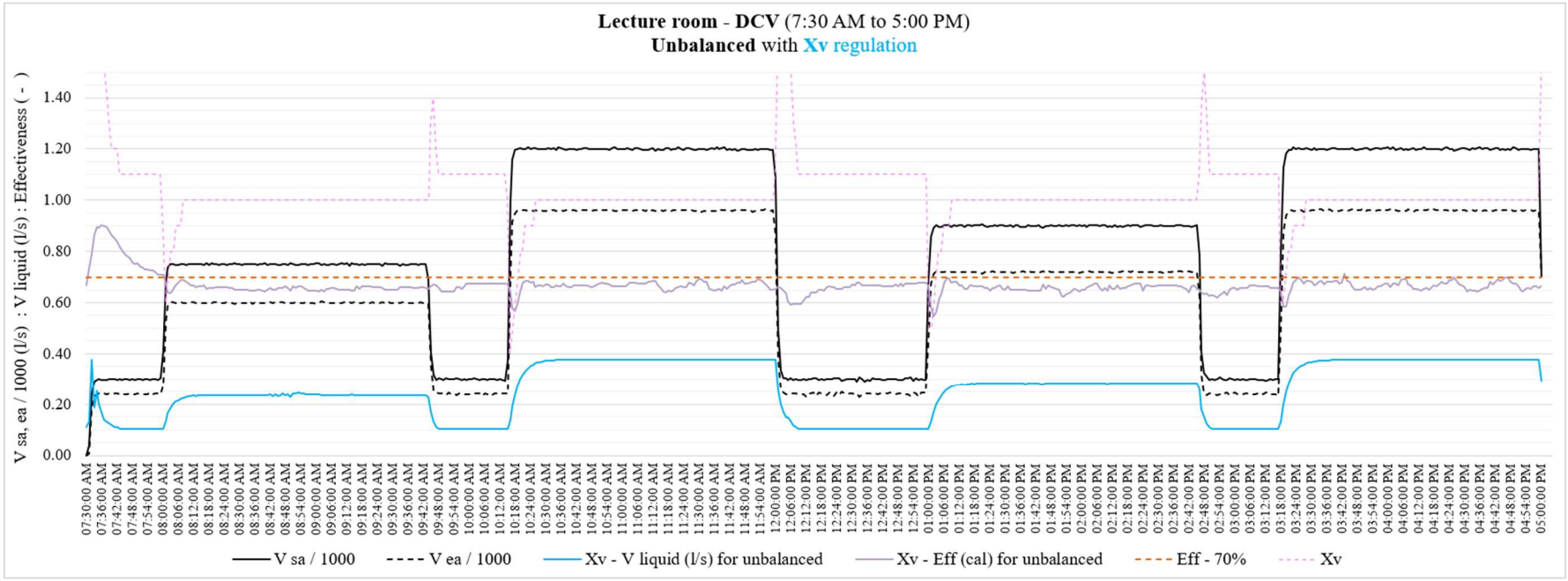

Figure 50: Novel control unit utilizing Xv regulation for an unbalanced demand-controlled ventilation (DCV) system in a lecture hall application.

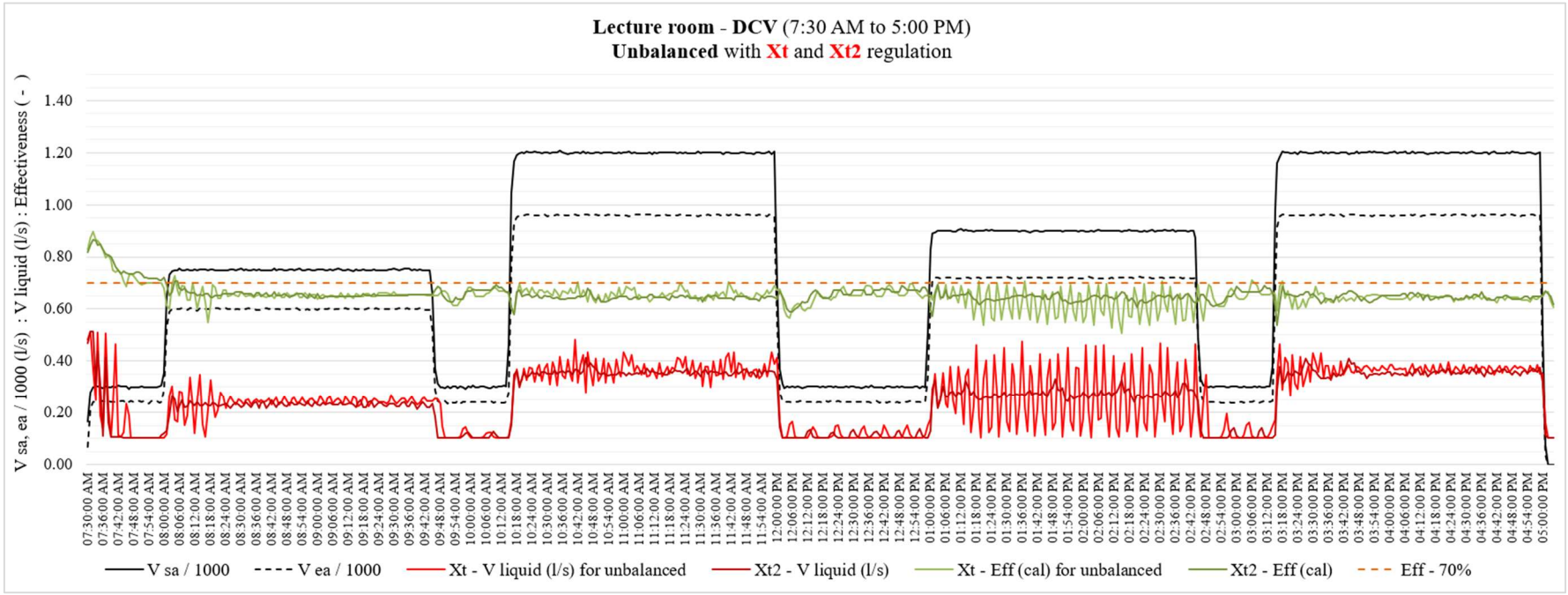

Figure 51: Comparison of Xt and Xt2 regulations for a unbalanced demand control ventilation (DCV) system in a lecture hall application.

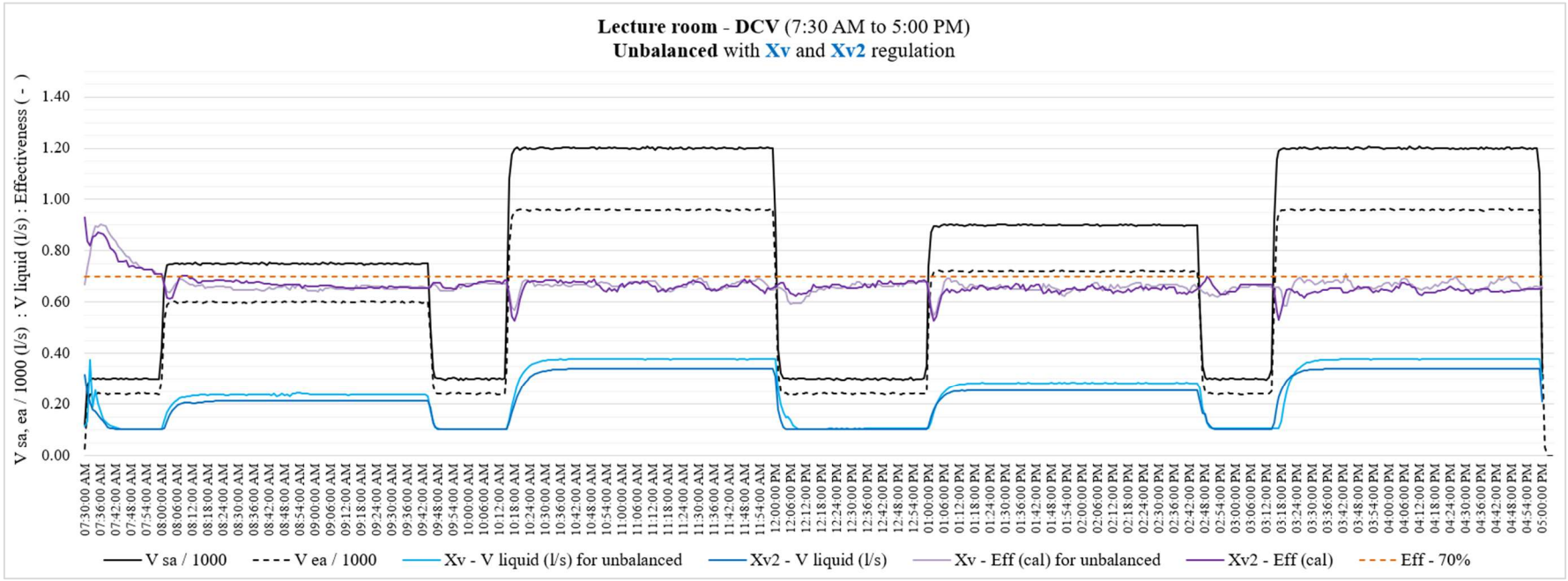

Figure 52: Comparison of Xv and Xv2 regulations for a unbalanced demand control ventilation (DCV) system in a lecture hall application.

In addition to the performance results illustrated in Figures 49 to 52 for Xt, Xv, Xt vs. Xt2 and Xv vs. Xv2 regulation methods for unbalanced DCV systems, the corresponding average effectiveness and liquid flow rate for each regulation strategy were analysed over different periods. These comparative results for the unbalanced ventilation system are summarized in Table 7 below.

Table 7: Comparison of average effectiveness and liquid flow rates during different time periods under Xt, Xt2, Xv, and Xv2 regulation methods in an unbalanced DCV system.

Schedule	Unbalanced DCV		Temperature based (Xt and Xt2)				Flowrate based (Xv and Xv2)			
	Supply (l/s)	Extract (l/s)	Effectiveness (Ave)		liquid flow (l/s) (Ave)		Effectiveness (Ave)		liquid flow (l/s) (Ave)	
			Xt2	Xt	Xt2	Xt	Xv2	Xv	Xv2	Xv
Start	300	240	77%	76%	0.18	0.20	78%	79%	0.13	0.13
Lecture 1	750	600	66%	65%	0.23	0.24	67%	66%	0.21	0.23
Break 1	300	240	66%	66%	0.11	0.13	67%	66%	0.11	0.11
Lecture 2	1200	960	64%	66%	0.35	0.36	66%	67%	0.33	0.37
Lunch break	300	240	66%	65%	0.11	0.12	66%	65%	0.11	0.12
Lecture 3	900	720	64%	62%	0.27	0.26	65%	66%	0.25	0.28
Break 2	300	240	65%	65%	0.11	0.13	66%	65%	0.12	0.12
Lecture 4	1200	960	65%	64%	0.35	0.33	64%	67%	0.33	0.36

Average effectiveness and liquid flow:

As shown in Table 7, the average effectiveness achieved with the Xt regulation method during the unbalanced DCV tests is generally comparable to that of the Xt2 regulation across most periods. However, the liquid flow rates for Xt are slightly higher than those for Xt2, except during Lecture periods 3 and 4. In these two periods, Xt regulation resulted in slightly lower effectiveness and reduced flow rates compared to Xt2. As illustrated in Figures 49 and 51, the Xt regulation struggled to stabilize during Lecture periods 3 and 4, particularly in period 3, where greater fluctuations occurred due to limited controller stability during this phase.

The effectiveness achieved with Xv regulation across all time periods closely aligns with the results from Xv2 regulation. However, the corresponding liquid flow rates for Xv are slightly higher, as evident in Figures 52. Particularly, both Xv and Xv2 regulation methods produced smoother liquid flow profiles compared to Xt and Xt2 under the tested unbalanced DCV conditions, as clearly illustrated in Figures 51 and 52.

Suitability of Xt and Xv regulations for unbalanced ventilation:

In this unbalanced ventilation tests, the extract air flow rate during each period was approximately 20% lower than the supply air flow rate. Based on the results, Xt and Xv regulation methods which operate based on inputs from the supply-side heat exchanger coil and airflow are well-suited for similar unbalanced DCV applications. These methods provide stable performance with slightly increased liquid flow rates, reflecting conditions more representative of real-world operation. In contrast, Xt2 and Xv2, which require combined input from both supply and extract coils and airflow measurements, introduce additional complexity without offering a significant improvement in performance for such unbalanced scenarios.

4.3 Effect of property selection (different EG%) on Xv regulation

Selection of thermophysical property:

The Xv regulation method in the novel control system adjusts the working fluid flow rate to maintain a heat capacity flow rate ratio of one, aiming to maximize the effectiveness of the run-around heat recovery unit. For Xv regulation to function accurately, it is essential to input the correct thermophysical properties of both air and the working fluid into the control system. These properties should be selected based on the expected operational temperature range, the testing environment, and the concentration of ethylene glycol used in the system.

In all primary tests, the thermophysical properties corresponding to a 30% ethylene glycol mixture were used. Specifically, a specific heat capacity of 3.88 kJ/kg·K and a density of 1023 kg/m³ were applied. These values provided consistency with the Xt regulation results and are therefore referred to throughout the remainder of this document as the 30% EG base case.

To analyse the impact of selecting incorrect thermophysical properties, for example when values are taken for a different ethylene glycol concentration, the effects of three concentrations were evaluated based on ASHRAE data. These include ASHRAE 20 percent, 30 percent, and 40 percent ethylene glycol concentrations. The corresponding thermophysical properties for each concentration were obtained from ASHRAE publications (from table 6 and 7 of chapter 31, ASHRAE fundamental 2021) and selected to match the relevant operating temperature range. These values are summarized in Table 8.

Table 8: Thermophysical properties corresponding to the selected ethylene glycol concentrations.

Selected working fluid concentration	specific heat capacity Cp [kJ/ kg.K]	density ρ [kg/ m^3]
30% EG - base case	3.88	1023
20% EG - ASHRAE	3.80	1031
30% EG - ASHRAE	3.63	1047
40% EG - ASHRAE	3.45	1061

*Note**:** For all cases in the table above, the **air properties** used in the control system remain the same. The selected values are a specific heat capacity of 1.00 kJ/kg·K and a density of 1.247 kg/m³.*

To evaluate the impact of incorrectly selecting thermophysical properties, a two-hour balanced DCV test cycle was carried out using each of the fluid concentrations listed above. The test was based on a lecture hall ventilation profile with a supply airflow of 300 l/s for the first 15 minutes, followed by 750 l/s for the remaining 1 hour and 45 minutes.

Estimation results:

Based on the selected test air flowrate and the consistent thermophysical properties of the air stream, the theoretical liquid flowrate required to achieve maximum effectiveness (corresponding to Xv = 1) can be determined for each of the working fluid concentrations listed in Table 8.

In addition, theoretical liquid flow rates corresponding to different heat capacity ratios, ranging from Xv = 0.3 to Xv = 1.8, were calculated for an air flow rate of 750 L/s. These values are presented in Table 8 for each working fluid concentration. For comparison, the measured liquid flow rates obtained during the primary testing using the 30% EG base case are also included in Table 9.

Table 9: Liquid flow rates corresponding to different Xv ratios for various working fluid concentrations.

Xv ratio	Liquid flowrate for air flow rate of 750 l/s [l/s]							
	30% EG - base case		20% EG - ASHRAE		30% EG - ASHRAE		40% EG - ASHRAE	
	estimated	measured	estimated	diff, base case %	estimated	diff, base case %	estimated	diff, base case %
0.3	0.08	-	0.08	- 0.5%	0.08	3%	0.08	7%
0.4	0.09	0.10	0.09	- 0.5%	0.10	3%	0.10	7%
0.5	0.12	0.12	0.12	- 0.5%	0.12	3%	0.13	7%
0.6	0.14	0.14	0.14	- 0.5%	0.15	3%	0.15	7%
0.7	0.17	0.16	0.17	- 0.5%	0.17	3%	0.18	7%
0.8	0.19	0.19	0.19	- 0.5%	0.19	3%	0.20	7%
0.9	0.21	0.21	0.21	- 0.5%	0.22	3%	0.23	7%
1.0	0.24	0.24	0.24	- 0.5%	0.24	3%	0.25	7%
1.1	0.26	0.26	0.26	- 0.5%	0.27	3%	0.28	7%
1.2	0.28	0.28	0.28	- 0.5%	0.29	3%	0.30	7%
1.3	0.31	0.30	0.31	- 0.5%	0.32	3%	0.33	7%
1.4	0.33	0.33	0.33	- 0.5%	0.34	3%	0.35	7%
1.5	0.36	0.35	0.35	- 0.5%	0.37	3%	0.38	7%
1.6	0.38	0.38	0.38	- 0.5%	0.39	3%	0.40	7%
1.7	0.40	0.40	0.40	- 0.5%	0.41	3%	0.43	7%
1.8	0.43	0.42	0.42	- 0.5%	0.44	3%	0.45	7%

According to the liquid flow rates presented in Table 9, the measured flow rates for the 30% EG base case closely matched the estimated values, demonstrating consistency between the control system response and the theoretical calculations. Among the ASHRAE-based fluid concentrations considered, 20%, 30%, and 40% EG-ASHRAE, the thermophysical properties of 20% EG-ASHRAE showed good alignment with the base case, while the 30% and 40% EG cases showed deviations in liquid flow rates of approximately 3% and 7%, respectively.

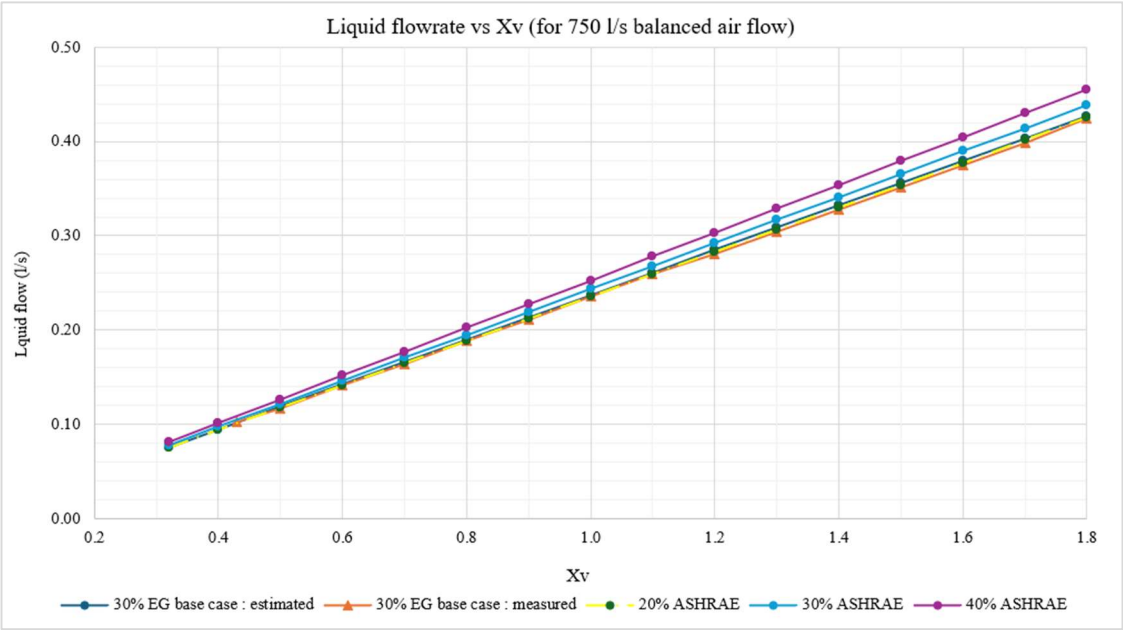

Figure 53: Estimated and measured liquid flow rates as a function of the Xv ratio for different EG concentrations.

Figure 53 illustrates these comparisons, showing both the estimated and measured liquid flow rates as a function of the Xv ratio. The deviations reflect the influence of thermophysical property selection on the control system's performance.

In addition to the above observations, as shown in Table 8, an increase in the EG concentration of the working fluid results in a decrease in its specific heat capacity, while its density increases. The overall impact on the required liquid flow rate is determined by the product of specific heat capacity and density for each selected EG concentration. These combined effects of thermophysical properties on fluid flow rates for different EG concentrations are summarized in Table 10.

Table 10: Overall influence of thermophysical properties on fluid flow rates for different EG concentrations.

Selected working fluid concentration	specific heat capacity Cp [kJ/ kg.K]	density ρ [kg/ m^3]	Overall effect in fluid flow rate	
			Cp x ρ	Deviation from base case (%)
30% EG - base case	3.88	1023	3969	-
20% EG - ASHRAE	3.80	1031	3922	(- 0.5%)
30% EG - ASHRAE	3.63	1047	3802	(- 4%)
40% EG - ASHRAE	3.45	1061	3664	(- 8%)

Test results:

Figures 54 and 55 present the test results of Xv regulation using different EG concentration properties implemented in the control system, compared with the preliminary results obtained using the base-case EG concentration.

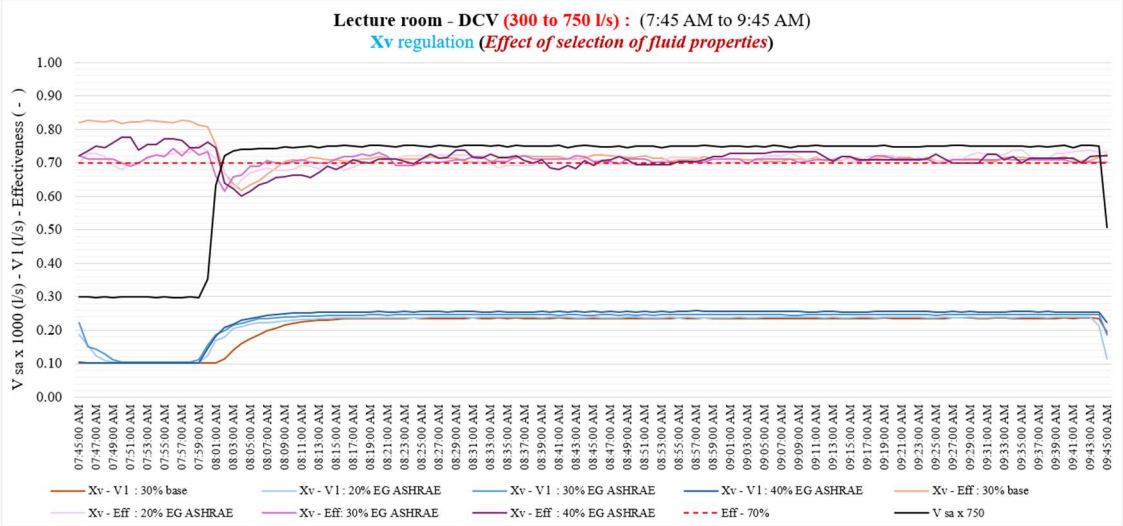

Figure 54: Effectiveness and liquid flow rate for DCV airflows ranging from 300 to 750 l/s using Xv regulation with varying ethylene glycol (EG) concentrations.

Based on the above Figures 54, the Xv regulation demonstrates consistent controller behaviour regardless of the selected thermophysical properties for different ethylene glycol concentrations. The resulting effectiveness and liquid flow rate profiles demonstrate similar trends and overall stability. However, as illustrated in Figure 55, the liquid flow rate increases when the controller uses thermophysical properties corresponding to higher EG concentrations.

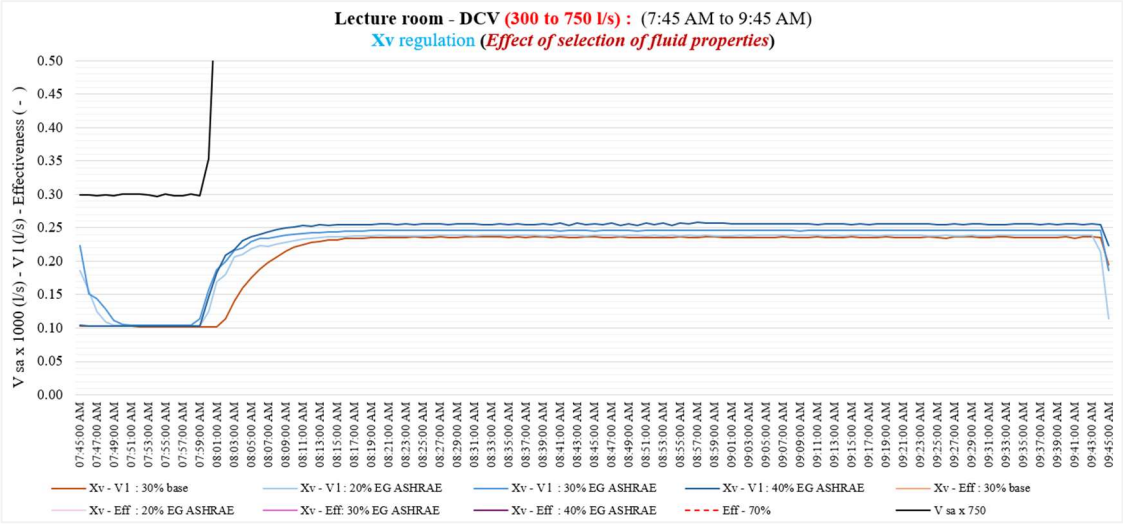

Figure 55: Liquid flow rate for DCV airflows ranging from 300 to 750 l/s using Xv regulation with varying ethylene glycol (EG) concentrations.

The average effectiveness and corresponding liquid flow rates during the 750 l/s airflow phase for each EG concentration test were determined and are presented in Table 11. For easier comparison, the table also includes the percentage change in liquid flow rate for each EG concentration relative to the base-case 30% EG.

Table 11: Comparison of average effectiveness and liquid flow rate at 750 l/s airflow using different EG concentration properties in the controller.

Remark	Effectiveness (%)							Liquid flowrate (l/s)						
	Base case (30%)	ASHRAE 20% EG		ASHRAE 30% EG		ASHRAE 40% EG		Base case (30%)	ASHRAE 20% EG		ASHRAE 30% EG		ASHRAE 40% EG	
		Eff	Diff	Eff	Diff	Eff	Diff		l/s	Diff %	l/s	Diff %	l/s	Diff %
Total duration 1:45 hrs	71%	71%	0%	71%	0%	70%	-1%	0.23	0.23	2.5%	0.24	6.5%	0.25	10.6%
After settling, duration of 1:15 hrs	71%	71%	0%	71%	0%	71%	0%	0.24	0.24	0.6%	0.25	4.3%	0.26	8.5%

According to the average results summarized in Table 11, the effectiveness remained consistent across all test cases, regardless of the EG concentration used in the controller. However, as the EG concentration increased, the required liquid flow rate also increased. These increases were approximately 0.6% for 20% EG, 4.3% for 30% EG, and 8.5% for 40% EG, aligning well with the trends identified in the theoretical estimates presented earlier in Figure 53 and Table 9.

Furthermore, a comparison between the overall thermophysical property effect (calculated as the product of specific heat capacity and density, $Cp \times \rho$) shown in Table 10, and the corresponding changes in liquid flow rate from Table 11, reveals a clear correlation. Specifically:

- For 20% EG (ASHRAE), the overall effect decreased by 0.5%, and the corresponding increase in flow rate was 0.6%.
- For 30% EG (ASHRAE), the overall effect decreased by 4%, with a flow rate increase of 4.3%.
- For 40% EG (ASHRAE), the overall effect decreased by 8%, and the flow rate increased by 8.5%.

These comparisons clearly indicate a direct relationship between the reduction in the thermophysical property product ($Cp \times \rho$) and the required increase in liquid flow rate. This correlation confirms the influence of selecting appropriate thermophysical properties on the system's performance and controller response.

According to the above, if thermophysical properties corresponding to a higher EG concentration are selected instead of those matching the actual working fluid concentration, the control unit regulates a fluid flow rate that exceeds the optimal requirement. Conversely, selecting properties associated with a lower EG concentration causes the controller to regulate a flow rate below the required level. Such deviations in property selection significantly affect the system's ability to maintain optimal effectiveness, resulting in reduced performance of the run-around heat recovery unit. This reduction occurs because the fluid flow rates become either excessive or insufficient, depending on how much higher or lower the selected EG concentration is compared to the actual concentration used in the system.

However, if the deviations in the selected thermophysical properties remain within ±10% of the actual concentration, the resulting effectiveness stays within an acceptable performance range. In such cases, the control unit is still able to maintain a reasonably stable and effective operation, despite minor mismatches in property selection.

5. Discussion

Unit performance:

The unit performance evaluation conducted at the rated airflow rate of 1000 l/s shows that the liquid flow rate corresponding to the maximum effectiveness obtained using the novel control system is in good agreement with the reference flowrate provided by the manufacturer. However, the measured maximum effectiveness is approximately 3% higher than the manufacturer's rated value. This deviation is primarily attributed to the measurement uncertainties associated with the temperature sensors in the laboratory test rig.

In comparison to the results from the previous laboratory tests, the maximum effectiveness recorded in the old lab setup is good aligned with the values obtained using the novel control method, showing only a minor deviation of approximately 1%. However, the corresponding liquid flow rate at this maximum effectiveness in the previous test was more than 10% lower than that observed with both the novel control system and the manufacturer's data. This deviation may be due to the differences in the thermophysical properties of the ethylene glycol solution used during the previous test, which can influence the heat capacity ratio and the measured liquid flow rate.

Effect of airflow rate on effectiveness:

The tested airflow rates of 500 l/s, 750 l/s, and 1000 l/s using a 30% ethylene glycol solution indicate that the maximum achievable effectiveness of the run-around heat recovery system decreases as the airflow rate increases. This trend is consistent with the findings of Mohamad [2], that simulation-based study showed a reduction in effectiveness at higher airflow rates, mainly due to a lower number of transfer units (NTU).

The optimum liquid flow rate corresponding to the maximum effectiveness varies for each tested airflow rate and increases with higher airflow rates. Additionally, the measured optimal heat capacity flow ratio also varies for each airflow rate. These results are consistent with the conclusions of Mohamad [2], which indicate that there is no single optimal heat capacity flow ratio applicable in all cases, as the optimal value depends on the airflow rate, the thermophysical properties of the coupling liquid and the number of coil circuit.

Furthermore, the measured heat capacity ratios at the point of maximum effectiveness for the tested airflow rates are equal to or greater than unity, which is also consistent with the conclusions presented by Mohamad [2].

Novel control unit performance with demand-controlled ventilation (DCV) application:

The novel control unit using the Xt-based regulation method demonstrates effective performance in achieving maximum effectiveness under demand-controlled ventilation conditions with balanced airflow. Based on the average heat capacity ratio of the supply and extract coils presented in Peter's study [1], the Xt2 regulation method was implemented to evaluate unbalanced airflow conditions. Test results show that Xt2 also performs well under unbalanced DCV scenarios, effectively optimizing the performance of the run-around heat recovery unit.

Particularly, the main Xt regulation method, which relies on temperature measurements from the supply air coil, also performs effectively under unbalanced ventilation conditions. In tests where the extract airflow rate was reduced by 20% compared to the supply airflow rate, the Xt-

based control method achieved effectiveness values similar to those obtained with Xt2. This confirms the robustness of the novel control unit, even when applied to unbalanced airflow scenarios.

Furthermore, the system's performance under unbalanced DCV conditions was comparable to that of the balanced airflow cases, with only about a 5% reduction in maximum effectiveness. In real building applications, where DCV strategies frequently result in unbalanced ventilation, control systems typically regulate based on the supply airflow rate. The findings in this study support the suitability of that approach, as the Xt-based regulation method consistently maintained reliable and efficient operation even under unbalanced airflow conditions.

Xt and Xv - similarity and gaps:

The flow-based regulation methods, Xv and Xv2, tested under both balanced and unbalanced ventilation conditions, also demonstrated good performance during demand-controlled ventilation operation. The liquid flow rates corresponding to the maximum effectiveness values were consistent with those observed in previous tests. However, the liquid flow rate regulated by the Xv-based method was slightly lower than that of the Xt-based control. This minor difference may be attributed to uncertainties in temperature measurements, which could influence the Xt-based regulation and result in slightly higher liquid flow rates. Despite this, the deviation in maximum effectiveness between the two methods remained within ±1%, indicating strong consistency and agreement between both regulation strategies based on the heat capacity ratio.

Another observation with Xv-based control was its ability to maintain a smoother and more stable liquid flow rate, with fewer fluctuations around the optimal value compared to Xt-based control. This difference is primarily due to the number of input signals involved in each method. Xt-based regulation requires four temperature sensors, which are more subject to ambient temperature variations, particularly on the outdoor and extract air streams. These fluctuations can introduce greater variability in the controller's response. In contrast, the flow-based signals used in Xv regulation are more stable with fixed thermophysical properties, enabling more consistent control of the liquid flow rate.

Effect of PI values:

The PID controller parameters of the novel controller unit were manually adjusted during each test to ensure stable and fast responsive regulation across varying airflow conditions and regulation methods. Appropriate proportional (P) and integral (I) values were identified to optimize controller performance, and it was observed that the optimal values differed between Xt-based and Xv-based regulation strategies. This difference is mainly due to the separate dynamic behaviour of temperature-based and flow-based inputs.

Although manual tuning of the P values was necessary during the experiments, the final selected values allowed the controller to perform effectively and maintain stable operation under both balance and unbalanced airflow conditions. These results confirm that, when properly tuned, the controller can achieve high heat recovery effectiveness across different ventilation scenarios.

However, further testing is recommended to determine the optimal PI values under a wider range of conditions, including different regulation methods and airflow rates. This would support the development of an automatic tuning mechanism in future applications, allowing the system to select appropriate P and I value autonomously in real building environments.

Effect of thermophysical properties on Xv regulation:

The test results show that Xv-based regulation maintains consistent controller behaviour even when slightly different ethylene glycol EG concentration properties are preset in the controller. While the overall system stability and effectiveness remain similar under minor variations in the thermophysical properties of EG, a slight mismatch between the actual and preset EG concentration can influence the liquid flow rate. When properties corresponding to a slightly higher EG concentration than the actual are used, the system tends to regulate a slightly higher liquid flow rate. On the other hand, using properties corresponding to a slightly lower EG concentration results in a slightly reduced flow rate.

This relationship highlights the importance of selecting thermophysical properties within an acceptable range for accurate flow-based control. Since the heat capacity flow rate is directly influenced by the specific heat and density of the coupling liquid, any significant deviation in these parameters can impact the flow regulation. Therefore, setting thermophysical properties within a reasonable range is essential for precise and efficient Xv-based control and for optimizing the system's overall performance.

6. Conclusion and Recommendations

With appropriate tuning of the PI controller parameters, the temperature-based control method (Xt) effectively optimized the heat recovery performance for balanced ventilation airflows. Moreover, test simulations based on modern demand-controlled ventilation systems showed that the Xt-based regulation efficiently optimized the system effectiveness for both balanced and unbalanced airflow conditions.

Additionally, the Xv regulation method, which relies on accurate flow rate measurement using the ultrasonic flow meter, also successfully optimized the effectiveness of the run-around heat recovery system under both balanced and unbalanced DCV conditions. The measured maximum effectiveness and corresponding liquid flow rates using Xv were very similar to those achieved using Xt, with only minor deviations observed.

Furthermore, the extended regulation methods for unbalanced ventilation systems, Xt2 and Xv2, also showed good performance. With reasonable parameter assumptions and educated estimations, these methods were able to optimize the effectiveness of the run-around heat recovery unit in DCV applications. Particularly, the Xt and Xv methods provided results comparable to Xt2 and Xv2 in scenarios with a 20% reduced extract airflow, indicating their flexibility and reliability.

In conclusion, the implemented temperature-based control system (Xt) presents a practical and robust solution for optimizing run-around heat recovery systems in both existing and new DCV applications, especially in cases where the thermophysical properties of the working fluid are uncertain or when precise liquid flow measurement is not feasible. With proper tuning of the control parameters, particularly the proportional (P) and integral (I) values, the system can dynamically maintain optimal effectiveness across varying operating conditions.

The novel control unit implemented in the laboratory test rig, together with a precise flow measuring device and accurate identification of the thermophysical properties of the coupling fluid, confirms that both regulation methods, temperature-based and flow rate-based, developed using the theoretical foundation of the heat capacity ratio, are capable of reliably optimizing the control of the run-around heat recovery unit to achieve maximum effectiveness.

Therefore, it can be recommended to implement the novel control unit in both new and existing run-around heat recovery systems. By incorporating both regulation methods and enabling switching between them as required, along with periodic tuning, the system can maintain efficient operation, achieve optimized effectiveness, and ensure stable and robust performance.

7. References

[1] Peter Filipsson, Anders Trüschel, Torbjörn Lindholm, Jan-Olof Dalenbäck. (2024). Liquid Flow Rate Control in Run-Around Heat Recovery Systems. 10.2139/ssrn.5012076.

[2] Mohammad Mahmoud, Peter Filipsson, Samuel Brunninge, Jan-Olof Dalenbäck, Flow rate optimization in run-around heat recovery systems, Applied Thermal Engineering, Volume 200, 2022, 117599, ISSN 1359-4311, https://doi.org/10.1016/j.applthermaleng.2021.117599.

[3] IEA (2022), Tracking Buildings, IEA, https://www.iea.org/energy-system/buildings#tracking accessed (2025-04-08).

[4] IEA (2020), Is cooling the future of heating?, IEA, https://www.iea.org/commentaries/is-cooling-the-future-of-heating _accessed (2025-04-08).

[5] IEA (2020), Energy Efficiency 2020, IEA, https://www.iea.org/reports/energy-efficiency-2020/buildings accessed (2025-04-08).

[6] REHVA COVID-19 guidance document, August 3, 2020.

[7] P. Filipsson, L. Ekberg "V¨atskekopplad v¨armeåtervinning - F¨orstudie " CIT Energy Management, G¨oteborg, December, 2018.

[8] Mardiana-Idayu, A., & Riffat, S. B. (2012). Review on heat recovery technologies for building applications. Renewable and Sustainable Energy Reviews, 16(2), 1241-1255. https://doi.org/10.1016/j.rser.2011.09.026

[9] Nelson, G. (2021). Optimizing Coil Loop Energy Recovery Systems. ASHRAE Journal, 63(11).

[10] United Nations, Sustainable Development Goals: 17 goals to transform our world, [Online]. Available: https://sdgs.un.org/goals accessed (2025-04-19).

[11] European Commission, The European Green Deal, 2019. [Online]. https://learning-corner.learning.europa.eu/learning-materials/eu-green-deal_en accessed (2025-04-19).

[12] ASHRAE, ASHRAE Handbook: Heating, Ventilating, and Air-Conditioning Applications (SI Edition), American Society of Heating, Refrigerating and Air-Conditioning Engineers, Inc., 2023.

[13] R.B. Holmberg, Heat Transfer in Liquid-Coupled Indirect Heat Exchanger Systems, ASME J. Heat Transfer. 97 (4) (November 1975) 499–503.

[14] W.M. Kays, and A.L. London, "Compact heat exchangers", United States, 1984.

[15] B.I. Forsyth, R.W. Besant, The design of a run-around heat recovery system, ASHRAE transactions. 94 (1988) 511–531.

[16] B.I. Forsyth, R.W. Besant, The performance of a run-around heat recovery system using aqueous glycol as coupling liquid, ASHRAE transactions. 94 (1988) 532–545.

[17] Y.Y. Zeng, R.W. Besant, K.S. Rezkallah, The effect of temperature-dependent properties on the performance of run-around heat recovery systems using aqueous-glycol coupling fluids, ASHRAE Trans. 98 (l) (1992) 551–562.

[18] I. Balen, P. Donjerkovic, I. Galaso, Analysis of the coil energy recovery loop system, Int. J. Energy Res. 27 (4) (2003) 363–376.

[19] ASHRAE (2021) ASHRAE Handbook—Fundamentals. SI Edition. Chapter 31: Physical properties of secondary coolants (brines). Atlanta, GA: American Society of Heating, Refrigerating and Air-Conditioning Engineers, Inc.

[20] Product data sheet of AHU eQ, FläktGroup, 2020

Appendix

A.1 : Calibration of temperature sensors

1. Introduction

Accurate temperature measurement is essential for the novel control system used in this test rig. The temperature sensors play a vital role in regulating and evaluating the performance of the run-around heat recovery unit. Errors in sensor readings can result in inaccurate calculations and reduced control-system efficiency. To ensure measurement reliability, an accuracy check was conducted on the major temperature sensors used in the test rig at the Chalmers Building Services Laboratory. The calibration aimed to identify any deviations, calculate correction factors, and establish an appropriate method for applying those factors.

This appendix presents the calibration methodology, the measurement results, and the proposed correction factors for the temperature sensors used in both the liquid media and air streams. The findings contribute to ensuring precise control and effective performance evaluation of the implemented novel control unit.

2. Temperature sensors evaluated

The eight major temperature sensors evaluated in this study are as follows:

2.1 Sensors used in liquid media:

1. GT40: measures the hot side temperature after the circulation pump and before the supply HX coil.
2. GT41: measures the cold side temperature after the supply air HX coil and before the extract air HX coil.
3. GT42: measures the hot side temperature before the circulation pump and after the extract air HX coil.

2.2 Sensors used in the air streams:

4. GT003: measures outdoor air temperature before the supply air HX coil.
5. GT018: measures supply air temperature after the supply air HX coil and just after the supply air fan.
6. GT011: measures extract air temperature before the extract air HX coil (moveable).
7. GT012: measures extract air temperature before the extract air HX coil (fixed).
8. GT019: measures exhaust air temperature after the extract air HX coil and just after the extract air fan.

The locations of these sensors are illustrated in the Figure A.1 below, extracted from the web application interface.

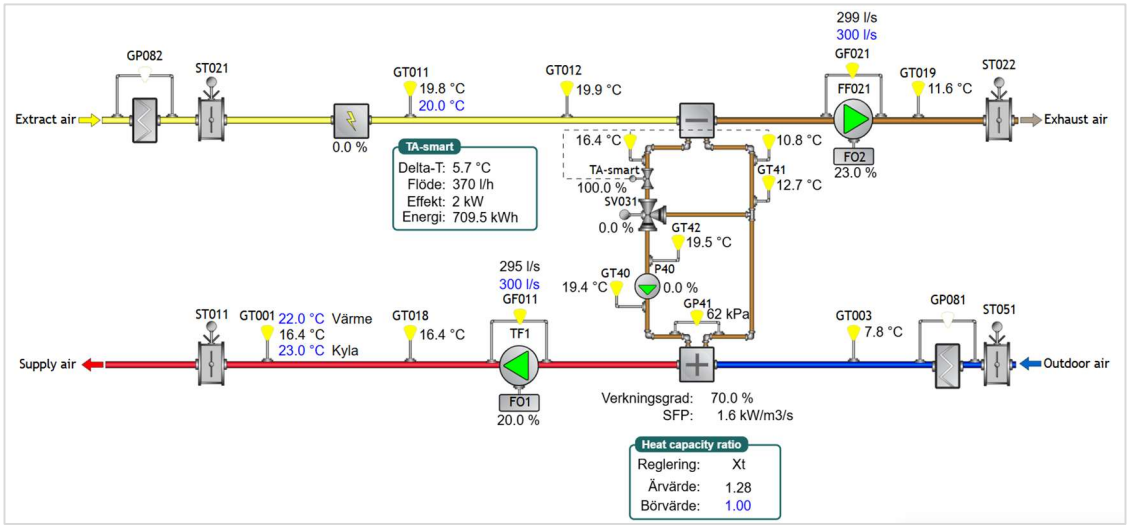

Figure A.1: Location of the temperature sensors

3. Methodology

To validate the accuracy of the temperature sensors, a comparative method was used with a highly accurate, calibrated Pt100 reference thermometer. The technical specifications and most recent calibration date of this reference thermometer are provided below.

Reference thermometer:

- Make: DOSTMANN electronic
- Model: P600
- Type: Pt100
- Accuracy: Pt100: ± 0.1°C
- Resolution: 0.01°C
- Calibration date: 29th October 2024

The methodology was divided into two parts:

1. Accuracy verification for all sensors except the fixed shielded type GT012: conducted using in-situ ice bath calibration.
2. Accuracy verification for the GT012 sensor: performed through comparison with a reference thermometer under steady-state conditions.

3.1 In-situ, ice bath calibration

For all sensors except GT012, an in-situ ice bath calibration (0 °C reference check) was conducted. This method provides a stable 0 °C reference point, enabling the identification of measurement deviations with high reliability.

Procedure:

- An ice–water mixture was prepared to create a stable 0 °C environment.
- The sensors were fully immersed in the ice bath, ensuring they did not contact the container walls.
- The reference thermometer (P600) was also placed in the bath under the same conditions.

- The system was allowed to stabilize for 10–15 minutes.
- Readings were recorded once the temperature stabilized.
- Each sensor's value was compared against the expected 0 °C reference, and deviations were calculated.

3.2 Comparison with a reference sensor under steady-state conditions

For the fixed air temperature sensor GT012, a calibrated reference sensor was positioned adjacent to the installed sensor to allow for direct comparison of readings.

Procedure:

- The calibrated reference sensor was placed as close as possible to the GT012 sensor to ensure consistent measurement conditions.
- The system was allowed to reach a steady-state condition to minimize temperature fluctuations.
- Temperature readings were recorded once the temperature stabilized.
- The differences between the readings were calculated to identify measurement deviations and determine appropriate correction factors.

4. Results

Deviations and corrections factors

The deviation of the measured values for each sensor is calculated as follows.

$$Deviation(\pm) = Measured\ value - Reference\ value$$

In addition to the main seven sensors, sensor GT011, a movable sensor placed in the extract air stream near the fixed GT012 sensor, was also calibrated. GT011 was used to measure the air temperature upstream of the supply fan, enabling estimation of the temperature rise caused by the fan.

Table A.1 presents the correction factors determined through deviation calculations based on the recorded dataset. The estimated correction for the supply air temperature due to fan heat contribution is also included in the same table.

Table A.1: Correction factors for the temperature sensors

Sensor	Temperature measurement	Deviation °C	**Correction factor** °C
GT40 ($T_{lw,2}$)	hot liquid, after pump	+ 0.3	- 0.3
GT41 ($T_{l,c}$)	cold liquid	+ 2.1 *1	- 2.1 *1
GT42 ($T_{l,w,1}$)	hot liquid, before	+ 0.5	- 0.5
GT003 (Toa)	outdoor air	+ 0.6	- 0.6
GT018 (Tsa)	supply air	- 0.5	+ 0.5
GT012 (Tea)	extract air	+ 0.3	- 0.3
GT019 (Tehu)	exhaust air	- 0.3	+ 0.3
GT011	before supply fan	+ 0.4	- 0.4
Correction to supply air temperature due to fan heat gain (at 1000 l/s air flowrate)			
GT018 (Tsa)	supply air	+ 0.77 *2	- 0.77 *2

Note :

*1: Before the novel controller was installed in the laboratory test rig, all liquid temperature sensors had similar wire lengths. With the integration of the new control system, the GT41 sensor is now connected to the liquid circulation control panel (Econet) via an additional wire extension of approximately 3 meters. This extension was necessary because the hydronic system is installed slightly away from the AHU unit compared to the setup in the previous lab. The increased wire length may introduce additional electrical resistance, potentially contributing to greater temperature deviations in GT41 readings compared to those of the GT40 and GT42 sensors.

*2: According to the table above, the overall correction factor for the supply air temperature sensor GT018 is calculated as (+0.50 – 0.77) = –0.27 °C. This value accounts for both the temperature sensor correction and the correction related to the fan's heat contribution.

Effect of applying temperature correction factors on effectiveness

Table A.2 presents a set of test measurements recorded during the evaluation at an airflow rate of 1000 l/s, conducted under Xt regulation. These results are used to evaluate the impact of applying the temperature correction factors listed in Table A.1. The corrected effectiveness values, obtained after applying these factors, are also included in Table A.2.

Table A.2: Test results at 1000 l/s using Xt, with corrected effectiveness after temperature calibration.

Measured temperature			Effectiveness measured	Effectiveness **corrected**
GT018 (Tsa)	GT003 (Toa)	GT012 (Tea)		
8.6	2.3	19.7	36%	37%
9.5	2.3	20	41%	42%
11.2	2.4	20.2	50%	50%
12.6	2.3	20.1	58%	59%
13.6	2.4	20.1	64%	64%
14.3	2.4	20	68%	68%
14.5	2.4	19.9	69%	70%
14.5	2.4	19.9	69%	70%
14.5	2.3	19.8	70%	70%
14.5	2.3	19.9	70%	70%
14.3	2.3	19.7	70%	70%
14.3	2.2	19.8	69%	70%
14.1	2.1	19.9	68%	68%
14	2	19.8	68%	68%

Figure A.2 below illustrates the variation in effectiveness with the liquid flow rate, based on the measured values. Additionally, the figure includes measured results from the previous lab test (manual PF), enabling a direct comparison of effectiveness between the current and previous setups.

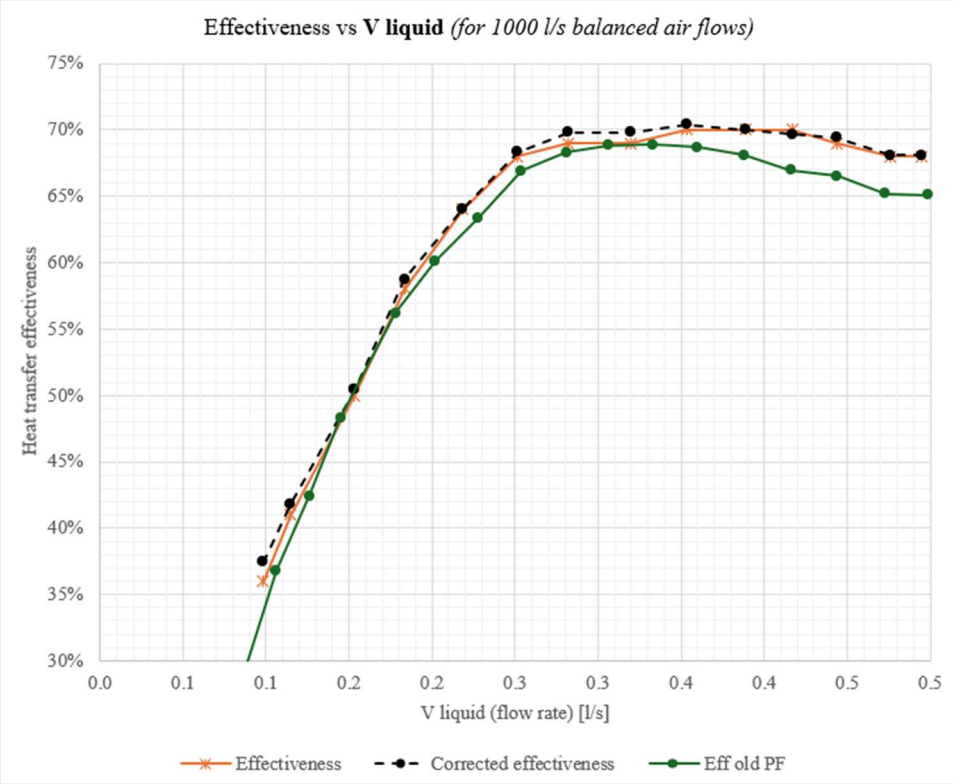

Figure A.2: Measured and corrected effectiveness vs. liquid flow rate

Based on the table and figure above, after applying the temperature correction factors for both air sensors and accounting for the fan heat contribution, the corrected effectiveness and the originally measured effectiveness at an airflow rate of 1000 l/s are nearly identical, showing no significant deviation in the graph.

5. Discussion and Conclusion

The accuracy check performed on the temperature sensors revealed that all sensors, except for GT41, demonstrated minor deviations within the acceptable limits for HVAC applications (± 0.5°C). This indicates that, overall, the sensors are reliable for use in regulating and evaluating the performance of the run-around heat recovery system. However, GT41 showed a significant deviation, which is most likely due to the extended wire length introduced during the installation in the new lab. This additional length may have contributed to increased electrical resistance, affecting the sensor's readings.

Despite the deviation in GT41, the use of correction factors derived from the calibration results effectively adjusted the sensor readings and minimized errors. The correction factors applied to both air sensors, along with the fan heat contribution, provided a more accurate understanding of the system's effectiveness. It was observed that, after applying the corrections, the corrected and original effectiveness values were nearly identical, with no significant deviation at the tested airflow rate of 1000 l/s.

Moreover, the reference thermometer (P600) was verified to be within its accuracy range through an ice bath test, confirming its reliability as a reference sensor.

DEPARTMENT OF ARCHITECTURE AND CIVIL ENGINEERING
CHALMERS UNIVERSITY OF TECHNOLOGY
Gothenburg, Sweden 2025
www.chalmers.se

CHALMERS
UNIVERSITY OF TECHNOLOGY